Journal of Hazardous Materials 404 (2021) 124082

Contents lists available at ScienceDirect

Journal of Hazardous Materials

journal homepage: www.elsevier.com/locate/jhazmat

Review

Heterogeneous Fenton catalysts: A review of recent advances

Nishanth Thomas [a,b], Dionysios D. Dionysiou [c], Suresh C. Pillai [a,b,*]

[a] Nanotechnology and Bio-engineering Research Group, Department of Environmental Science, Institute of Technology Sligo, Sligo, Ireland
[b] Centre for Precision Engineering, Materials and Manufacturing Research (PEM), Institute of Technology Sligo, Sligo, Ireland
[c] Environmental Engineering and Science Program, Department of Chemical and Environmental Engineering, University of Cincinnati, Cincinnati, OH, USA

A B S T R A C T

Heterogeneous Fenton catalysts are emerging as excellent materials for applications related to water purification. In this review, recent trends in the synthesis and application of heterogeneous Fenton catalysts for the abatement of organic pollutants and disinfection of microorganisms are discussed. It is noted that as the complexity of cell wall increases, the resistance level towards various disinfectants increases and it requires either harsh conditions or longer exposure time for the complete disinfection. In case of viruses, enveloped viruses (e.g. SARS-CoV-2) are found to be more susceptible to disinfectants than the non-enveloped viruses. The introduction of plasmonic materials with the Fenton catalysts broadens the visible light absorption efficiency of the hybrid material, and incorporation of semiconductor material improves the rate of regeneration of Fe(II) from Fe(III). A special emphasis is given to the use of Fenton catalysts for antibacterial applications. Composite materials of magnetite and ferrites remain a champion in this area because of their easy separation and reuse, owing to their magnetic properties. Iron minerals supported on clay materials, perovskites, carbon materials, zeolites and metal-organic frameworks (MOFs) dramatically increase the catalytic degradation rate of contaminants by providing high surface area, good mechanical stability, and improved electron transfer. Moreover, insights to the zero-valent iron and its capacity to remove a wide range of organic pollutants, heavy metals and bacterial contamination are also discussed. Real world applications and the role of natural organic matter are summarised. Parameter optimisation (e.g. light source, dosage of catalyst, concentration of H_2O_2 etc.), sustainable models for the reusability or recyclability of the catalyst and the theoretical understanding and mechanistic aspects of the photo-Fenton process are also explained. Additionally, this review summarises the opportunities and future directions of research in the heterogeneous Fenton catalysis.

1. Introduction to photo-Fenton chemistry

The growing scarcity of water in the world today forces researchers to investigate more deeply various water conservation schemes and explore new water purification technologies. There is also a need to find solutions for the increasing presence of microbial and chemical pollutants in water (Brillas et al., 2009; Shannon et al., 2008). The scientific community has demonstrated the suitability of advanced oxidation processes (AOPs) for degrading contaminants present in wastewater. In AOPs, generally, the pollutants undergo mineralisation into different inorganic compounds such as salts, CO_2, and water or they will be converted to readily degradable small organic molecules if treatment time is optimized (Oller et al., 2011; Comninellis et al., 2008; Pérez et al., 2006). The typical chemical feature that connects the AOPs is the formation of the hydroxyl radicals ($^{\bullet}OH$) (Malato et al., 2009). A broader definition of AOPs also includes the techniques that involve oxidants such as $SO_4^{\bullet-}$ and $Cl^{\bullet}$ (Sun et al., 2012; Tan et al., 2011). The major areas in which research is undertaken on the photocatalytic degradation of contaminants in water are the Fenton process (Clarizia et al., 2017; Rahim Pouran et al., 2015; Herney-Ramirez et al., 2010; Pera-Titus et al., 2004; Babuponnusami and Muthukumar, 2014) and TiO_2 photocatalysis (Pelaez et al., 2012; Kumar and Devi, 2011; Sin et al., 2012; Zaleska, 2008; Mccullagh et al., 2007; Fagan et al., 2016; Ola and Maroto-Valer, 2015).

The history of Fenton reaction began in 1894 when H.J.H. Fenton performed a reaction with iron ions and oxidizing agents. He observed a higher oxidative capacity of the mixture in comparison to its components (Koppenol, 1993). Even though the Fenton reaction was initially formulated for Fe(II) and H_2O_2 many redox-active metals such as Cu, Mn, and Ni also display Fenton-like reactions (Masarwa et al., 1988; Goldstein et al., 1993).

The general mechanism of the Fenton process can be represented as follows.

$$Fe(II)+H_2O_2 \rightarrow Fe(III)+{}^{\bullet}OH+OH^- \quad k = 40–80\ M^{-1}\ s^{-1} \tag{1}$$

$$Fe(III)+H_2O_2 \rightarrow Fe(II)+HO_2^{\bullet}+H^+ \quad k = 0{\cdot}001–0{\cdot}01\ M^{-1}\ s^{-1} \tag{2}$$

$$\text{Organic matter}+{}^{\bullet}OH \rightarrow \text{degradation products} \tag{3}$$

Hydrogen peroxide reacts with Fe(II) to generate $^{\bullet}OH$. However, it is a challenging task to recover the Fe(II) (Eq. 2) because of the inherently

* Corresponding author at: Nanotechnology and Bio-engineering Research Group, Department of Environmental Science, Institute of Technology Sligo, Sligo, Ireland.
E-mail address: pillai.suresh@itsligo.ie (S.C. Pillai).

https://doi.org/10.1016/j.jhazmat.2020.124082
Received 11 July 2020; Received in revised form 18 September 2020; Accepted 21 September 2020
Available online 2 October 2020

slow Fe(III) to Fe(II) reduction kinetics (Wang, 2008). Studies report that a Fenton reaction proceeds through a non-radical iron(IV)-oxo ($Fe^{IV}O)^{2+}$ species, but its mechanism awaits a proper experimental validation (Gonzalez-Olmos et al., 2011; Shen et al., 1992; Chen, 2019). Also, various studies illustrate the use of electrical energy (Nidheesh and Gandhimathi, 2012; Li et al., 2018; Plakas et al., 2016) and light energy (Feng et al., 2006) in speeding up the regeneration of Fe(II) in the Fenton reaction (Zhang et al., 2007; Rubio et al., 2013; Lin et al., 2014).

Since sunlight can accelerate the Fenton process, it is explored as a cheap alternative. Here, $[Fe(OH)]^{2+}$ is the crucial photoactive Fe(III) complex under solar light and is predominantly present at low pH of 2.8. In the presence of light irradiation, $[Fe(OH)]^{2+}$ species get reduced to Fe (II), and that in turn generates further $^{\bullet}OH$ and enhances the contaminant degradation.

$$[Fe(OH)]^{2+}+h\nu \rightarrow Fe(II)+{}^{\bullet}OH \quad (4)$$

The most desirable pH for the homogeneous photo-Fenton reaction is reported to be 2.8 (Clarizia et al., 2017). Even though photo-Fenton reactions are highly efficient in oxidising different contaminants, a pre and post-treatment of water is required to perform the reaction at pH 2.8. Also, when the pH of the solution is increased to neutral, that leads to iron sludge precipitation as iron hydroxides (Giannakis et al., 2016). The major pitfalls associated with the homogeneous photo-Fenton reaction is its narrow pH range and the need to remove iron sludge after the reaction; both these add up to the cost of water treatment. However, the heterogeneous photo-Fenton reaction can perform the water treatment at around neutral pH (Soon and Hameed, 2011). So advanced methods, or materials are warranted for performing the reaction at circum-neutral pH (O'Dowd and Pillai, 2020). Therefore, the development of low cost, efficient, visible-light responsive materials for performing the Fenton reaction at around neutral pH is an active area of research in AOPs (Lv et al., 2010; Hou et al., 2013). There are different techniques employed for achieving this target. In the current review, various advanced materials developed for Fenton and photo-Fenton processes are discussed. The readers are redirected to other reviews for a detailed understanding of the reactor design, usage of chelates *etc* (O'Dowd and Pillai, 2020; Ganiyu et al., 2018; Wang et al., 2016; Babuponnusami and Muthukumar, 2014; Clarizia et al., 2017).

2. Mechanism of reactive oxygen species (ROS) formation and disinfection

Illumination of semiconductors such as iron oxides, TiO_2, ZnO etc. with light having energy equal or higher than the bandgap of the material leads to the formation of electrons and holes (Lee and Park, 2013). Those photo-induced electrons (excited from the valence band to the conduction band) transfer to an acceptor molecule and the molecule undergoes reduction. At the valence band, the generated hole (electron vacancy) receives an electron from a molecule which is adsorbed to the system, and that molecule gets oxidised. In the O_2 atmosphere, generally O_2 acts as an acceptor molecule and generates the superoxide anion ($O_2^{\bullet-}$). Also, the adsorbed hydroxyl groups (OH^-) capture the holes to produce hydroxyl radicals ($^{\bullet}OH$). Similarly, many organic moieties will get oxidised to other smaller compounds. Various reactive oxygen species (ROS) have different capacity for oxidation and selectivity. The $^{\bullet}OH$ and $O_2^{\bullet-}$ are the two dominant reactive oxygen species involved in the Fenton reaction (Cai et al., 2016; He et al., 2016; Wang et al., 2020c). The $^{\bullet}OH$ with a half-life of 10^{-9} s and high reduction potential (+2.80 V vs SCE, $^{\bullet}OH/H_2O$; under acidic conditions) is the most reactive oxygen species involved (Feng et al., 2018; He et al., 2016). Since $^{\bullet}OH$ are short-lived, it is generally produced in-situ by the illumination of UV light on H_2O_2 or O_3 (Cho et al., 2010; Hodges et al., 2018). It is also possible to generate the H_2O_2 through the photo electrocatalytic mechanism, and that in-situ generated H_2O_2 can take part in the Fenton reaction and produce $^{\bullet}OH$. The $^{\bullet}OH$, which is the most active ROS, also has the capacity to disrupt the cell wall of microorganisms and can perform disinfection of water. One of the hindrances associated with $^{\bullet}OH$ based disinfection is the scavenging of $^{\bullet}OH$ by natural organic matter (NOM) present in the wastewater, which may diminish the efficiency of wastewater disinfection (Brame et al., 2014).

At the initial stages of the development of photo-Fenton reaction, it was thought to be impractical to acidify the wastewater to perform the disinfection and removal of contaminants (Giannakis et al., 2016). As time progressed, researchers came up with the photo-Fenton methods of performing the disinfection of *Escherichia coli* (*E. coli*) at around neutral pH (Ruales-Lonfat et al., 2014; Rincon and Pulgarin, 2006; Spuhler et al., 2010; Rodriguez-Chueca et al., 2014). The mechanism of disinfection of microorganisms through a heterogeneous catalyst can occur through two pathways. At first, the normal semiconductor action resulting in the formation of electron-hole pairs and then to the creation of $^{\bullet}OH$. The $^{\bullet}OH$ formation can also occur via the photo-Fenton action of H_2O_2 and Fe(II). A simplified summary of the mechanism of disinfection is given in Fig. 1. The complexity of the cell wall of microorganisms can be related to their capacity to get inactivated by photocatalytic action. As the complexity of cell wall increases, it needs either harsh conditions or longer exposure time for the complete disinfection. The resistance level of different classes of bacteria and viruses towards various disinfectants are compared in Fig. 2. Due to the unique barrier properties of the outer membrane of gram-negative bacteria, it is observed to be more tolerant to disinfectants compared to the gram-positive bacteria. In case of viruses, enveloped viruses (e.g. SARS-CoV-2) seem to be more susceptible to disinfectants than the non-enveloped viruses (Chu et al., 2019). Enveloped viruses consist of three building blocks; genetic material (DNA, RNA), protein capsid, and lipid bilayer. Non-enveloped viruses lack the outer lipid bilayer membrane (Holland Cheng et al., 1995). In general, disinfectants act on the lipid bilayer membrane of the enveloped viruses and deactivate the viruses (Chu et al., 2019). $^{\bullet}OH$ generated by solar photo-Fenton processes are capable of inactivating viruses by photo-oxidation of capsid protein (Giannakis et al., 2016).

3. Mechanism of heterogeneous Fenton catalysis

Iron-based materials are usually treated as superior heterogeneous Fenton catalysts because of their low cost, negligible toxicity levels, high catalytic activity and easy methods for recovery (Pereira et al., 2012; Nidheesh, 2015; Fu et al., 2014; Garrido-Ramírez et al., 2010; Rahim Pouran et al., 2014). A heterogeneous Fenton system can generate the $^{\bullet}OH$ by two methods. Either it could be the true heterogeneous catalytic mechanism or the homogeneous Fenton reaction occurring because of the leached iron from the solid catalyst (He et al., 2016). In 1998 Lin and Gurol (1998) proposed the widely accepted mechanism of heterogeneous catalytic decomposition of H_2O_2 by studying the reactions of H_2O_2 on the solid iron oxide catalyst (goethite).

$$\equiv Fe^{III}\text{-}OH+H_2O_2 \leftrightarrow (H_2O_2)_s \quad (5)$$

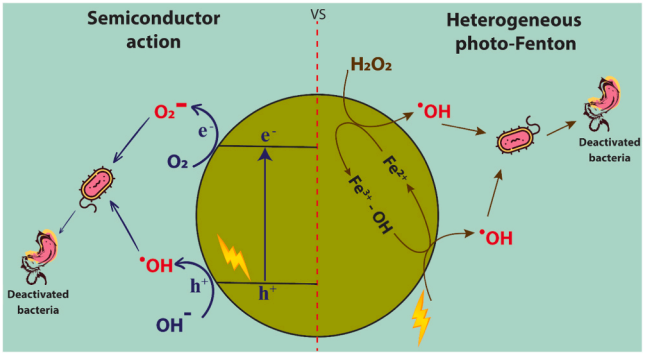

Fig. 1. Schematic illustration depicting the photo-assisted semiconductor action and heterogeneous photo-Fenton action of bacterial inactivation.

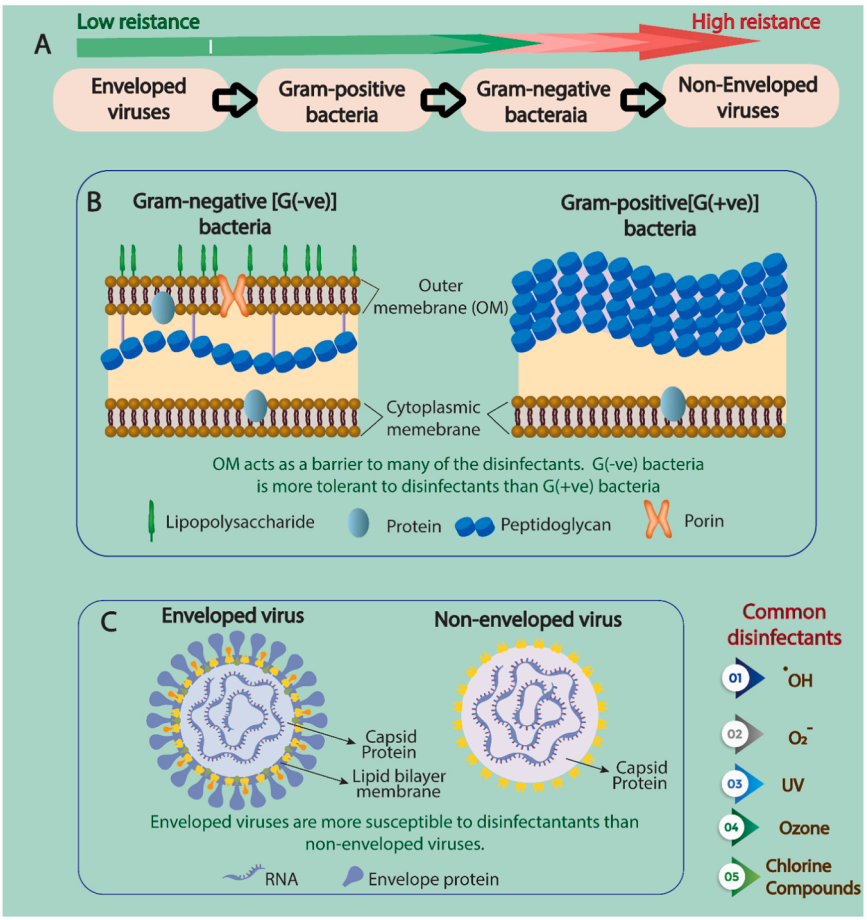

Fig. 2. (a) An arrangement of infectious agents according to their resistance towards disinfectants. Comparing the resistance level of two different classes of bacteria (b) and viruses (c) to withstand disinfectants.

$$(H_2O_2)_s \leftrightarrow (\equiv Fe^{II}{}^{\bullet}O_2H) + H_2O \quad (6)$$

$$(\equiv Fe^{II}{}^{\bullet}O_2H) \rightarrow \equiv Fe^{II} + HO_2^{\bullet} \quad (7)$$

$$\equiv Fe^{II} + H_2O_2 \rightarrow \equiv Fe^{III}\text{-}OH + {}^{\bullet}OH \quad (8)$$

In the mechanism, the symbol ≡ Fe^{III} represents the iron present on the surface. Here the interaction of H_2O_2 at the goethite surface (≡Fe^{III}-OH) forms the complex $(H_2O_2)_s$ (Eq. 5). Then a ligand to metal charge transfer leads to the formation of a transition state complex (≡ Fe^{II} $^{\bullet}O_2H$) (Eq. 6). Subsequently, the complex dissociates and forms hydroperoxyl radical (Eq. 7), and later $^{\bullet}OH$ is generated in the presence of ≡Fe^{II} and H_2O_2. (Eq. 8). The mechanism depicts the recycling of Fe (III) and Fe (II) on the surface, so here goethite is treated as a heterogeneous catalyst.

Apart from the pure heterogeneous Fenton process, the iron leached out from the solid catalyst enhances the reaction rate by homogeneous Fenton pathway (Ramirez et al., 2007; Wang et al., 2010; Hartmann et al., 2010). Zeng and Lemley (2009) reported the leaching of iron from amberlyst-15 ion-exchange resin while studying the kinetic modelling of degradation of the herbicide 4,6-dinitro-*o*-cresol (DNOC). Also, a faster rate of degradation of DNOC was observed during the addition of hydrochloric acid owing to the higher amounts of the leached ferrous ion at lower pH values. In another study, FeO_x supported on $CuFe_2O_4$ and TiO_2 was used as model systems for understanding the role of leached iron species in the heterogeneous Fenton reaction. This study pointed out that the methods such as gravimetry, X-ray fluorescence and energy dispersive X-ray analysis are not sensitive enough to account for the low metal ion leaching from the heterogeneous Fenton catalyst (Kuan et al., 2015). So, they have monitored the 4-chlorophenol (4-CP) degradation using inductively coupled plasma optical emission spectroscopy (ICP-OES) and UV–vis spectroscopy under continuous pH monitoring. Time-dependent leaching of metal ions was observed with the pH variations, and even μM/sub-ppm concentrations of dissolved metal ions were responsible for the increase in degradation rate of 4-CP in the heterogeneous Fenton system.

4. Various Fe-based materials related to the Fenton process

4.1. Iron-oxide based Fenton catalysts

Iron oxides are generally considered to be biodegradable, non-toxic and environmentally friendly (Nidheesh, 2015; Pouran et al., 2014; Ruales-lonfat et al., 2015a; Xu et al., 2012). Usually, the physical properties of synthesised materials are dependent on their specific surface area, particle size, morphology etc. and these properties vary greatly based on their synthesis strategies. Some of the popular methods adopted for the synthesis of iron-based materials include solvothermal procedure, hydrothermal procedure, thermal decomposition, micro-emulsion process and co-precipitation method (Nidheesh, 2015). Until now, sixteen pure faces of oxides, hydroxides and oxy-hydroxides are reported in the literature (Giannakis et al., 2016; Usman et al., 2018).

Iron oxides have the potential to act as photo-catalysts because of their semiconducting properties. The possible semiconducting mechanism of iron oxides can be detailed as follows (Cai et al., 2016; Ruales-Lonfat et al., 2015a).

$$\text{Iron Oxide} + h\nu \rightarrow \text{Iron Oxide } (h^+ + e^-) \quad (9)$$

$$e^-(cb) + O_2 \rightarrow O_2^{\bullet -} \quad (10)$$

$$h^+(vb)+H_2O \rightarrow H^+ + {}^\bullet OH \quad (11)$$

$$h^+(vb)+OH^- \rightarrow {}^\bullet OH \quad (12)$$

$$H_2O_2 + e^- \rightarrow {}^\bullet OH + OH^- \quad (13)$$

$$Fe(III) + e^- \rightarrow Fe(II) \quad (14)$$

Upon light irradiation, the heterogeneous Fenton reaction gets enhanced by the production of Fe(II) from the reduction of Fe(III) to Fe (II).

$$Fe(III)+h\nu+OH^- \rightarrow Fe(II)+{}^\bullet OH \quad (15)$$

Also on the particle surface, $^\bullet$OH is generated by the heterogeneous Fenton reaction between Fe(II) and H_2O_2 (Eq. 1). Later the $^\bullet$OH reacts with organic matter leading to their degradation (Eq. 3).

In the iron oxide systems, the ferrous ion is part of the crystal system of oxides. This feature enhances the stability of the catalyst towards the splitting of H_2O_2, and thus the leaching of ferrous ions from the catalyst is reduced. Magnetite (Munoz et al., 2015; Zubir et al., 2015; Du et al., 2017; Nguyen et al., 2017; Nidheesh et al., 2014; Costa et al., 2006), ferrihydrite (Zhu et al., 2018; Xu et al., 2017; Xu et al., 2016b; Zhang et al., 2014; Zhu et al., 2018), hematite (Pradhan et al., 2013; Patra et al., 2016; Jaramillo-Paez et al., 2017; Chen et al., 2016; Huang et al., 2016), goethite (Xu et al., 2016c; Wang et al., 2017; Hou et al., 2017; Krumina et al., 2017; Jin et al., 2017; Qian et al., 2018), schwertmannite (Duan et al., 2016; Yang et al., 2016; Wang et al., 2013), lepidocrocite (He et al., 2017; Sheydaei et al., 2014), and maghemite (Wang et al., 2008; Ma et al., 2018) are some of the classes of iron minerals utilised as Fenton-catalysts. The recent developments regarding these heterogeneous Fenton catalysts are discussed in the upcoming sections.

4.1.1. Ferrihydrite and plasmonic systems

Ferrihydrite (Fh) is a naturally occurring iron oxyhydroxide mineral used as a Fenton catalyst because of its large specific surface area (Liu et al., 2010; Zhang et al., 2014). In some of the recent studies Ag/AgBr/ferrihydrite (Ag/AgBr/Fh) and Ag/AgCl/ferrihydrite (Ag/AgCl/Fh) was established as heterogeneous Fenton catalysts (Zhu et al., 2018a, 2018b). AgBr is a semiconductor which absorbs light in the visible region (bandgap of 2.6 eV). Ag nanoparticles absorb visible light because of their surface plasmon resonance (SPR) effect. Here, by introducing Ag/AgBr/Fh hybrid system, the study demonstrates the direct injection of electrons from the Ag/AgBr to the ferrihydrite (Zhu et al., 2018b). On the ferrihydrite surface, electrons help in the regeneration of Fe(II) which leads to an enhancement in catalytic degradation of bisphenol A (BPA, is an endocrine disruptor and one of the emerging contaminants of concern present in drinking water (Rubin, 2011).). Since the electrons from catalyst are directly performing the recycling of Fe(II), the reaction is also efficient in terms of the amount of H_2O_2 consumed. XPS analysis was employed to determine the chemical state of different elements present in the catalyst such as Fe, O, Ag and Br (Zhu et al., 2018b). The peak at 711.72 eV in the Fe 2p spectrum was attributed to the Fe(III) coordinated to the oxygen on Fh. In Ag 3d spectra two peaks at 368.5 and 374.5 eV values represent the silver in the zero-oxidation state, and the peaks at 367.9 and 373.9 eV were associated with the Ag^+ in AgBr (Zhu et al., 2018b). In a similar study, Ag/AgCl/Fh hybrid catalyst also demonstrated BPA degradation (Zhu et al., 2018a). Ag/AgCl/Fh was synthesised by an impregnation-precipitation strategy followed by a photo-reduction under UV light. The rate of degradation of BPA by six percentage Ag/AgCl/Fh (6% weight ratio of Ag added to Fh) was measured to be 0.0506 min^{-1} which is about five times the rate of pure Fh ($k = 0.0099\ min^{-1}$).

Another strategy to enhance the rate of regeneration of Fe (II) is to introduce electrons from semiconductors to the heterogeneous Fenton catalyst. In another study, a $BiVO_4$/ferrihydrite ($BiVO_4$/Fh) system was synthesised to understand the decolourisation efficiency of acid red-18 at near-neutral pH (Xu et al., 2017). EPR spectrum showed that the introduction of $BiVO_4$ to the ferrihydrite enhanced the generation of $^\bullet$OH. XPS studies and 1,10-phenanthroline spectrophotometric method concluded the increase in the concentration of Fe(II) on the surface of the $BiVO_4$/Fh. Furthermore, enhanced H_2O_2 consumption was observed for $BiVO_4$/Fh system compared to the pure ferrihydrite. This was rationalised by the Fe(II) regeneration on the surface, by the photo-generated electrons from $BiVO_4$. Similarly, a 15% doped composite of cerium oxide (CeO_2) and Fh showed 98.7% degradation of tetracycline antibiotic (Huang et al., 2020). Here, the mechanism details the critical role of Ce^{4+}/ Ce^{3+} cycle in helping the regeneration of Fe(II). Furthermore, 7%TiO_2/Fh nanohybrid depicted the efficient removal of cefotaxime antibiotic under UV light (Jiang et al., 2019).

In a recent report, a composite material of oxidised multi walled carbon nanotubes (CNTs) and ferrihydrite (CNTs/Fh) was prepared and evaluated in the degradation of BPA (Zhu et al., 2020). A 3% CNTs/Fh system depicted seven times higher efficiency compared to simple Fh in degrading the pollutant. Cyclic voltammetry (CV) studies revealed a 14 mV lowering of half-wave potential ($E_{1/2}$) of CNTs/Fh (0.827 V vs. RHE) compared to Fh (0.841 V vs. RHE) revealing the fast reduction of Fe (III) (thermodynamic aspect). Also, the effective transfer of electrons from H_2O_2 to Fh was considered as the dynamic aspect of the increase in the rate of Fenton reaction. The possible mechanism deduced from DFT calculations, and CV characterisation is summarised in Fig. 3.

4.1.2. Ferrites and magnetite

Transition metal-doped iron oxides with a spinel structure are normally named as ferrites. They have a general formula of $M_xFe_{3-x}O_4$ (M is a bivalent transition metal ion) with a face-centred cubic lattice formed by oxide ions. Among the different iron-based materials tested as heterogeneous photo-Fenton catalysts, the ferrites are of particular interest because of their narrow bandgap (1.9 eV, for $ZnFe_2O_4$) and high stability (Sharma et al., 2015; Hou et al., 2013; Valdés-Solís et al., 2007; Wang et al., 2014). Ferrites are preferred as heterogeneous Fenton catalysts because of their easiness in recovery and reuse owing to their magnetic properties (Laurent et al., 2008; Polshettiwar et al., 2011; Sharma and Singhal, 2015). Ferrites are chemically stable (Yang et al., 2013), and because of their narrow bandgap, they are also active catalysts under visible light (Wang et al., 2011). Sharma and Singhal (2015) demonstrated the synthesis of magnetic nano-spinel having formula MFe_2O_4 (M=Cu, Zn, Ni and Co) using a sol-gel method. Among all the four ferrites, $CuFe_2O_4$ was found to be best ($k = 0.228\ min^{-1}$) for the degradation of azo dye RB5, which was attributed to the coupling between Fe^{3+}/Fe^{2+} and Cu^{2+}/Cu^+ redox pairs leading to the efficient production of more $^\bullet$OH radicals. Similar studies also reported the use of copper ferrites for gallic acid removal (Fontecha-Cámara et al., 2016), degradation of sulfonamide antibiotic (Gao et al., 2018), and antibacterial therapy (Liu et al., 2019). Fontecha-Cámara et al. (2016) studied three commercially available iron oxides; copper ferrite, magnetite

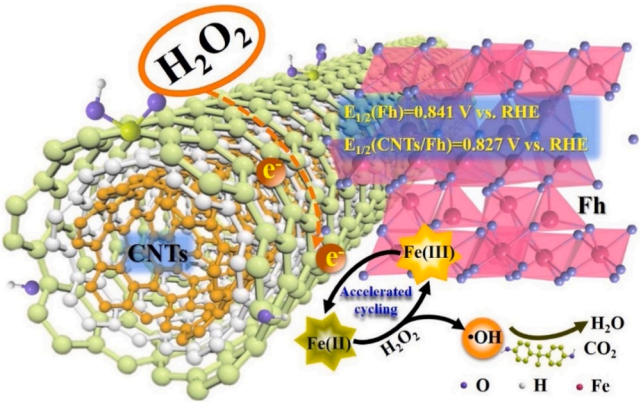

Fig. 3. Scheme showing the electron transfer process and the BPA degradation in CNTs/Fh composite. Copyright (2020), Elsevier.
Reproduced with permission from ref (Zhu et al., 2020).

and ilmenite ($FeTiO_3$) for the removal of gallic acid and the highest catalytic activity was displayed by copper ferrites. Cu^{2+} occupied the octahedral site of the copper ferrite spinel, and the collective effect of iron and copper ions significantly improved the rate of Fenton reaction by generating more $^{\bullet}OH$ radicals. In another study, $ZnFe_2O_4$ was synthesised from precursors such as $Fe(NO_3)_3$ and $Zn(NO_3)_3$ through a hydrothermal treatment procedure and depicted the visible light degradation of orange II (Cai et al., 2016). Experiments performed with various radical scavengers such as *tert*-butanol, sodium oxalate and *iso*-propanol showed that $^{\bullet}OH$ generated on the surface was the key species responsible for the degradation. A generalised scheme of the mechanism of generation of $^{\bullet}OH$ and the regeneration of Fe(II) on the surface of ferrites is summarised in Fig. 4. The stability of the catalyst was understood by performing multiple runs with the recycled catalyst. After the first cycle, the reaction rate constant was observed to be 0.0468 min^{-1}. Even after five cycles, the catalyst showed a similar reaction rate constant ($k = 0.0483\ min^{-1}$). Also, the amount of H_2O_2 decomposed by the catalyst during the five cycles was equivalent. Invariably all these indicate the reusability of the catalyst. Xiang et al. (2020) prepared $ZnFe_2O_4$ nanoparticles having yolk-shell structure and evaluated in the degradation of tetracycline under visible light. The yolk-shell structured $ZnFe_2O_4$ nanoparticles had a higher specific surface area and presented better visible light absorption capacity in comparison to the spherical $ZnFe_2O_4$ nanoparticles. The higher visible light absorption was correlated to the possibility of multi-scatterings of light in the inner yolk-shell structure of $ZnFe_2O_4$.

Later, Hermosilla et al. (2020) reported an environmentally friendly synthesis of manganese ferrites (Mn–Fe_2O_4) via routes such as sol-gel, combustion and reverse microemulsion. Bio-recalcitrant compounds such as ciprofloxacin (a fluoroquinolone antibiotic) (Davis et al., 1996) and carbamazepine (anti-depressive drug) (Ballenger and Post, 1980) were successfully degraded by the photo-Fenton action of visible light active Mn–Fe_2O_4. The magnetisation is one of the crucial characteristics of a material for its separation and reusability. α-Fe_2O_3 (hematite) is reported as a weak ferromagnet, and its content has a trivial contribution to the magnetisation of the material (Raming et al., 2002). Here, the magnetisation value of the sol-gel synthesised Mn–Fe_2O_4 came to be 41.0 emu g^{-1} and the lowest value was reported for Mn–Fe_2O_4 synthesised by reverse microemulsion route (3.7 emu g^{-1}). The relative content of α-Fe_2O_3 was lowest in the sol-gel Mn–Fe_2O_4, and it was associated with its higher values of magnetisation.

Some of the recent studies report the use of magnetite (Fe_3O_4) or its composites for disinfection of *E. coli* in water (Tong et al., 2020; Feng et al., 2019; Arshad et al., 2019). A composite material of Fe_3O_4 and flower-like MoS_2 (Fe_3O_4/MoS_2) effectively inactivated *E. coli* up to six log scale within 30 min (Tong et al., 2020). The Fe_3O_4/MoS_2 was active at a broad pH from 3.5 to 9.5, and the catalyst could be separated magnetically owing to its saturation magnetization value of 40.6 emu g^{-1}. Similarly, a graphene composite of Fe_3O_4 was successful in inhibiting the growth of *Pseudomonas aeruginosa* and *S. aureus* (Tong et al., 2020). Wang and co-workers developed a therapeutic approach by combining the copper ferrite antibacterial therapy with photothermal therapy (PTT) (Liu et al., 2019). The hydrothermally prepared haemoglobin functionalized copper ferrite nanoparticle (Hb-CFNPs), effectively generated the $^{\bullet}OH$ and initiated the cell membrane disruption. Further shining 808 nm laser light (near-Infrared, NIR) increased the cell membrane permeability by hyperthermia and resulted in leakage of bacterial contents. *In-vitro* experiments revealed the broad-spectrum antibacterial activity over the *E. coli* (100% removal), and *S. aureus* (96.4% removal) bacteria and the therapeutic method showed significant results in the *S. aureus* infected abscess treatment. The coupling between Fe^{3+}/Fe^{2+} and Cu^{2+}/Cu^{+} redox pairs catalysed the production of $^{\bullet}OH$ and promoted the oxidative damage of bacterial cells. A brief illustration of the synthetic strategy and the therapeutic application of Hb-CFNPs is outlined in Fig. 5.

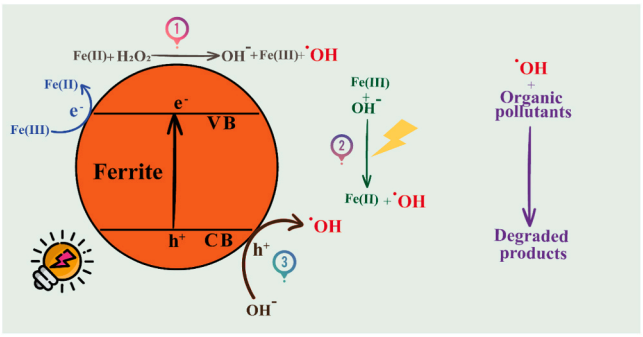

Fig. 4. The schematic illustration of photo-Fenton degradation of organic pollutants by the ferrites upon visible light irradiation. Three specific pathways leading to $^{\bullet}OH$ generation are highlighted with numbers 1–3.

4.1.3. Other major classes of iron minerals

There are various reports of the application of iron oxide family of materials for wastewater treatment and microbial inactivation (Nieto-Juarez and Kohn, 2013; Pecson et al., 2012; Xu et al., 2012). In 2015, Ruales-Lonfat et al. (2015b) studied the microbial inactivation efficiency of four commercially available iron oxides. Hematite, goethite and wustite used O_2 as electron acceptor and performed the photocatalytic activity even in the absence of H_2O_2. However, the magnetite was only active in the presence of H_2O_2. It is important to note that no bacterial growth was observed after the photo-Fenton treatment. These results are very significant because excluding H_2O_2 from the reaction decreases the cost of the water treatment to a great extent. The concentration of the catalyst used was 0.6 mg/L Fe^{3+}, and iron concentration similar to this scale is usually observed in natural water sources. This seems to be a useful strategy in a large-scale application for bacterial inactivation.

Size and morphology of the nanomaterials have a significant correlation with the physical and chemical characteristics exhibited by them (Mai et al., 2005; Kundu and Jayachandran, 2013; Xie et al., 2013). Hematite (α-Fe_2O_3) having morphology such as microtubes, nanorods, nanorings are reported in the literature (Xiong et al., 2011; Vayssieres et al., 2005; Hu et al., 2007). Xiao et al. (2018) studied the morphological evolution of

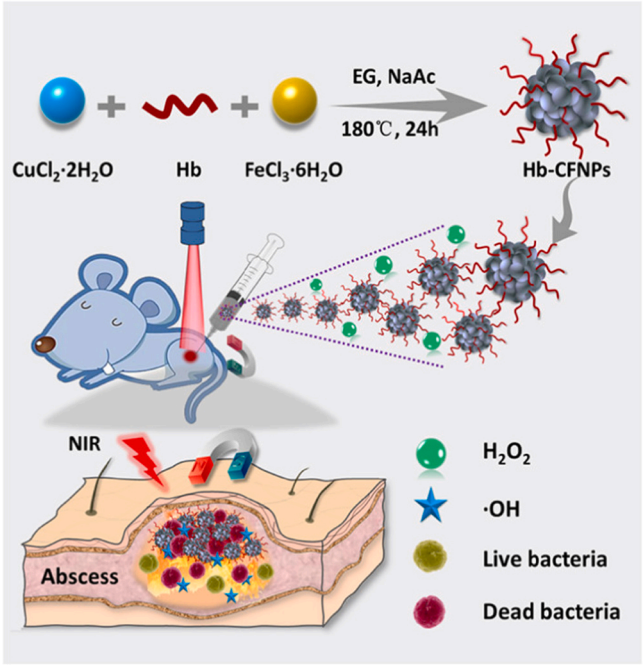

Fig. 5. Schematic representation of preparing Hb-CFNPs and the synergistic antibacterial action by Fenton reaction followed by NIR irradiation. Copyright (2019), American Chemical Society.
Reproduced with permission from ref (Liu et al., 2019).

hematite by adjusting the hydrothermal reaction time. After 6 h of hydrothermal treatment, the nanoparticles attained a spherical morphology, and upon further heating, elliptical, olive-like and burger-like morphologies were observed at 12, 18, 24 h, respectively. Burger-like α-Fe_2O_3 was found to be better in the removal of acid red G in comparison to other morphologies of α-Fe_2O_3, and a 98% degradation efficiency was observed under visible light within 90 min.

Recently, a composite material of schwertmannite/graphene oxide (SCH/GO) was synthesised through an oxidation-co-precipitation route and demonstrated removal of tetracycline antibiotic under visible light. The photo-Fenton catalytic tests were performed in real wastewater matrices such as raw food wastewater and biogas fluid of anaerobically digested food. The SCH/GO nanocomposite was efficient in selectively degrading the tetracycline in the presence of a comparable concentration of moieties such as chlorides, sulfates, phosphates and nitrates. The SCH/GO system showed fifteen times higher rate constant of tetracycline degradation compared to the SCH, because of its improved optical absorption property and separation of electron-hole pairs (Ma et al., 2020).

Similar to the Fenton reaction in the presence of H_2O_2, Fe(II/III)-oxalate system also reported having the superior capacity to degrade organic pollutants (Wei et al., 2013; Liu et al., 2012; Lan et al., 2008). A $FeWO_4$ nanosheet material synthesised by a hydrothermal method showed facet dependent surface Fenton chemistry in the presence of oxalic acid (Li et al., 2019). Density functional theory (DFT) studies concluded that the {001} facets were efficient in producing reactive oxygen species in comparison to {010} facets. Also, DFT analysis confirmed that $^{\bullet}OH$ generated on the {001} facets diffused faster to the solution and kept the {001} facets vacant for the continuous activation of oxalic acid molecules into radicals.

4.2. Catalyst loaded on materials

Apart from directly employing various iron minerals as heterogeneous Fenton catalysts, iron minerals can be incorporated into numerous supporting materials like zeolites (Soon and Hameed, 2011; Nidheesh, 2015; Hartmann et al., 2010), metal-organic frameworks (MOFs) (Liu et al., 2017; Cheng et al., 2018), clays (Garrido-ramírez et al., 2010; Navalon et al., 2010), graphene oxide (GO) (Nidheesh, 2017; Wang et al., 2019), silica (Gan and Li, 2013; Zhong et al., 2011) etc. Some of the desirable properties needed for the supporting materials for holding the iron-based catalysts for photo-Fenton reaction can be their ability to perform the reaction for multiple cycles and the lesser leaching of the Fe ions. Moreover, they need to be durable against highly reactive radicals. In this section, recent reports on various supporting materials for heterogeneous Fenton processes and their desirable properties are discussed.

4.2.1. Clay-based catalysts

The incorporation of iron into clays can be performed by pillaring (Guimarães et al., 2019; Tabet et al., 2006), impregnation (Herney-Ramirez et al., 2008; Hassan and Hameed, 2011) etc. Generally, inorganic supporting materials provide thermal stability, resistance to organic solvents and high mechanical strength (Cheng et al., 2006).

4.2.1.1. Pillared clays. Clay materials are abundantly present in the earth crust, but they may not be used as excellent Fenton catalysts because of their low iron content in them. Even though the layered clay materials have a large surface area, their interlamellar space is mostly inaccessible because of higher electrostatic interaction present between the layers (Garrido-ramírez et al., 2010). These shortcomings are circumvented by pillaring of clays. Among the different clay materials, pillared clays are of special interest because of their catalytic and adsorption properties. Through the pillaring process, (stacking and then connecting the 2D layers) various large-sized poly oxo-hydroxy metal cations are incorporated into the structure of clays by replacing the smaller ions (Aznarez et al., 2015; Nogueira et al., 2011). This process makes the interlamellar space accessible for the reactants and leads to a significant increase in the porosity and surface area of the material. Pillaring process also exposes some of the catalytic sites, and additional catalytic sites are added in case iron compounds make the pillars (Navalon et al., 2010). Since the crystal structures and other characteristic properties of the pure clay materials are well-defined, the difference in catalytic activity mainly arises from the pillars incorporated (Baloyi et al., 2018). Further, the Fe(III) species can be considered as immobilised in the interlayer spacing of pillared clays. So, the ion species is stable against the differences in solution pH, and that results in limited leaching of iron (Herney-Ramirez et al., 2010). There are various reports of the use of pillared clays for the degradation of dyes (Li et al., 2015; Ayari et al., 2019), pharmacologically important compounds (Hurtado et al., 2019; Khankhasaeva et al., 2017), and phenolic compounds (Hadjltaief et al., 2015; Catrinescu et al., 2012). However, the applications of pillared clay-based systems in more complex matrices, especially those with heavy organic load, are rare in literature. Recently, the photo-Fenton activity of Al-Fe smectite pillared clay has been demonstrated for the treatment of winery wastewater with high amounts of recalcitrant polyphenolic compounds (Guimaraes et al., 2019). The catalyst was prepared by intercalating poly-hydroxy aluminium ($Al_3(OH)_4^{+5}$) and ($Fe_3(OH)_4^{+5}$) species between the layers of natural smectite. The photo-Fenton studies performed under UV-C light radiation resulted in a 75.2% percentage total organic carbon (TOC) removal of the winery wastewater. In another study, Xu et al. (2016b) used hydroxy-iron montmorillonite (Fe/Mt) as a host material, and $BiVO_4$ semiconductor was loaded into the interlayers of Fe/Mt. An 8% $BiVO_4$/Fe/Mt composite demonstrated an 85.2% TOC removal of acid red-18 under visible light irradiation. The remarkable $^{\bullet}OH$ generation capacity of the system was associated with the synergistic effect between $BiVO_4$ and Fe/Mt and the photo-induced injection of electrons from $BiVO_4$ to Fe(III) ions.

Similar to the examples of the addition of plasmonic systems with the ferrites, Ag/AgCl was impregnated onto sepiolite clay which was modified with hydroxy iron (Ag/AgCl/Fe-S) (Liu et al., 2017). This catalyst exhibited excellent activity in degrading BPA. Electrochemical impedance spectroscopy (EIS) was performed to understand the charge transfer resistance (CTR) and ease of separation of electron-hole pairs in the catalyst. In a three-electrode electrochemical system, 0.1 mol/L KCl was used as an electrolytic solution, and a glassy carbon electrode modified with prepared catalysts was employed as a working electrode. Several reports suggest that a lower charge transfer resistance can be correlated with facile separation of electrons and holes (Ganiyu et al., 2018). Here among the three catalytic systems studied, Ag/AgCl/Fe-S was reported with the lover CTR, and that corroborate the enhanced degradation of the BPA.

4.2.1.2. Layered double hydroxides (LDH). Layered double hydroxides (LDHs) are a class of clay-based materials having brucite-like sheet structures made of metal hydroxides (Gursky et al., 2006; Shao et al., 2013). Their intercalated anions/cations can be easily exchanged by cation exchange to alter their properties (Zhang et al., 2014; Zhang et al., 2012). The strong electrostatic interaction observed between the layers and interlayer anions provides a well-oriented structure for the LDHs (Zhang et al., 2020). This ordered layered structure endows the LDHs with plenty of sites for the interaction of pollutants and H_2O_2 (Jack et al., 2015). The general hydrophilic nature provided by the hydroxyl groups promotes distinct interaction of hydrophilic contaminants and H_2O_2 with the active catalytic sites on the surface (Yang et al., 2020). Bai et al. (2017) synthesised a Co/Fe LDH through a co-precipitation strategy and demonstrated the Fenton-like removal of nitrobenzene. The mechanism of the process was studied by an $^{\bullet}OH$ scavenger, and $^{\bullet}OH$ was identified to be the key radical involved. In another study, a Fe–Ni LDH was reused for the synthesis of a magnetic catalyst (Ni_3Fe/Fe_3O_4). Here, Fe–Ni LDH was treated with the orange II dye and heated under

nitrogen atmosphere to obtain the novel catalyst (Ni_3Fe/Fe_3O_4). The thermo-magnetic curves depicted the superior magnetic properties of the synthesised catalyst. In the past decade, there have been various reports of using copper-containing LDHs for the mineralisation of phenol, a major waste generated in the petrochemical industry (Zhang et al., 2010a, 2010b). But in those scenarios, the degree of mineralization of phenol was comparatively low, and the system utilized a higher dosage of H_2O_2. Even though many of the studies discuss the synergistic effect of copper with other metals present, yet studies concerning the in-depth understanding of phenol degradation mechanism remains unaddressed (Zhou et al., 2011). In a similar perspective, Wang et al. (2018) prepared a series of CuNiFe LDHs by varying the Cu/Ni ratios. The specific band observed in the Raman spectra at 460 cm^{-1}, and 533 cm^{-1} corresponds to the lattice vibration in LDHs. For the samples where the Cu/Ni ratio is higher than 0.5, a particular band is observed at 294 cm^{-1}, attributed to the $Cu(OH)_2$. The intensity of this band increases with the increase in Cu/Ni ratio. Experiments revealed that the catalytic activity (phenol mineralisation) increased upon decreasing the Cu/Ni ratio. It is remarkable to mention that, when the concentration of H_2O_2 was kept near the theoretical value ($M_{\text{Hydrogen peroxide}}/M_{\text{phenol}}$ =14) they observed mineralisation of 90% phenol. At lower Cu/Ni ratios, electron transferred from Ni^{2+} to Cu^{2+} and facilitated the generation of Cu^{+} species. Here Cu^{+} reacted with H_2O_2 in a Fenton like mechanism and produced the $^{\bullet}OH$. The mechanism is summarised in Fig. 6.

The large-scale applications of these materials vary depending upon the local availability of the particular clay materials. Currently, many of the Fenton related studies using clay materials concentrate on the degradation and mineralisation of dyes. Extensive research is needed to develop new catalysts with disinfection properties and the capacity for removal of antibiotics.

4.2.2. *Iron contained perovskites*

Perovskites are a class of ABX_3 compounds in which the X anion is mainly O^{2-} (Ferri and Forni, 1998; Zhu and Thomas, 2009). Perovskite compounds have a cubic geometry with A cation surrounded by 12 X anions, and B cation surrounded by 6 X anions (Smith et al., 2019; Quan et al., 2019). These compounds received their generic nomenclature from the mineral perovskite ($CaTiO_3$). In the last decade, ABO_3 perovskite family of oxides such as $EuFeO_3$ (Ju et al., 2011) , $LaFeO_3$ (Nie et al., 2015), $BiFeO_3$ (Rusevova et al., 2014; Luo et al., 2010) garnered a great deal of attention as heterogeneous photo-Fenton catalysts for the degradation of various organic pollutants. A nano-$BiFeO_3$ perovskite catalytic-system was demonstrated to have the degradation capacity of BPA. They have studied the capping action of various organic ligands such as oxalic acid (OA), formic acid (FA), glycine (Gly), nitriloacetic acid (NTA), and ethylenediaminetetraacetic acid (EDTA) on the nano-$BiFeO_3$ catalyst. Studies show that the EDTA_$BiFeO_3$ system was accelerating the BPA degradation and the efficiency of OA_$BiFeO_3$ system was lower than the bare $BiFeO_3$ catalyst (Wang et al., 2011). To further understand the system, density functional theory (DFT) studies were carried out on the OA_$BiFeO_3$ and EDTA_$BiFeO_3$ models. DFT studies gave the insight that unique hydrogen bonding interaction observed in the EDTA_$BiFeO_3$ catalyst was responsible for the weakening of the O-O bond and the generation of $^{\bullet}OH$ (Fig. 7).

In a recent effort, Cu-substituted $LaFeO_3$ perovskite was used for the degradation of BPA (Pan et al., 2020). Using a citric acid complexation method (Zhao et al., 2016), by altering the copper doping ratio they demonstrated the synthesis of novel Cu-substituted $LaFeO_3$ catalysts. The generation of oxygen vacancy in the Cu-substituted $LaFeO_3$ played a critical role in redistributing charge on the surface of the catalyst, and that helped the efficient decomposition of H_2O_2. The XRD phase evolution studies depicted that at calcination temperature of 700 ºC, the XRD spectrum became narrower and sharper. Also, the $LaFeO_3$ perovskite structure of $LaCu_xFe_{1-x}O_{3-\delta}$ solid solution was retained when the x values changed from 0.1 to 0.5. The peaks corresponding to Miller indices (121) and (240) got widened and the observed peak-offset was attributed to the lattice contraction of the crystal. Theoretical calculations showed an approximate 0.05-angstrom decrease in the Fe–O, and La–O bond lengths after copper substitution and that also portrays the volume contraction of the $LaCu_xFe_{1-x}O_{3-\delta}$ unit cell. These parameters undoubtedly suggested that copper got incorporated into the $LaFeO_3$ perovskite replacing Fe in the structure (Pan et al., 2020).

In a similar study, Cu-doped $LaFeO_3$ was used as a visible-light active catalyst for the photo Fenton degradation of methyl orange (To et al., 2018). The performance of 15 mol% Cu-doped catalyst was better than that of pure $LaFeO_3$ catalyst. In another study, Cu-doped $BiFeO_3$ was synthesised by a sol-gel method, and it depicted the degradation of 2-chlorophenol under visible light (Soltani and Lee, 2017). In the above cases of copper doping, along with Fe(II), Cu(I) was also acting as an active species in a Fenton like manner in splitting the H_2O_2 to $^{\bullet}OH$. In a different study, Chu et al. (2018) used the Ag-doped $LaCaFeO_{3-\delta}$ (Ag-$LaCaFeO_{3-\delta}$) perovskite as a peroxymonosulfate (PMS) activating agent for the effective removal of bacterial pathogens. EIS studies have suggested an increase in lattice oxygen vacancies in Ag-$LaCaFeO_{3-\delta}$ than $LaCaFeO_{3-\delta}$. A synergistic effect of free radicals ($SO_4^{\bullet-}$ and $^{\bullet}OH$) and silver ions towards the bacterial inactivation was observed. The studies demonstrated the antimicrobial effect of the catalyst on the *E. coli* and *S. aureus* (a methicillin antibiotic-resistant bacteria). The study also

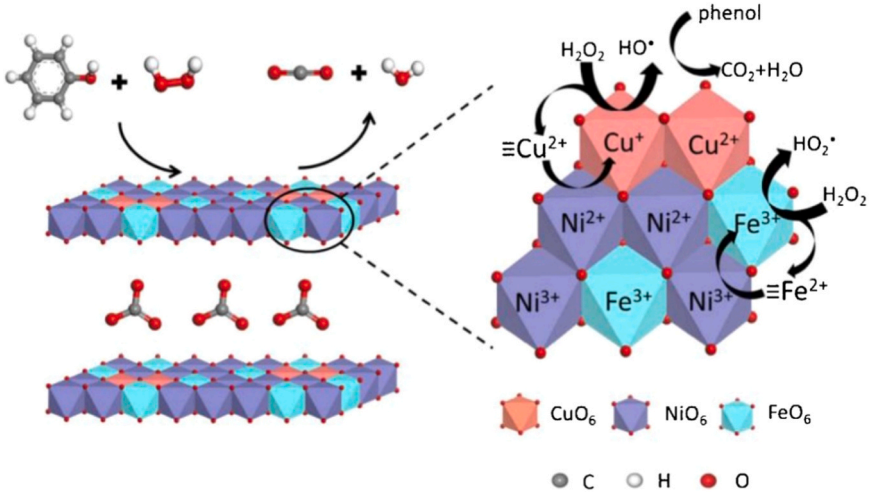

Fig. 6. Schematic representation of phenol mineralisation by the CuNiFe layered double hydroxides. Copyright (2018), Elsevier. Reproduced with permission from ref (Wang et al., 2018).

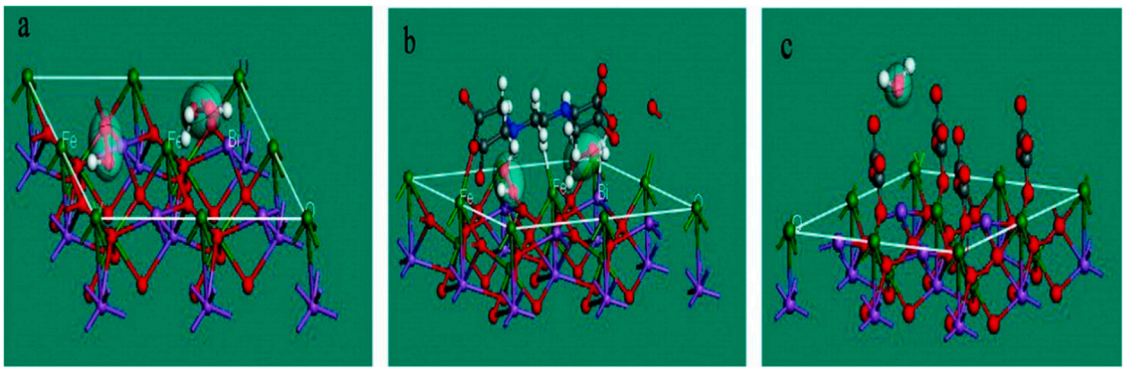

Fig. 7. Various configurations of the H_2O_2 adsorption obtained from the DFT studies on the surface of (a) bared, (b) EDTA_adsorbed and (c) OA_adsorbed $BiFeO_3$ nanoparticles. The red, white, purple, green, and blue spheres stand for O, H, Bi, Fe, and N atoms, respectively. Copyright (2011), American Chemical Society. (For interpretation of the references to colour in this figure legend, the reader is referred to the web version of this article.)
Reproduced with permission from ref (Wang et al., 2011).

displays that the silver leaching observed after 48 h of the reaction was 0.09 mg/L, which comes below the guidelines of the World Health Organization (WHO) for safe drinking water.

4.2.3. *Two-dimensional carbon-based materials*

Carbon-based materials namely carbon nanotubes (CNTs) (Yao et al., 2016; Yang et al., 2018), activated carbon (AC) (Yao et al., 2013; Navalon et al., 2011), biochar (Fang et al., 2015; Yan et al., 2017), graphene oxide (GO) (Nidheesh, 2017; Divyapriya and Nidheesh, 2020), *g*-C_3N_4 (Sudhaik et al., 2018; Hasija et al., 2019) etc. have been exploited in the heterogeneous Fenton reactions. The recent developments in using two-dimensional carbon-based materials for Fenton related applications are discussed here.

4.2.3.1. Graphene and related materials. Many researchers have shown that incorporating carbon materials with heterogeneous Fenton catalysts helps in quick reduction of Fe(III) to Fe(II), because of its fast single electron transfer ability. Graphene is a two-dimensional monolayer of carbon atoms with superior electron mobility, mechanical stability and electrical conductivity (Dai, 2013; Bekyarova et al., 2013). It is reported that the presence of graphene provides support to the Fenton catalyst, and it enhances the performance of the Fenton reaction (Nidheesh, 2017; Divyapriya and Nidheesh, 2020; Han et al., 2014). In a GO–Fe_3O_4 Fenton catalyst, GO is considered as a sacrificial electron donor (Zubir et al., 2015). The unpaired π electrons present in the sp^2 carbon domains (C═C) of GO transfer electron to the iron centres of Fe_3O_4 and accelerate the reduction of Fe(III) to Fe(II) (Zubir et al., 2014). XPS analysis on the GO–Fe_3O_4 system evidenced a continuous reduction of Fe(III) to Fe(II). Hence the strong electron transfer ability depicted by the graphene-related materials is a crucial factor that contributes to the enhanced catalytic efficiency of graphene-based material supported heterogeneous Fenton catalysts. The GO–Fe_3O_4 catalyst showed a 97% removal of Acid Orange 7 (AO7) whereas Fe_3O_4 was only effective in removing 65% of AO7 under photo Fenton conditions. Similar recyclability of Fe (II) species is reported for CNTs supported FeS systems (Ma et al., 2015). The several chemical moieties present on the GO (carboxyl, hydroxyl, hydrophobic groups etc.) and the higher specific surface area promotes the adsorption of organic pollutants to the surface of GO and contributes to the effective removal of pollutants (Bagri et al., 2010; Suárez-Iglesias et al., 2017). The hydrogen bonding, π-π interaction, hydrophobic interaction and electrostatic interaction are the four possible interactions that cause the better adsorption of pollutants to the GO surface (Wang et al., 2019).

Boruah et al. (2017) prepared a magnetically recoverable Fenton catalyst by decorating Fe_3O_4 nanoparticles on an amide-functionalized graphene sheet. The specific π-π and electrostatic interaction between the sp^2 carbon system of graphene and organic pollutants assisted the mineralisation of various phenolic compounds under sunlight irradiation. The catalyst was stable up to ten cycles, and lower electron-hole recombination was inferred from the photoluminescence studies. In a similar study, Wan and Wang (2017) used polyol process and an impregnation method to prepare Fe_3O_4/Mn_3O_4/reduced graphene oxide hybrid material. Under the optimum conditions (H_2O_2 =6 mM, catalyst =0.5 g/L, pH = 3) catalyst showed a 98% degradation of sulfamethazine, one of the pharmaceutically active compound. Zheng et al. (2018) loaded Fe_3O_4 nanoparticles on the functionalized graphene oxide (GO) nanosheets through urushiol molecules as a linker (Fe_3O_4–U-rGO). Urushiol is known for its strong coordinating ability to the metal oxides, and it bonds with various materials through its phenolic hydroxyl groups (Zheng et al., 2011, 2014). The composite catalytic material prevented the iron sludge formation and unfavourable decomposition of H_2O_2 to H_2O and O_2. Hence the Fenton catalytic performance was significantly improved and the process exhibited complete degradation of rhodamine B and methylene blue. The catalyst also exhibited excellent reuse stability up to seven cycles with minimal sludge formation. The synthesis method of the composite catalyst and its reaction pathway are summarised in Fig. 8. Graphene oxide membranes showed tremendous potential in water filtration technologies, but their low permeation flux was hindering their large-scale applications (Wang et al., 2016; Yin et al., 2016; Gao et al., 2013). Recently, a composite material of GO and metal-organic framework (MOF) exhibited six times higher permeation flux (26.3–30.6 L m^{-2} h^{-1} bar^{-1}) with an enhanced separation efficiency, compared to GO nano-sheets. Also, a forty-minute visible light photo-Fenton action on the material removed 97.27% of BPA compound (Xie et al., 2020).

The need to remove iron sludge after the wastewater treatment makes the homogeneous Fenton process non-viable (Zhu et al., 2019). Guo et al. (2017) used a low amount of graphene (0–2 wt%) to modify the ion-sludge obtained from homogeneous Fenton process to prepare a heterogeneous Fenton catalyst named as iron sludge-graphene (Fe–G). The Fe–G catalyst was characterised as FeOOH particles entrapped inside graphene sheet. Owing to the mesoporous structure and the increased adsorption ability of Fe–G catalyst, it showed an improved degradation rate of metronidazole (an antibiotic) compared to the bare iron sludge.

The development of graphene oxide (GO) composites for innovative disinfection technologies is an emerging research topic (Arshad et al., 2019; Moreira et al., 2018; Singh et al., 2020). Hu et al. (2018) prepared a hybrid material of reduced graphene oxide (rGO), silver nanoparticles (AgNP), and $Bi_2Fe_4O_9$ (rGO-Ag/BFO) through an evaporation process. The hybrid material exhibited 100% bactericidal performance (> 6 logs) of *E. coli*. Generally, 3 logs of photocatalytic bacterial disinfection is achieved in 1–4 h; (Laxma Reddy et al., 2017) however in the process using the hybrid catalyst, approximately 6 logs of disinfection was

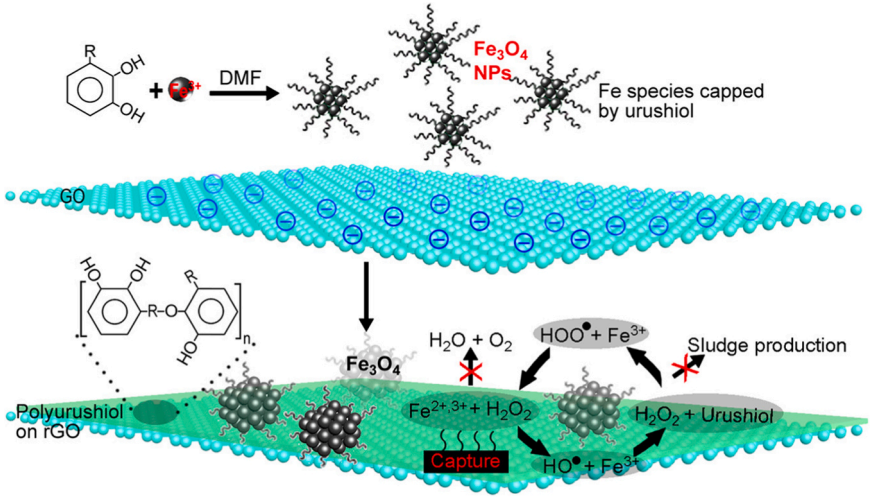

Fig. 8. The diagrammatic representation of the crosslinking reaction of urushiol capped Fe_3O_4 nanoparticles on the functionalised graphene oxide nanosheets. The R group on urushiol consist of 15–17 carbon atoms. Copyright (2018), American Chemical Society.
Reproduced with permission from ref (Zheng et al., 2018).

achieved in 20 min. High performance of the material was associated with the synergistic effect of various mechanisms such as rGO/AgNP co-assisted photocatalysis, photo-Fenton reaction, and rGO assisted silver ion release. The rGO-Ag/BFO was also excellent in the disinfection of gram-negative *P. aeruginosa* and gram-positive *S. aureus*.

4.2.3.2. g-C_3N_4 composites. Graphitic carbon nitride is a polymeric medium band-gap material (2.7 eV) with efficient photocatalytic property (Zhao et al., 2015; Cao et al., 2015; Wang et al., 2012). Its remarkable thermal and chemical stability have set the stage for preparation of various state-of-the-art nanocomposites for solving the energy storage and environmental pollution issues (Sudhaik et al., 2018; Hasija et al., 2019; Wu et al., 2013; Liu et al., 2016). The Fe doped *g*-C_3N_4 modified with mesoporous carbon was effective in removing Acid Red 73 dye for a wide pH ranging from 4 to 10 (Ma et al., 2017). The XPS analysis identified the Fe–N species formed on the N-rich C_3N_4 as the active sites for the Fenton reaction. Cyclic voltammetry (CV) experiments verified that the mesoporous carbon could accelerate the Fe (III) to Fe (II) cycle. Similarly, Hu et al. (2019) doped the *g*-C_3N_4 with different ratios of Fe(III) and the obtained Fe–g–C_3N_4 catalyst was successful in removing phenol, BPA and 2,4-dicholorophenol. The study reported that 5% doping of Fe in *g*-C_3N_4 was the optimum iron concentration for phenol removal, and the catalyst was efficient in degrading the components of a complex wastewater system such as cooking wastewater. Fe(III) forms strong σ and π bonds with the triazine ring skeleton of the *g*-C_3N_4, and that helps the material to act as an efficient heterogeneous Fenton catalyst upon light irradiation.

Many of the studies that deal with Fenton chemistry and disinfection only take care of inactivating bacteria in the system; but genetic material could stay active in the medium (Tong et al., 2020; Thakur et al., 2020). Through the horizontal gene transfer process, it is possible to transfer the antibiotic resistance gene (ARG) from one bacterium to another bacterium which does not possess the antibiotic resistance (Koonin et al., 2001; Thomas and Nielsen, 2005). Therefore, methodologies need to be developed to eliminate ARGs from the wastewater to prevent the rapid growth of antibiotic-resistant bacteria (ARB). A ternary nanocomposite system prepared by Saha et al. (2020) was successful in inactivating the commercially available plasmids pUC18 and pBR322 containing the ampicillin resistance gene (amp^R). The synthesis of ternary nanocomposite of reduced graphene oxide (rGO), iron oxide and *g*-C_3N_4 was carried out by in-situ mixing of all the precursor chemicals. The fragmentation route of the plasmids was confirmed by agarose gel electrophoresis studies performed after treating the system with ternary catalyst, H_2O_2 and visible light. Initially, the plasmids were at a super-coiled fashion, and upon light irradiation over the system, plasmids transferred to a relaxed and single-stranded form. After an exposure time of around 30 min, the plasmids disintegrated into smaller fragments. The various phenomena that lead to the inactivation of plasmids involve photocatalytic activity by iron oxide and *g*-C_3N_4, photo-Fenton activity, relaxation of charge carriers by rGO etc. and are summarised in Fig. 9 (Adapted from reference (Saha et al., 2020)).

Recent advancements show that incorporating goethite or hematite with the *g*-C_3N_4 can result in a heterogeneous photo-Fenton catalyst, capable of degrading tetracycline antibiotic under visible light (Wang et al., 2020b; Zhao et al., 2020). The combination of hematite (α-Fe_2O_3) and *g*-C_3N_4 resulted in a solid-state Z-scheme type catalyst (Wang et al., 2020b). In a similar perspective, a co-calcination approach of melamine (Hughes, 1941) (a cyclic compound of formula $C_3H_6N_6$) with Fe-based metal-organic framework (MIL-53(Fe)), resulted in the formation of Z-scheme heterostructure catalyst α-Fe_2O_3 @*g*-C_3N_4 (Guo et al., 2019). The photoluminescence emission spectra suggested the enhanced separation ability of photo-generated electron-hole pairs. The higher number of electrons participated in the regeneration of Fe(II) boosted the production of $^{\bullet}OH$ and resulted in higher degradation of tetracycline antibiotic. Many-a-times, the large quantity of commercial H_2O_2 needed in the Fenton reaction considerably increases the operating cost of the reaction and hinders its industrial-scale applications (Comninellis et al., 2008). The *g*-C_3N_4 having a negative conduction band (CB) potential compared to the reduction potential of O_2/H_2O_2, can transfer two electrons to the oxygen and result in an in-situ production of H_2O_2 (Kofuji et al., 2016; Moon et al., 2017). It is significant to note that, in the α-Fe_2O_3/*g*-C_3N_4 system, H_2O_2 was produced on the *g*-C_3N_4 and the in-situ produced H_2O_2 was decomposed to $^{\bullet}OH$ on the α-Fe_2O_3 surface. Also, the hole in the VB of hematite was capable of oxidising OH^- to $^{\bullet}OH$. These characteristics make the *α*-Fe_2O_3/*g*-C_3N_4 a promising candidate for wastewater purification applications (Wang et al., 2020b).

4.2.4. Zeolite based catalysts

Zeolites are framework aluminosilicate structures composed of linked MO_4 tetrahedra (M= Si^{4+}, Al^{3+}) (Suib, 1993; Armbruster and Gunter, 2001; Weckhuysen and Yu, 2015). An array of zeolites are available with specific pore sizes. So they find distinct applications in separating mixtures of molecules based on size and they are also called as molecular sieves (Kita et al., 1997; Jia et al., 1994; Primo and Garcia, 2014). One of the striking features associated with zeolites is their selectivity towards the guest molecules compared to other high surface

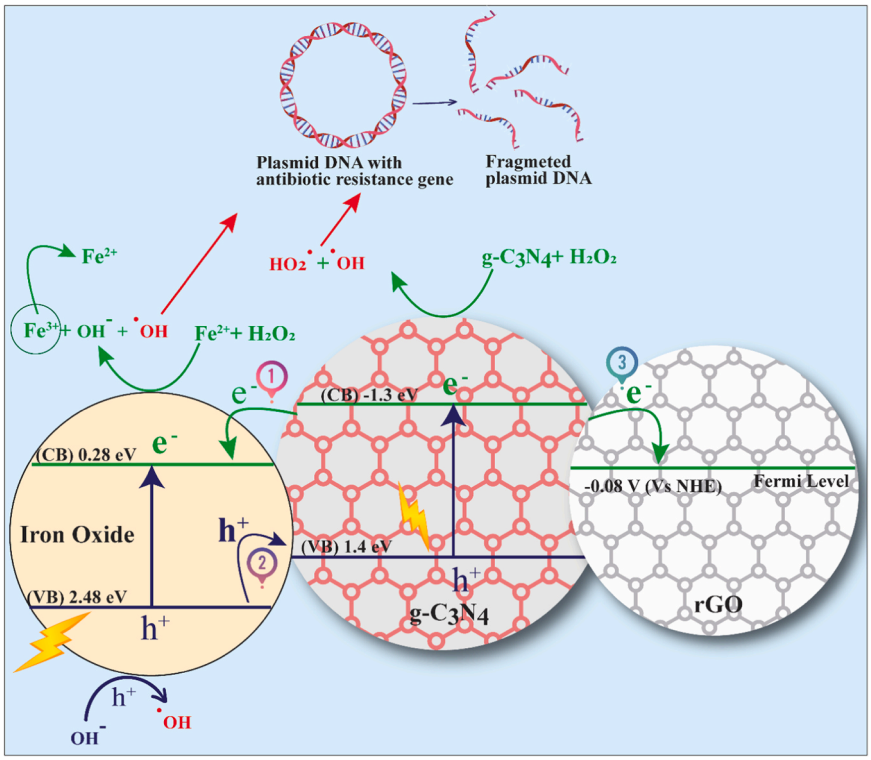

Fig. 9. A schematic representation of all the possible pathways that lead to the fragmentation of plasmids by the ternary nanocomposite system of reduced graphene oxide (rGO), iron oxide and g-C_3N_4. Three different electron transfer processes that minimise the possibility of electron-hole recombination are highlighted with numbers 1–3.

area materials such as activated carbon and silica gel (Lesthaeghe et al., 2007; Martinez-Macias et al., 2015). Fe-containing zeolites are widely studied because of their structural uniformity and high catalytic activity in removing different contaminants (Aleksic et al., 2010; Gonzalez-Olmos et al., 2009; Hartmann et al., 2010; Navalon et al., 2010). Different studies show the enhancement in the catalytic degradation rate by shining UV light on Fe-zeolite systems (Kasiri et al., 2008; Kusic et al., 2006; Noorjahan et al., 2005). Gonzalez-Olmos et al. (2012) reported the mineralisation of phenol and imidacloprid (an insecticide) using iron-containing zeolites, Fe-ZSM5 and Fe-beta. Studies performed at near-neutral pH demonstrated that Fe-ZSM5 catalyst was efficient in producing •OH compared to Fe-Beta. They also performed these experiments in a pilot-scale under the solar light using a compound parabolic collector (CPC) (Gonzalez-Olmos et al., 2012). In a similar perspective, Fe-ZSM5 catalyst was prepared by an ion-exchange method and used for removal of diclofenac, an anti-inflammatory drug. Characterisation by scanning electron microscopy (SEM) and inductively coupled plasma mass spectrometry (ICP-MS) gave insights about the morphology and composition of the catalyst. After two hours of treating diclofenac under optimal conditions ($[H_2O_2] = 50$ mM, $[Fe]_{FeZSM5} = 2.0$ mM, UV-A), they reported low toxicity and biodegradability. Catalyst also gave a similar performance in consecutive runs (Perisic et al., 2016). In another study, Fe_3O_4 nanoparticles were deposited on zeolite-Y through a wet impregnation method (Yang et al., 2019). A 9% iron-loaded zeolite degraded 90% phenol at neutral pH within two hours. The possible adsorption of phenol on the catalyst and the splitting of H_2O_2 to generate •OH is schematically represented in Fig. 10.

The ideas of improving the efficiency of Fenton catalyst are well explored in literature, but the strategies for improving the H_2O_2 utilization are relatively ignored. Since the Fenton reaction is applied for treating wastewater with massive loads of contaminants, it needs the external addition of large amounts of H_2O_2. Optimization of H_2O_2 amount could make the Fenton reaction considerably cheaper. Here the idea is to reduce the self-decomposition of H_2O_2 to H_2O and O_2 and to prevent the reaction of excess H_2O_2 with •OH. In a recent study, Wang et al. (2020a) prepared a Fe_3O_4-zeolite-cyclodextrin catalyst (F-Z-C), which acted as a nano-reactor capable of controlling the local reactant concentration. Cyclodextrins are known for forming inclusion complexes with the guest molecules through van der Waals forces, chemical bonds etc (Saenger, 1980). In this process, the dispersed contaminants (e.g. methylene blue) adsorb on the F-Z-C catalyst which result in increased contaminant concentration over a local region. Then the •OH generated on the catalyst-water interface reacts with the adsorbed contaminants and degrades them. Also, the F-Z-C catalyst can store excess H_2O_2 and release it once necessary. This 'storage- release' effect prevents the self-decomposition of H_2O_2 and improves the H_2O_2 utilization efficiency.

4.2.5. *Metal-organic frameworks (MOFs) and composites*

Metal-organic frameworks (MOFs) are a class of supramolecular assemblies formed from the interaction of various metal ions and organic

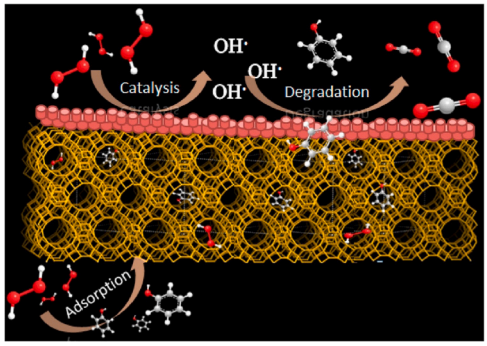

Fig. 10. A structural representation of the porous framework of zeolites and the possible pathway for phenol degradation. Copyright (2018), Elsevier. Reproduced with permission from ref (Yang et al., 2019).

ligands (Deria et al., 2014; O'Keeffe and Yaghi, 2012; Howarth et al., 2016). The high porosity, excellent surface area and capacity to act as nano-reactors attracted wide attention on MOFs for various applications such as gas storage, liquid-phase separations, catalysis, drug delivery *etc* (Li et al., 2011; Wang et al., 2015; Kuppler et al., 2009; Denny et al., 2016; Wang and Astruc, 2020; Horcajada et al., 2012; Li et al., 2009). In the past decade, a surge has been observed in the utilization of iron-contained MOFs for heterogeneous Fenton reactions owing to their efficient $^{\bullet}OH$ generation capacity (Liu et al., 2017; Cheng et al., 2018; Sharma and Feng, 2019). Fe-MOFs have a higher tendency for the recombination of generated electron-hole pairs resulting in lower photocatalytic activity (Liang et al., 2015; Liu et al., 2018). Nowadays, preparation of composite materials with Fe-MOFs and semiconductor is devised as a successful strategy to promote the charge transfer efficiency (Chandra et al., 2016; Shen et al., 2015). MIL (Materials Institute Lavoisier) group of metal-organic frameworks are one of the most explored classes of MOFs in the field of environmental remediation (Farha and Hupp, 2010; Janiak and Vieth, 2010). Li et al. (2018) formulated a one-pot solvothermal synthesis method for the preparation of TiO_2 @MOF (TiO_2 @NH_2-MIL88B-Fe) heterostructures (abbreviated as SU-3, where three stands for the optimal molar ratio of Ti: Fe). The TiO_2 @MOF displayed enhanced photodegradation of methylene blue (MB) under visible LED light. To identify the key reactive species in the Fenton system, experiments were performed with EDTA (h^+ scavenger), *p*-benzoquinone ($O_2^{\bullet-}$ scavenger) and *tert*-butyl alcohol ($^{\bullet}OH$ scavenger). The excess addition of *tert*-butyl alcohol slowed down the degradation of MB, and it indicated the vital role of $^{\bullet}OH$ in the Fenton reaction. Electron spin resonance (ESR) technique employed using 5,5-dimethyl-1-pyrroline N-oxide (DMPO) as a spin trapper resulted in a characteristic four peak signal (ratio 1:2:2:1) attributed do the DMPO-$^{\bullet}OH$, indicating the presence of $^{\bullet}OH$ (Du et al., 2017). A plausible mechanism of the photocatalytic decomposition of MB by SU-3 is represented in Fig. 11.

In another study, Fe_3O_4 and carbon aerogel (CA) were combined with the MIL-100(Fe) and the composite material was evaluated for the removal of tetracycline hydrochloride (TC), a contaminant of emerging concern, under UV light. The CA incorporated nanocomposite with a higher surface area (389 $m^2\ g^{-1}$) enhanced the performance by 1.6 times compared to MIL-100(Fe)@ Fe_3O_4. Also combining the system with CA resulted in improvement of the water stability of the MOF (Rasheed et al., 2018). In a similar study, Wu et al. (2020) prepared a series of Fe-MOFs and studied the role of Fe-oxo clusters in the framework for the degradation of TC. Fe-oxo clusters were regarded as the absorption antennae, and Fe-MOFs showed substantial absorption in the visible region. Among the MIL-101, MIL-53 and MIL-88B, photo-Fenton activity was highest in the MIL-101, because of its higher number of coordinatively unsaturated iron sites. Generally, the metal centres in a MOF are fully occupied by the organic ligands, and this inhibits the metal sites from activating H_2O_2. So, introducing coordinatively unsaturated metal sites becomes a successful strategy in activating H_2O_2. Tang and Wang (2018) prepared the CUS-MIL-100(Fe) having open iron centres and reported 100% degradation of sulfamethazine (a commonly used sulfonamide antibiotic). Also the Fenton experiments performed for multiple cycles, revealed excellent structural stability of the catalyst and minimal leaching of iron which is lower than the environmental standards demanded by European Union (<2 mg/L).

In a recent report, distinct nano-architectures of road-like, spindle-like, and diamond-like MIL-88A-Fe were prepared and studied to examine the correlation of different exposed crystal facets towards catalytic performance (Liao et al., 2019). The shape-selective synthesis of the catalyst was achieved by simply varying the water/DMF ratio during the solvothermal synthesis, and the contribution of (100) facet decreased upon increasing the quantity of DMF. The peak area analysis of XRD pattern showed that (100) facet has a ratio of 60%, 30% and 15% in the road-MIL-88A-Fe, spindle-MIL-88A-Fe and diamond-MIL-88A-Fe, respectively. Also, DFT studies revealed the easier activation of H_2O_2 on the (100) crystal facet compared to (101), and the rod-MIL-88A-Fe was chosen as the best catalyst for Fenton reaction.

4.3. Zero-Valent iron (ZVI) based catalysts

Zero-valent iron (ZVI) with a standard reduction potential of E_H^0 (Fe^{2+}/Fe^0) = −440 mV is considered as an effective reducing agent (Fu et al., 2014). ZVI can give out two electrons in the presence of H_2O_2 or O_2 and form the Fe(II) species responsible for Fenton reaction (Eq. 16 and 17). ZVI is known for reacting differently in aerobic and anaerobic conditions. In aerobic conditions, it acts by oxidizing contaminants and in anaerobic condition by reducing contaminants (He et al., 2016).

$$Fe^0 + O_2 + 2\ H^+ \rightarrow Fe(II) + H_2O_2 \quad (16)$$

$$Fe^0 + H_2O_2 + 2\ H^+ \rightarrow Fe(II) + 2\ H_2O \quad (17)$$

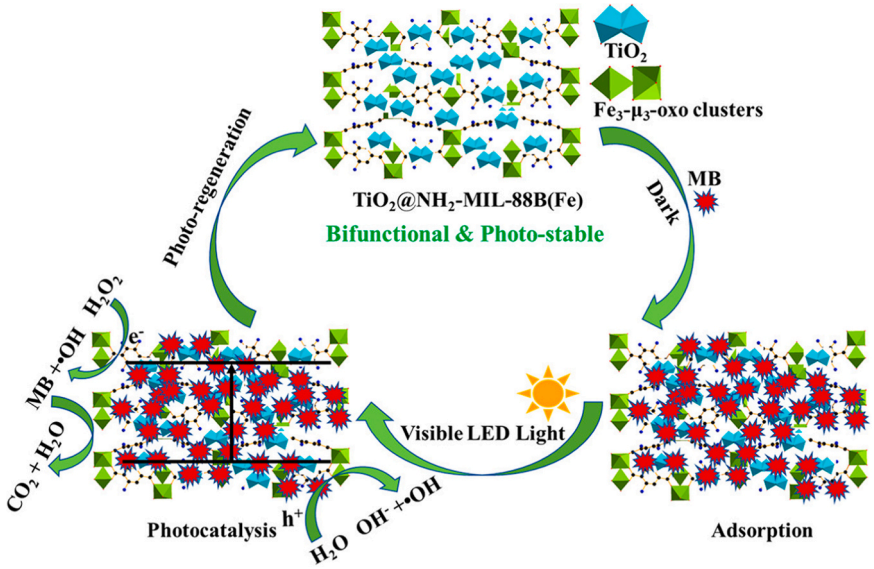

Fig. 11. Schematic representation of adsorption and photocatalytic dye degradation on the SU-3 catalyst upon visible LED light irradiation. Copyright (2018), American Chemical Society.
Reproduced with permission from ref (Li et al., 2018).

$$Fe(II)+H_2O_2 \rightarrow Fe(III)+{}^{\cdot}OH+OH^{-} \quad (18)$$

Over the past decade, ZVI was demonstrated for treating different varieties of organic and inorganic contaminants such as dyes (Wang et al., 2017), phenolic compounds (Ambika et al., 2020; Minella et al., 2019), antibiotics (Zhou et al., 2019), nitroaromatic compounds (NACs) (Zarei et al., 2019), arsenic (Tucek et al., 2017), heavy metals (Li et al., 2017), chlorinated organic compounds (Ezzatahmadi et al., 2017), nitrates *etc* (Ezzatahmadi et al., 2017*)*. The heavy metal iron content in wastewater poses significant challenges during its treatment (Demirbas, 2008; Fu and Wang, 2011). In the last decade, ZVI emerged as a catalyst for treating wastewater, having a large load of heavy metal content (Vilardi et al., 2018; O'Carroll et al., 2013). Li et al. (2017) tested conventional adsorbents and precipitants such as activated alumina, Ca $(OH)_2$, Fe_3O_4, nanoTiO_2 etc. for removing heavy metal ions and compared their performance with the ZVI. However, only the ZVI demonstrated simultaneous removal of multiple heavy metals present (Ni(II), Zn(II), As(V) and Cu(II)). Since the standard reduction potential of copper is more positive compared to that of ZVI, it can easily receive electrons from ZVI. Interestingly, the chemical reduction method of Cu (II) and As(V) using ZVI is less susceptible to changes by the difference in pH or introduction of chelates. For metal ions such as Zn (II) and Ni(II) having standard reduction potential more negative than that of ZVI, precipitation, adsorption and electrostatic attraction are the major methods for the metal ion removal (Li et al., 2017). The oxyanions of arsenic were primarily removed by co-precipitation with Fe(II).

Zero-valent iron microspheres have shown to be efficient catalyst for UV light photo-Fenton processes with a TOC removal of 99% for phenol and 83% for oxalic acid (Blanco et al., 2016). The studies also demonstrated the degradation of 90% 1,4-dioxane by ZVI microspheres under solar irradiation for 180-minutes. The results of this study showed similar values of degradation at various pH values and indicate that iron solubilisation is not an essential step in this process and the photo-Fenton reaction is taking place on the surface of the catalyst (Barndok et al., 2016). In a similar study, nano-ZVI was evaluated for the removal of ciprofloxacin antibiotic. With a ratio of 5:1 for nZVI: H_2O_2, a 99.3% removal of ciprofloxacin was achieved in 120 min at neutral pH. The experiment performed under UV light demonstrated a 100% degradation of ciprofloxacin within 25 min (Mondal et al., 2018). Kakavandi et al. (2019) reported the use of nZVI supported on kaolinite (a layered silicate mineral) for the removal of acid black 1 (AB1) dye. The reaction was performed at pH 2.0 with 0.3 g/L of catalyst, and even after four cycles the catalyst was efficient in removing 72% of the dye, indicating catalyst durability and potential for reuse. In a recent study, Jiang et al. (2020) investigated the role of formic acid in the pathway for degradation of prechlorinated organic contaminants. One of the major concerns about chlorinated contaminants is their resistance to degradation via an oxidative pathway. In the study, formic acid acted as a scavenger of $^{\bullet}OH$ and generated carbon dioxide radical ($CO_2^{\bullet-}$). Carbon dioxide radical is known for transferring one of its electrons to chlorinated contaminants and performing the degradation by a reductive pathway. They studied the role of formic acid in the generation of $CO_2^{\bullet-}$ and confirmed the presence of carbon dioxide radical by electron paramagnetic resonance (EPR) analysis. The generalised mechanism for oxidative and reductive routes of degradation followed by ZVI is summarised in Fig. 12.

The first report of inactivation of two waterborne viruses ΦX174 and MS-2 using ZVI came in 2005 (You et al., 2005; Hossain et al., 2014). Later Lee et al. (2018) demonstrated that nano zero-valent iron (nZVI) could act as a potent bactericide under anaerobic conditions. Under aerobic conditions, a more significant amount of nZVI was required for inactivation, possibly due to the surface corrosion and oxidation of nZVI by oxygen. Another study in 2009 by Diao and Yao (2009) reported the inactivation of *Pseudomonas fluorescens* (gram-negative bacteria), *Bacillus subtilis* var. *niger* (gram-positive bacteria) and *Aspergillus versicolor* (fungus) using nZVI. A sulfidated micro zero-valent iron (S-mZVI) was studied for the removal of antibiotic-resistant *E. coli* bacteria and antibiotic-resistant gene (ARG) TetB. The S-mZVI was prepared in a planetary ball mill by mixing sulfur and mZVI in a molar ratio of 20 (Fe/S). $SO_4^{\bullet-}$ and $^{\bullet}OH$ radicals generated was attributed to the effective removal of ARG (Zhang et al., 2020). Similarly, a Fe/Ni nanoparticle system was synthesised by a liquid-phase reduction method using $NaBH_4$. Here the bimetallic system displayed superior activity compared to the ZVI in the removal of f2 bacteriophage. An optimum ratio of 5:1 (Fe/Ni) showed the highest catalytic performance and both metals existed in the nanoparticle as Fe^0 and Ni^0 (Cheng et al., 2019).

Chlorination is one of the popular methods employed for disinfection of drinking water, but it produces carcinogenic disinfection byproducts (DBPs) like chloroform, chloroacetic acid etc (Hrudey, 2009; Hua and Reckhow, 2007). Therefore, ZVI is of interest since it will not result in the production of any DBPs. Two of the limiting factors that prevent the practical application of ZVI include poor dispersibility and its low disinfection efficiency. Because of the lower disinfection efficiency, a higher dosage of ZVI is required, and that adds to the cost of the process. The electrostatic and magnetic interactions between ZVI particles lead to its aggregation and poor dispersibility. Also, under aerobic conditions, the iron oxide layers formed over the ZVI decelerates the electron transfer from the ZVI core to the exterior (Fu et al., 2014; Sun et al., 2019). Recently Sun et al. (2019) prepared amorphous zerovalent iron microspheres (A-mZVI) and crystalline nanoscale zerovalent iron (C-nZVI) for studying the efficiency of removal of *E. coli* under aerobic

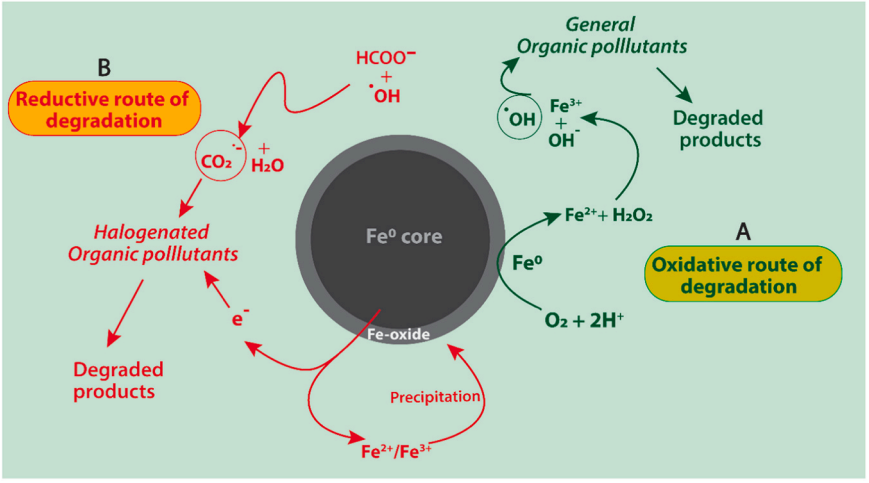

Fig. 12. Scheme showing degradation mechanism of (a) general organic pollutants and (b) halogenated organic pollutants by the ZVI. The oxidative and reductive routes of pollutant degradation are denoted by green and red colour schemes respectively.

conditions. C-nZVI produced •OH on the surface of a catalyst but A-mZVI generated •OH by the iron dissolution and oxygen activation in the solution. SEM and TEM images of the *E. coli* treated with C-nZVI depicted the spherical nanoparticles on the surface of bacteria. But the sample treated with A-mZVI showed a thick covering of interconnected flakes on the surface of *E. coli* bacteria. In the A-mZVI, a fast dissolution of Fe^{2+} was observed, and later it deposited on the *E. coli* as iron oxy-hydroxy species. A thicker adsorption of oxide layers over the bacteria resulted in better inactivation efficiency by A-mZVI. Also, the magnetization studies revealed that the corrosion products of A-mZVI are essentially non-magnetic. Therefore, the sedimentation of the reaction mixture after treatment with A-mZVI was not influenced by a magnet. The difference in the mode of action of C-nZVI and A-mZVI and their physical mode of separation are schematically represented in Fig. 13. Since this technique employs direct gravitational precipitation of the inactivated bacteria covered by iron oxides, it can also prevent the release of ARG into the water (Sun et al., 2019).

ZVI is an abundantly available, non-toxic, and comparably low-cost material that has also shown applications as heterogeneous Fenton catalyst (Fu et al., 2014). It has successfully demonstrated the removal of microorganisms, heavy metals, and contaminants of emerging concern from drinking water, and it also functions without formation of toxic disinfection by-products (DBP) (Giannakis et al., 2016; Sun et al., 2019; Du et al., 2020). Because of its versatility, it has great potential for future applications in large-scale water treatment plants. However, it is a challenging task to understand the complex mechanism of action of ZVI because its mechanisms of action may involve oxidation, reduction, co-precipitation, surface adsorption etc. Its mechanism also varies according to the contaminants which it reacts with. Also, ZVI treatment may result in the formation of smaller quantities of corrosion products such as $Fe(OH)_2$, $Fe(OH)_3$, Fe_2O_2 etc. and they could be detrimental to the pipelines in water distribution channels (Fu et al., 2014). Table 1. summarises operational parameters used for performing the Fenton reaction and the catalytic activity observed for different classes of heterogeneous Fenton catalysts.

5. Real world applications and the role of natural organic matter

The implementation of Fenton reaction for real-water applications becomes complicated due to the presence of a complex matrix of organic substances present in real water called as Natural Organic Matter (NOM) (Giannakis et al., 2016). Various studies have shown the positive impact of NOM in enhancing the efficiency of Fenton reaction (Spuhler et al., 2010; Huling et al., 2001; Georgi et al., 2007; Vione et al., 2006; Moncayo-Lasso et al., 2009). Fe(III) can form complexes with the NOM (Fe^{3+}-NOM), and this complex is less prone to precipitation and depict higher absorption in the UV–visible range (Voelker et al., 1997; Walte and Morel, 1984). Georgi et al. (2007) reported that the presence of humic acid (a type of NOM) in the Fenton system (50–100 mg/L) had shifted the optimum pH of the reaction towards the neutral condition. Ruales-Lonfat et al. (2015a) compared the *E. coli* inactivation of hematite with the Milli-Q water and water collected from Geneva lake. The natural water was not interfering with the photocatalytic semiconducting action of hematite (hematite/light/water) and with both water samples complete *E. coli* inactivation was observed within 120 min. When H_2O_2 was introduced to the system (hematite/light/water/H_2O_2), natural water system showed slightly higher inactivation rate in comparison to Milli-Q water. This observation could be related to the photo Fenton action showed by iron species which got complexed and solubilised by the NOM. The formed complex enhances the reaction rate by participating in the homogeneous Fenton reaction.

On the contrary, some other studies report the inhibition of Fenton process in the presence of NOM (Bogan and Trbovic, 2003; Lindsey and Tarr, 2000; Lindsey and Tarr, 2000). Fenton experiments performed to degrade polycyclic aromatic hydrocarbons in the presence of humic acid, and fulvic acid (classes of NOM) exhibited the inhibition of •OH formation (Lindsey and Tarr, 2000). In a similar study Lindsey and Tarr (2020) observed four times lower radical formation in natural water compared to pure water. Since the classes of NOM present in real water varies depending on the source of water, detailed localised studies are needed to understand the effect of NOM and its interaction with the heterogeneous Fenton catalyst in either enhancing or inhibiting the Fenton reaction process.

6. Parameter optimisation

Various parameters such as light source, dosage of catalyst etc. need to be optimised for the efficient performance of Fenton reaction. Choice of the perfect light source for the photo Fenton reaction is a critical aspect considering its economic viability. The optimum light radiation required for the photo Fenton process is in the UV region and near-visible spectrum up to 560 nm wavelength (Carra et al., 2015). Solar light is a sustainable source of energy, and in areas where the availability of sunshine is limited, artificial light sources are required. Mercury UV-lamps were the common source of light for photo Fenton reaction (Guimarães et al., 2019). But considering its low energy efficiency and possible mercury contamination, Xenon lamp-based sun

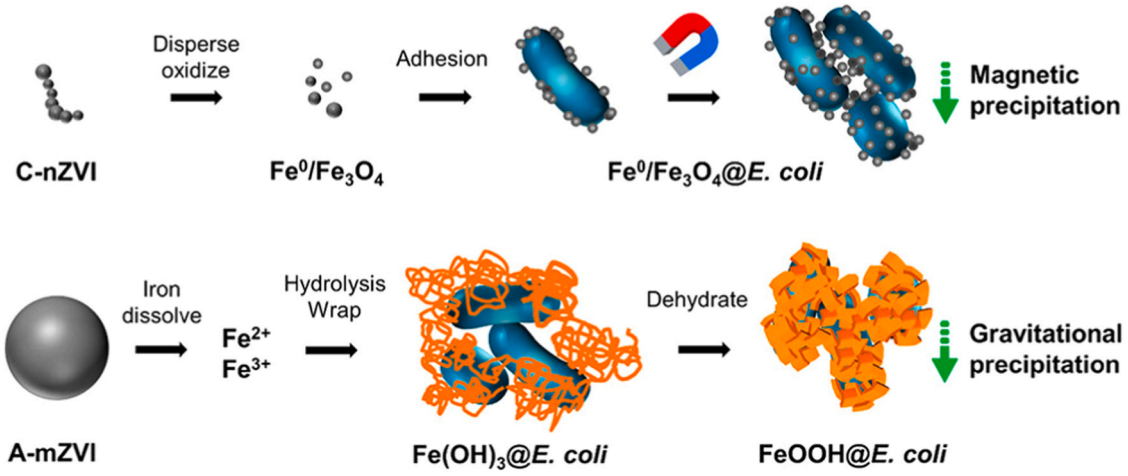

Fig. 13. Schematic diagram representing the mode of disinfection and physical separation process by the C-nZVI and A-mZVI. Copyright (2019), American Chemical Society.
Reproduced with permission from ref (Sun et al., 2019).

Table 1
Summary of catalytic activity and operational conditions of different classes of heterogeneous Fenton materials.

Catalyst	Catalyst dose added	Light source	H_2O_2 concentration and pH of system (pH_0=initial pH)	Pollutants	Duration	Catalytic activity or removal efficiency of pollutant	Ref.
Ferrihydrites							
8%Ag/AgBr/Fh	1.0 g/L	Visible light (LED lamp)	10 mM $pH_0 = 3$	BPA (30 mg/L)	60 min	0.0370 min^{-1} (8%Ag/AgBr/Fh) 0.0101 min^{-1} (Pure Fh)	(Zhu et al., 2018)
6%Ag/AgCl/Fh	1.0 g/L	Visible light (LED lamp)	10 mM $pH_0 = 3$	BPA (30 mg/L)	60 min	0.0506 min^{-1} (6%Ag/AgCl/Fh) 0.0099 min^{-1} (Pure Fh)	(Zhu et al., 2018)
Ferrites							
$ZnFe_2O_4$	0.5 g/L	Visible light (Xenon lamp)	5 mM $pH_0 = 6$	Orange II (100 mg/L)	60 min	0.0468 min^{-1}	(Cai et al., 2016)
$ZnFe_2O_4$ (yolk-shell structure)	0.3 g/L	Visible light (LED lamp)	20 mM $pH_0 = 2$	Tetracycline (60 mg/L)	40 min	0.070 min^{-1}	(Xiang et al., 2020)
Pillared clays							
Al-Fe smectite pillared clay	3.0 g/L	UV-C (mercury vapour lamp)	98 mM $pH_0 = 3$	Winery wastewater	240 min	67.1% TOC removal	(Guimarães et al., 2019)
Layered double hydroxides							
CuNiFe LDH	1.0 g/L	Without light irradiation	$M_{H2O2}/M_{phenol} = 37$ $pH_0 = 6.5$	Phenol	60 min	98.9% TOC removal	(Wang et al., 2018)
Fe-Perovskites							
$LaCu_xFe_{1-x}O_{3-\delta}$ (x = 0.5)	1.0 g/L	Without light irradiation	12 mM $pH_0 = 6$	BPA (20 mg/L)	120 min	0.021 min^{-1}	(Pan et al., 2020)
Graphene related materials							
Fe_3O_4-Mn_3O_4/reduced graphene oxide	0.5 g/L	Without light irradiation	6 mM $pH_0 = 3$	Sulfamethazine (0.07 mmol/L)	120 min	98% removal	(Wan and Wang, 2017)
g-C_3N_4 composites							
Fe-g-C_3N_4/Graphitised mesoporous carbon	0.8 g/L	Visible light	40 mM (pH range 4–10)	Acid Red 73 (50 mg/L)	40 min	99.2% removal	(Ma et al., 2017)
5% Fe-doped g-C_3N_4	3.0 g/L	Visible light (Xenon lamp)	16 mM ($pH_0 = 3$)	Cooking wastewater	60 min	TOC value reduced from 25.3 mg/L to 8.1 mg/L	(Hu et al., 2019)
Metal-organic frameworks (MOFs) and composites							
TiO_2 @NH_2-MIL88B-Fe	0.2 g/L	Visible light (LED lamp)	20 mM ($pH_0 = 7$)	Methylene blue (100 mg/L)	150 min	100% degradation	(Li et al., 2018)
Zero-valent iron (ZVI) based catalysts							
Nano-ZVI@kaolinite	0.3 g/L	Without light irradiation	4 mM (pH_0 =2)	Acid Black 1 (30 mg/L)	120 min	98% decolourisation	(Kakavandi et al., 2019)

simulators are widely used for photo Fenton reactions (Hu et al., 2019; Cai et al., 2016). Recent studies report the use of light emitting diodes (LEDs) as an energy-efficient light source in the heterogeneous photo Fenton reaction (Zhu et al., 2018a, 2018b). LEDs have a longer lifespan compared to Xenon lamps, and they convert less amount of energy in the form of heat (Carra et al., 2015; Matafonova and Batoev, 2018).

Optimising the dosage of catalyst, H_2O_2 etc. is an important procedure in minimising the operating cost and achieving the highest catalytic efficiency of Fenton reaction. The amount of natural NOM, carbohydrates, proteins and inorganic species (carbonate, nitrate, sulphate, etc.) present in water are the specific parameters that define a water matrix (Lado Ribeiro et al., 2019). Photo Fenton inactivation experiments performed on *E. coli.* bacteria in the urban wastewater sample resulted in a 2.43 log disinfection (Rodríguez-Chueca et al., 2012). When the water matrix was changed to distilled water, a log 5.81 inactivation was observed. In a recent report, Ling et al. (2018) studied the effect of chloride and phosphate on the ZVI in a Fenton reaction. Chloride ions were shown to have accelerated the decomposition of H_2O_2 and enhanced the reaction rate, but the phosphate ions were observed to inhibit the H_2O_2 decomposition. It was assumed that the insoluble iron phosphate layer formed on the ZVI surface could have blocked the catalytic sites on ZVI and thus resulted in a decreased reaction rate. A proper investigation of the critical parameters of the water matrix can provide a rational understanding of the possible interactions of catalyst and H_2O_2 with organic/inorganic compounds of the water matrix and obtain insights on the potential effects on Fenton reaction rate.

7. Sustainable model of reusing catalyst

Reusability/recyclability of heterogeneous Fenton catalysts is an essential parameter in view of its economic implications. Multiple cycles of Photo Fenton reaction performed with ammonia modified graphene/Fe_3O_4 catalyst resulted in the lowering of pollutant degradation efficiency of the catalyst (Boruah et al., 2017). The first cycle showed 92.43% degradation of phenol whereas, at the 10th cycle phenol degradation reduced to 75.50%. A similar decrease in the catalytic efficiency over multiple runs is observed for almost all types of heterogeneous Fenton catalysts (Tang and

Wang 2018). An environmentally friendly sustainable model of reusing/recycling the heterogeneous Fenton catalyst is a highly sought-after area of research. Recently Serrà et al. (2020) reported an interesting zero-carbon-emission circular process resulting in water remediation and energy production. Spirulina microalgae was cultivated in wastewater which was rich in iron and heavy metals. During the photosynthetic process, spirulina utilised carbon dioxide and released oxygen to the atmosphere. This microalgal biomass was fermented and produced bioethanol. The resultant biomass was dried and burnt for thermal energy generation. The iron-rich ash obtained after combustion was utilised as heterogeneous photo Fenton catalyst under sunlight for wastewater treatment. Finally, the mineralised water was reused for cultivating the next batch of microalgae and completed the cycle. The research area of zero-carbon-emission circular processes using heterogeneous Fenton catalysts is expecting significant advances in recent years. A large scale implementation of similar techniques will effectively contribute to tackling the current global issues like excessive CO_2 emission and atmospheric pollution (Keijer et al., 2019).

8. Theoretical understanding and mechanistic aspects

Even though most reports on Fenton catalysts are successful in showing better results of degradation of organic contaminants and transformation of inorganic contaminants, more work and insights are needed to understand the mechanistic aspects of the reactions involved. Theoretical understanding of the underlying mechanisms of the Fenton and Fenton-like reactions by density functional theory (DFT) studies can provide new insights and information in this area of research (Buda et al., 2001). DFT studies help in understanding the role of surface defects in enhancing the catalytic activity of heterogeneous Fenton reactions. Only by the in-depth understanding of the mechanism, further improvements in the catalyst performance can be achieved. Recently, static and dynamic DFT calculations performed by Hsing-Yin Chen and co-workers on the intermediates of Fenton reaction concluded that $^{\bullet}OH$ is the predominant species below pH 2.2 (English for Writing Research Papers Useful Phrases, 2016). This study also reported that as the pH increases from 2.2 to 4.6, iron(IV)-oxo complex $[(H_2O)_5Fe^{IV}O]^{2+}$ was the major complex and at pH >7.9 a deprotonated dihydroxy species, $[(H_2O)_3Fe^{IV}O(OH)_2]$ was the active intermediate. Nonetheless, the high-level ab initio calculations question the presence of dihydroxy species in aqueous Fenton reactions and yet there are no reports of the successful synthesis and characterisation of $[(H_2O)_3Fe^{IV}O(OH)_2]$ species in the literature. Likewise, it is essential to explore the electron transfer mechanism in the Fenton catalyst by quantum chemical calculations (Qin et al., 2017; Vorontsov, 2019). Later the theoretical studies should be validated with necessary experimental evidence.

9. Prospects and future directions

The lack of standardised procedures for reporting the catalytic activity is a major concern in the heterogeneous photo-Fenton process. Different groups of researchers use various ratios of concentrations of catalyst: H_2O_2 for performing the reactions (See the catalytic activity summarised in Table1). Therefore, a standardised procedure for comparing the efficiency of the catalyst is inevitable. In many cases, even though the authors argue about carrying out the reaction at a neutral pH, the reaction pH changes during the experiment. Usually, the pH of the reaction mixture decreases due to the formation of smaller degradation products such as oxalic acid, formic acid etc (Kuan et al., 2015). Hence, use of buffers and/or continuous monitoring of pH is necessary while performing the reaction. Another challenge that needs to be addressed is the leaching of iron species from the catalyst and deactivation of catalytic sites by the adsorption of impurities from wastewater. So, more work is needed to understand catalyst stability and longevity as well as technologies that can use the catalyst in a sustainable way.

2-dimensional (2D) nanomaterials with high surface area have played a significant role in various energy and environmental applications. 2D materials such as MXene composites are less explored in the Fenton chemistry, and a great deal of attention should be paid on them to unveil their potential. Also, many of the reports on heterogeneous Fenton catalysis show higher activity in the ultraviolet region of the electromagnetic spectrum. Since the sun can be a low-cost source of energy (i.e., depending on the technology for capturing and utilizing the radiation) and because of its inexhaustible nature, researchers need to target more on the synthesis of catalysts which are visible light active and have high activity under visible light spectrum. When it comes to the broad-scale application of photo-Fenton reaction for water treatment, materials that utilize a broader spectrum of sunlight and doing so at high quantum yields will have more potential for practical applications. Nowadays, the research community is witnessing computer-aided design of various catalysts. So, researchers should come forward for applying *in silico* tools in designing novel catalytic materials having excellent activity for photo Fenton reaction (Poree and Schoenebeck, 2017).

The toxicity of nanomaterials is itself a widely debated topic. The nanoparticles embedded in different matrices get released into the environment, and they interact with the living cells in a dynamic fashion (Hamers, 2017). Nanomaterials which are synthesised with distinct properties, may undergo chemical changes once they are released into the environment. Hence a comprehensive understanding of the interaction of nanoparticles with the living matter is necessary for the large-scale application of these catalysts and for avoiding any future health hazards. Different reports present great achievements in degrading various contaminants of emerging concern via Fenton and Fenton-like processes, but excellent outcomes in complex wastewater matrices are still rare in the literature. So, opportunities for combining heterogeneous photo Fenton process with other established wastewater treatment technologies should be explored for commercial-scale applications.

Photo-Fenton reaction is proved to be a promising method for the removal of bacterial and fungal pathogens from wastewater (O'Dowd and Pillai, 2020; García-Fernández et al., 2012). Also, there are successful reports on the removal of MS2 coliphage (bacteriophage having similar properties to that of human enteric viruses) from wastewater through photo-Fenton treatment (Nieto-Juarez et al., 2010; Ortega-Gómez et al., 2015). Nieto-Juarez and Kohn (2013) investigated the fate of MS2 coliphage upon photo-Fenton treatment with four commercially available iron oxide species (hematite, goethite, magnetite and amorphous $Fe(OH)_3$. The study reported 99.9% virus removal by all the iron species studied via a photo-Fenton process combined with physical removal such as adsorption. A recent study reports the effectiveness of homogeneous solar photo-Fenton for inactivation of hepatitis A virus (an extremely resistant non-enveloped virus) in water (Polo et al., 2018). Since the SARS-CoV-2 is an enveloped virus, which remains more susceptible to disinfectants compared to a non-enveloped virus (Chu et al., 2019), photo-Fenton reaction offers the possibility of effectively deactivating SARS-CoV-2 virus present in wastewater. Therefore, future studies should aim at identifying suitable heterogeneous Fenton catalysts for virus removal with respect to their inactivation efficiency and absorption capacity. The research area of heterogeneous photo-Fenton has a lot of room for development, and it has remarkable potential in addressing pressing challenges in industrial-scale water treatment.

10. Conclusions

Photo-Fenton treatment of wastewater is an evolving technology for removing organic, inorganic, and microbial contaminants from water. In comparison to the homogeneous Fenton reaction, heterogeneous catalysts have displayed great potential for commercial applications in view of their wide pH range of application, low sludge formation, and reusability. Along with the recent literature reports on the advances in materials for heterogeneous Fenton reaction, schematic illustrations in this review provide a basic understanding of the electron transfer mechanisms and the formation of reactive oxygen species in Fenton reactions. The excellent magnetic properties of materials such as ferrites, magnetite, and their composites

have enabled significant developments, due to easy separation and reusability of such materials after wastewater treatment. The incorporation of plasmonic materials with iron minerals to broaden their visible light absorption capacity is highlighted as a growing area of research. Various supporting materials used in the heterogeneous Fenton catalytic systems have a specific role in altering the catalytic activity of the system. Incorporation of semiconductor nanoparticles and carbon-based two-dimensional materials with iron minerals to speed-up the electron transfer and Fe (II) regeneration has shown promise and is expected to receive more attention in the coming years. The higher specific surface area provided by graphene-related supporting materials leads to enhanced adsorption of pollutants on the Fenton catalytic surface. Pillaring process of clay materials exposes the active site of the catalyst and the specific hydrophilic nature of LDHs assists the interaction of hydrophilic contaminants with LDHs. Literature review on studies on the application of Fenton, Fenton-like, and photo-Fenton technologies show these processes play important role in the inactivation of pathogenic microorganisms and destruction of contaminants of emerging concern in various types of wastewaters. Along these lines, there is potential for further enhancement of process performance when introducing catalysts of good selectivity, synergistic action, and versatility for the treatment of various types of source waters/wastewaters polluted with a variety of pathogenic microorganisms, organic and inorganic contaminants of concern. Fe-contained perovskites are seeing growing interest in Fenton-like processes, especially on aspects related to innovative strategies to dope or modify perovskites materials to achieve higher catalytic activity and better process performance. New developments on the synthesis and applications of MOFs and zeolite materials, especially for water treatment, demonstrate there have been important advances in recent years and point towards further progress, especially on topics focused on tailor-designed framework structures with improved functionality and higher activity for more efficient Fenton-like applications. Zero-valent iron-based technologies have seen huge interest in both mechanistic studies and field applications for the treatment of numerous pollutants due to the environmental compatibility of iron and versatility of the process towards oxidation or reduction reactions. It is expected that more applications will be seen in the future, especially if challenges on n-ZVI dispersibility, longevity, and reactivity control are addressed. The materials which can in-situ produce the H_2O_2 by a two-electron transfer to oxygen and the techniques that improve the H_2O_2 utilisation by reducing its self-decomposition can considerably decrease the operating cost of the reaction and pave the way for commercial-scale applications of Fenton reaction. Therefore, a sea of opportunities is wide open in this area for the cost optimisation of the existing technology and to develop brand new materials with extraordinary catalytic efficiency.

Declaration of Competing Interest

The authors declare that they have no known competing financial interests or personal relationships that could have appeared to influence the work reported in this paper.

Acknowledgement


This project has received funding from the European Union's Horizon 2020 Research and Innovation Programme under grant agreement number 820718, and is jointly funded by the European Commission and the Department of Science Technology of India (DST). Dionysiou also acknowledges support from the University of Cincinnati through the Herman Schneider Professorship in the College of Engineering and Applied Sciences.

References

Aleksic, M., Kusic, H., Koprivanac, N., Leszczynska, D., Bozic, A.L., 2010. Heterogeneous Fenton type processes for the degradation of organic dye pollutant in water - the application of zeolite assisted AOPs. Desalination 257, 22–29. https://doi.org/10.1016/j.desal.2010.03.016.

Ambika, S., Devasena, M., Nambi, I.M., 2020. Single-step removal of hexavalent chromium and phenol using meso zerovalent iron. Chemosphere 248, 125912. https://doi.org/10.1016/j.chemosphere.2020.125912.

Armbruster, T., Gunter, M.E., 2001. Crystal structures of natural zeolites. Rev. Miner. Geochem. 45, 1–67. https://doi.org/10.2138/rmg.2001.45.1.

Arshad, A., Iqbal, J., Mansoor, Q., 2019. Graphene/Fe 3 O 4 nanocomposite: solar light driven Fenton like reaction for decontamination of water and inhibition of bacterial growth. Appl. Surf. Sci. 474, 57–65. https://doi.org/10.1016/j.apsusc.2018.05.046.

Ayari, F., Manai, G., Khelifi, S., Trabelsi-Ayadi, M., 2019. Treatment of anionic dye aqueous solution using Ti, HDTMA and Al/Fe pillared bentonite. Essay to regenerate the adsorbent. J. Saudi Chem. Soc. 23, 294–306. https://doi.org/10.1016/j.jscs.2018.08.001.

Aznarez, A., Delaigle, R., Eloy, P., Gaigneaux, E.M., Korili, S.A., Gil, A., 2015. Catalysts based on pillared clays for the oxidation of chlorobenzene. Catal. Today 246, 15–27. https://doi.org/10.1016/j.cattod.2014.07.024.

Babuponnusami, A., Muthukumar, K., 2014. A review on Fenton and improvements to the Fenton process for wastewater treatment. J. Environ. Chem. Eng. 2, 557–572. https://doi.org/10.1016/j.jece.2013.10.011.

Babuponnusami, A., Muthukumar, K., 2014. A review on Fenton and improvements to the Fenton process for wastewater treatment. J. Environ. Chem. Eng. 2, 557–572. https://doi.org/10.1016/j.jece.2013.10.011.

Bagri, A., Mattevi, C., Acik, M., Chabal, Y.J., Chhowalla, M., Shenoy, V.B., 2010. Structural evolution during the reduction of chemically derived graphene oxide. Nat. Chem. 2, 581–587. https://doi.org/10.1038/nchem.686.

Bai, J.F., Liu, Y., Yin, X.H., Duan, H.T., Ma, J.H., 2017. Efficient removal of nitrobenzene by Fenton-like process with Co-Fe layered double hydroxide. Appl. Surf. Sci. 416, 45–50. https://doi.org/10.1016/j.apsusc.2017.04.117.

Ballenger, J.C., Post, R.M., 1980. Carbamazepine in manic-depressive illness: a new treatment. Am. J. Psychiatry 137, 782–790. https://doi.org/10.1176/ajp.137.7.782.

Baloyi, J., Ntho, T., Moma, J., 2018. Synthesis and application of pillared clay heterogeneous catalysts for wastewater treatment: a review. RSC Adv. 8, 5197–5211. https://doi.org/10.1039/c7ra12924f.

Barndok, H., Blanco, L., Hermosilla, D., Blanco, A., 2016. Heterogeneous photo-Fenton processes using zero valent iron microspheres for the treatment of wastewaters contaminated with 1,4-dioxane. Chem. Eng. J. 284, 112–121. https://doi.org/10.1016/j.cej.2015.08.097.

Bekyarova, E., Sarkar, S., Wang, F., Itkis, M.E., Kalinina, I., Tian, X., Haddon, R.C., 2013. Effect of covalent chemistry on the electronic structure and properties of carbon nanotubes and graphene. Acc. Chem. Res. 46, 65–76. https://doi.org/10.1021/ar300177q.

Blanco, L., Hermosilla, D., Merayo, N., Blanco, A., 2016. Assessing the use of zero-valent iron microspheres to catalyze Fenton treatment processes. J. Taiwan Inst. Chem. Eng. 69, 54–60. https://doi.org/10.1016/j.jtice.2016.08.014.

Bogan, B.W., Trbovic, V., 2003. Effect of sequestration on PAH degradability with Fenton's reagent: roles of total organic carbon, humin, and soil porosity. J. Hazard. Mater. 100, 285–300. https://doi.org/10.1016/S0304-3894(03)00134-1.

Boruah, P.K., Sharma, B., Karbhal, I., Shelke, M.V., Das, M.R., 2017. Ammonia-modified graphene sheets decorated with magnetic Fe3O4 nanoparticles for the photocatalytic and photo-Fenton degradation of phenolic compounds under sunlight irradiation. J. Hazard. Mater. 325, 90–100. https://doi.org/10.1016/j.jhazmat.2016.11.023.

Brame, J., Long, M.C., Li, Q.L., Alvarez, P., 2014. Trading oxidation power for efficiency: differential inhibition of photo-generated hydroxyl radicals versus singlet oxygen. Water Res. 60, 259–266. https://doi.org/10.1016/j.watres.2014.05.005.

Brillas, E., Sirés, I., Oturan, M.A., 2009. Electro-Fenton process and related electrochemical technologies based on Fenton's reaction chemistry. Chem. Rev. 109, 6570–6631. https://doi.org/10.1021/cr900136g.

Buda, F., Ensing, B., Gribnau, M.C.M., Baerends, E.J., 2001. DFT study of the active intermediate in the Fenton reaction. Chem. A Eur. J. 7, 2775–2783. https://doi.org/10.1002/1521-3765(20010702)7:13<2775::AID-CHEM2775>3.0.CO;2-6.

Cai, C., Zhang, Z.Y., Liu, J., Shan, N., Zhang, H., Dionysiou, D.D., 2016. Visible light-assisted heterogeneous Fenton with ZnFe2O4 for the degradation of Orange II in water. Appl. Catal. B Environ. 182, 456–468. https://doi.org/10.1016/j.apcatb.2015.09.056.

Cai, C., Zhang, Z., Liu, J., Shan, N., Zhang, H., Dionysiou, D.D., 2016. Visible light-assisted heterogeneous Fenton with ZnFe2O4 for the degradation of Orange II in water. Appl. Catal. B Environ. 182, 456–468. https://doi.org/10.1016/j.apcatb.2015.09.056.

Cao, S., Low, J., Yu, J., Jaroniec, M., 2015. Polymeric photocatalysts based on graphitic carbon nitride. Adv. Mater. 27, 2150–2176. https://doi.org/10.1002/adma.201500033.

Carra, I., Sánchez Pérez, J.A., Malato, S., Autin, O., Jefferson, B., Jarvis, P., 2015. Application of high intensity UVC-LED for the removal of acetamiprid with the photo-Fenton process. Chem. Eng. J. 264, 690–696. https://doi.org/10.1016/j.cej.2014.11.142.

Catrinescu, C., Arsene, D., Apopei, P., Teodosiu, C., 2012. Degradation of 4-chlorophenol from wastewater through heterogeneous Fenton and photo-Fenton process, catalyzed by Al-Fe PILC. Appl. Clay Sci. 58, 96–101. https://doi.org/10.1016/j.clay.2012.01.019.

Chandra, R., Mukhopadhyay, S., Nath, M., 2016. TiO2@ZIF-8: a novel approach of modifying micro-environment for enhanced photo-catalytic dye degradation and

high usability of TiO2 nanoparticles. Mater. Lett. 164, 571–574. https://doi.org/10.1016/j.matlet.2015.11.018.
Chen, H.Y., 2019. Why the reactive oxygen species of the Fenton reaction switches from oxoiron(iv) species to hydroxyl radical in phosphate buffer solutions? a computational rationale. ACS Omega 4, 14105–14113. https://doi.org/10.1021/acsomega.9b02023.
Cheng, R., Kang, M., Zhuang, S., Wang, S., Zheng, X., Pan, X., Shi, L., Wang, J., 2019. Removal of bacteriophage f2 in water by Fe/Ni nanoparticles: optimization of Fe/Ni ratio and influencing factors. Sci. Total Environ. 649, 995–1003. https://doi.org/10.1016/j.scitotenv.2018.08.380.
Cheng, M., Lai, C., Liu, Y., Zeng, G., Huang, D., Zhang, C., Qin, L., Hu, L., Zhou, C., Xiong, W., 2018. Metal-organic frameworks for highly efficient heterogeneous Fenton-like catalysis. Coord. Chem. Rev. 368, 80–92. https://doi.org/10.1016/j.ccr.2018.04.012.
Cheng, M.M., Ma, W.H., Chen, C.C., Yao, J.N., Zhao, J.C., 2006. Photocatalytic degradation of organic pollutants catalyzed by layered iron(II) bipyridine complex-clay hybrid under visible irradiation. Appl. Catal. B Environ. 65, 217–226. https://doi.org/10.1016/j.apcatb.2006.01.010.
Chen, X.J., Chen, F.G., Liu, F.L., Yan, X.D., Hu, W., Zhang, G.B., Tian, L.H., Xia, Q.H., Chen, X.B., 2016. Ag nanoparticles/hematite mesocrystals superstructure composite: a facile synthesis and enhanced heterogeneous photo-Fenton activity. Catal. Sci. Technol. 6, 4184–4191. https://doi.org/10.1039/c6cy00080k.
Cho, M., Kim, J., Kim, J.Y., Yoon, J., Kim, J.H., 2010. Mechanisms of *Escherichia coli* inactivation by several disinfectants. Water Res. 44, 3410–3418. https://doi.org/10.1016/j.watres.2010.03.017.
Chu, C., Ryberg, E.C., Loeb, S.K., Suh, M.J., Kim, J.H., 2019. Water disinfection in rural areas demands unconventional solar technologies. Acc. Chem. Res. 52, 1187–1195. https://doi.org/10.1021/acs.accounts.8b00578.
Chu, Y., Tan, X., Shen, Z., Liu, P., Han, N., Kang, J., Duan, X., Wang, S., Liu, L., Liu, S., 2018. Efficient removal of organic and bacterial pollutants by Ag-La0.8Ca0.2Fe0.94O3-Δ perovskite via catalytic peroxymonosulfate activation. J. Hazard. Mater. 356, 53–60. https://doi.org/10.1016/j.jhazmat.2018.05.044.
Clarizia, L., Russo, D., Di Somma, I., Marotta, R., Andreozzi, R., 2017. Homogeneous photo-Fenton processes at near neutral pH: a review. Appl. Catal. B Environ. 209, 358–371. https://doi.org/10.1016/j.apcatb.2017.03.011.
Clarizia, L., Russo, D., Di Somma, I., Marotta, R., Andreozzi, R., 2017. Homogeneous photo-Fenton processes at near neutral pH: a review. Appl. Catal. B Environ. 209, 358–371. https://doi.org/10.1016/j.apcatb.2017.03.011.
Clarizia, L., Russo, D., Di Somma, I., Marotta, R., Andreozzi, R., 2017. Homogeneous photo-Fenton processes at near neutral pH: a review. Appl. Catal. B Environ. 209, 358–371. https://doi.org/10.1016/j.apcatb.2017.03.011.
Comninellis, C., Kapalka, A., Malato, S., Parsons, S.A., Poulios, I., Mantzavinos, D., 2008. Advanced oxidation processes for water treatment: advances and trends for R&D. J. Chem. Technol. Biotechnol. 83, 769–776. https://doi.org/10.1002/jctb.1873.
Costa, R.C.C., Lelis, M.F.F., Oliveira, L.C.A., Fabris, J.D., Ardisson, J.D., Rios, R., Silva, C.N., Lago, R.M., 2006. Novel active heterogeneous Fenton system based on Fe3-xMxO4 (Fe, Co, Mn, Ni): the role of M2+ species on the reactivity towards H2O2 reactions. J. Hazard. Mater. 129, 171–178. https://doi.org/10.1016/j.jhazmat.2005.08.028.
Dai, L., 2013. Functionalization of graphene for efficient energy conversion and storage. Acc. Chem. Res. 46, 31–42. https://doi.org/10.1021/ar300122m.
Davis, R., Markham, A., Balfour, J.A., 1996. Ciprofloxacin: an updated review of its pharmacology, therapeutic efficacy and tolerability. Drugs 51, 1019–1074. https://doi.org/10.2165/00003495-199651060-00010.
Demirbas, A., 2008. Heavy metal adsorption onto agro-based waste materials: a review. J. Hazard. Mater. 157, 220–229. https://doi.org/10.1016/j.jhazmat.2008.01.024.
Denny, M.S., Moreton, J.C., Benz, L., Cohen, S.M., 2016. Metal-organic frameworks for membrane-based separations. Nat. Rev. Mater. 1, 1–17. https://doi.org/10.1038/natrevmats.2016.78.
Deria, P., Mondloch, J.E., Karagiaridi, O., Bury, W., Hupp, J.T., Farha, O.K., 2014. Beyond post-synthesis modification: Evolution of metal-organic frameworks via building block replacement. Chem. Soc. Rev. 43, 5896–5912. https://doi.org/10.1039/c4cs00067f.
Diao, M.H., Yao, M.S., 2009. Use of zero-valent iron nanoparticles in inactivating microbes. Water Res. 43, 5243–5251. https://doi.org/10.1016/j.watres.2009.08.051.
Divyapriya, G., Nidheesh, P.V., 2020. Importance of graphene in the electro-Fenton process. ACS Omega 5, 4725–4732. https://doi.org/10.1021/acsomega.9b04201.
Duan, H., Liu, Y., Yin, X., Bai, J., Qi, J., 2016. Degradation of nitrobenzene by Fenton-like reaction in a H2O2/schwertmannite system. Chem. Eng. J. 283, 873–879. https://doi.org/10.1016/j.cej.2015.08.033.
Du, Q., Li, G., Zhang, S., Song, J., zhao, Y., Yang, F., 2020. High-dispersion zero-valent iron particles stabilized by artificial humic acid for lead ion removal. J. Hazard. Mater. 383, 121170 https://doi.org/10.1016/j.jhazmat.2019.121170.
Du, D., Shi, W., Wang, L.Z., Zhang, J.L., 2017. Yolk-shell structured Fe3O4@void@TiO2 as a photo-Fenton-like catalyst for the extremely efficient elimination of tetracycline. Appl. Catal. B Environ. 200, 484–492. https://doi.org/10.1016/j.apcatb.2016.07.043.
Du, D., Shi, W., Wang, L., Zhang, J., 2017. Yolk-shell structured Fe3O4@void@TiO2 as a photo-Fenton-like catalyst for the extremely efficient elimination of tetracycline. Appl. Catal. B Environ. 200, 484–492. https://doi.org/10.1016/j.apcatb.2016.07.043.
English for Writing Research Papers Useful Phrases, (2016) 9–16. ⟨http://www.springer.com/cda/content/document/cda_downloaddocument/Free+Download+-+Useful+Phrases.pdf?SGWID=0-0-45-1543172-p177775190⟩.
Ezzatahmadi, N., Ayoko, G.A., Millar, G.J., Speight, R., Yan, C., Li, J.H., Li, S.Z., Zhu, J.X., Xi, Y.F., 2017. Clay-supported nanoscale zero-valent iron composite materials for the remediation of contaminated aqueous solutions: a review. Chem. Eng. J. 312, 336–350. https://doi.org/10.1016/j.cej.2016.11.154.
Fagan, R., McCormack, D.E., Dionysiou, D.D., Pillai, S.C., 2016. A review of solar and visible light active TiO2 photocatalysis for treating bacteria, cyanotoxins and contaminants of emerging concern. Mater. Sci. Semicond. Process. 42, 2–14. https://doi.org/10.1016/j.mssp.2015.07.052.
Fang, G., Liu, C., Gao, J., Dionysiou, D.D., Zhou, D., 2015. Manipulation of persistent free radicals in biochar to activate persulfate for contaminant degradation. Environ. Sci. Technol. 49, 5645–5653. https://doi.org/10.1021/es5061512.
Farha, O.K., Hupp, J.T., 2010. Rational design, synthesis, purification, and activation of metal-organic framework materials. Acc. Chem. Res. 43, 1166–1175. https://doi.org/10.1021/ar1000617.
Feng, J.Y., Hu, X.J., Yue, P.L., 2006. Effect of initial solution pH on the degradation of Orange II using clay-based Fe nanocomposites as heterogeneous photo-Fenton catalyst. Water Res. 40, 641–646. https://doi.org/10.1016/j.watres.2005.12.021.
Feng, S., Wang, R., Bai, Y., Yang, S., Ma, Q., Yilihamu, A., Yang, S.T., Luo, J., 2019. Fe3O4/SiO2/C nanocomposites for the fenton-like disinfection of Escherichia coli in water. Mater. Res. Express 6, 0–7. https://doi.org/10.1088/2053-1591/ab0585.
Feng, M., Wang, Z., Dionysiou, D.D., Sharma, V.K., 2018. Metal-mediated oxidation of fluoroquinolone antibiotics in water: a review on kinetics, transformation products, and toxicity assessment. J. Hazard. Mater. 344, 1136–1154. https://doi.org/10.1016/j.jhazmat.2017.08.067.
Koppenol, W.H., 1993. The centennial of the Fenton reaction. Free Radic. Biol. Med. 15, 645–651. https://doi.org/10.1016/0891-5849(93)90168-T.
Ferri, D., Forni, L., 1998. Methane combustion on some perovskite-like mixed oxides. Appl. Catal. B Environ. 16, 119–126. https://doi.org/10.1016/s0926-3373(97)00065-9.
Fontecha-Cámara, M.A., Moreno-Castilla, C., López-Ramón, M.V., Álvarez, M.A., 2016. Mixed iron oxides as Fenton catalysts for gallic acid removal from aqueous solutions. Appl. Catal. B Environ. 196, 207–215. https://doi.org/10.1016/j.apcatb.2016.05.032.
Fu, F., Dionysiou, D.D., Liu, H., 2014. The use of zero-valent iron for groundwater remediation and wastewater treatment: a review. J. Hazard. Mater. 267, 194–205. https://doi.org/10.1016/j.jhazmat.2013.12.062.
Fu, F., Wang, Q., 2011. Removal of heavy metal ions from wastewaters: a review. J. Environ. Manag. 92, 407–418. https://doi.org/10.1016/j.jenvman.2010.11.011.
Ganiyu, S.O., Zhou, M., Martínez-Huitle, C.A., 2018. Heterogeneous electro-Fenton and photoelectro-Fenton processes: a critical review of fundamental principles and application for water/wastewater treatment. Appl. Catal. B Environ. 235, 103–129. https://doi.org/10.1016/j.apcatb.2018.04.044.
Ganiyu, S.O., Zhou, M., Martínez-Huitle, C.A., 2018. Heterogeneous electro-Fenton and photoelectro-Fenton processes: a critical review of fundamental principles and application for water/wastewater treatment. Appl. Catal. B Environ. 235, 103–129. https://doi.org/10.1016/j.apcatb.2018.04.044.
Gan, P.P., Li, S.F.Y., 2013. Efficient removal of Rhodamine B using a rice hull-based silica supported iron catalyst by Fenton-like process. Chem. Eng. J. 229, 351–363. https://doi.org/10.1016/j.cej.2013.06.020.
Gao, P., Liu, Z., Tai, M., Sun, D.D., Ng, W., 2013. Multifunctional graphene oxide-TiO2 microsphere hierarchical membrane for clean water production. Appl. Catal. B Environ. 138–139, 17–25. https://doi.org/10.1016/j.apcatb.2013.01.014.
Gao, J., Wu, S., Han, Y., Tan, F., Shi, Y., Liu, M., Li, X., 2018. 3D mesoporous CuFe2O4 as a catalyst for photo-Fenton removal of sulfonamide antibiotics at near neutral pH. J. Colloid Interface Sci. 524, 409–416. https://doi.org/10.1016/j.jcis.2018.03.112.
García-Fernández, I., Polo-López, M.I., Oller, I., Fernández-Ibáñez, P., 2012. Bacteria and fungi inactivation using Fe 3+/sunlight, H 2O 2/sunlight and near neutral photo-Fenton: a comparative study. Appl. Catal. B Environ. 121–122, 20–29. https://doi.org/10.1016/j.apcatb.2012.03.012.
Garrido-Ramírez, E.G., Theng, B.K.G., Mora, M.L., 2010. Clays and oxide minerals as catalysts and nanocatalysts in Fenton-like reactions - a review. Appl. Clay Sci. 47, 182–192. https://doi.org/10.1016/j.clay.2009.11.044.
Garrido-ramírez, E.G., Theng, B.K.G., Mora, M.L., 2010. Applied clay science clays and oxide minerals as catalysts and nanocatalysts in Fenton-like reactions — a review. Appl. Clay Sci. 47, 182–192. https://doi.org/10.1016/j.clay.2009.11.044.
Georgi, A., Schierz, A., Trommler, U., Horwitz, C.P., Collins, T.J., Kopinke, F.D., 2007. Humic acid modified Fenton reagent for enhancement of the working pH range. Appl. Catal. B Environ. 72, 26–36. https://doi.org/10.1016/j.apcatb.2006.10.009.
Giannakis, S., Inmaculada, M., López, P., Spuhler, D., Antonio, J., Pérez, S. , Fernández, P., Applied Catalysis B : Environmental Solar disinfection is an augmentable , in situ -generated photo-Fenton reaction — Part 1 : A review of the mechanisms and the fundamental aspects of the process, 199 (2016) 199–223. https://doi.org/10.1016/j.apcatb.2016.06.009.
Giannakis, S., Lopez, M.I.P., Spuhler, D., Perez, J.A.S., Ibanez, P.F., Pulgarin, C., 2016. Solar disinfection is an augmentable, in situ-generated photo-Fenton reaction-Part 1: a review of the mechanisms and the fundamental aspects of the process. Appl. Catal. B Environ. 199, 199–223. https://doi.org/10.1016/j.apcatb.2016.06.009.
Giannakis, S., Lopez, M.I.P., Spuhler, D., Perez, J.A.S., Ibanez, P.F., Pulgarin, C., 2016. Solar disinfection is an augmentable, in situ-generated photo-Fenton reaction Part 2: a review of the applications for drinking water and wastewater disinfection. Appl. Catal. B Environ. 198, 431–446. https://doi.org/10.1016/j.apcatb.2016.06.007.
Goldstein, S., Meyerstein, D., Czapski, G., 1993. The Fenton reagents. Free Radic. Biol. Med. 15, 435–445.
Gonzalez-Olmos, R., Holzer, F., Kopinke, F.D., Georgi, A., 2011. Indications of the reactive species in a heterogeneous Fenton-like reaction using Fe-containing zeolites. Appl. Catal. A Gen. 398, 44–53. https://doi.org/10.1016/j.apcata.2011.03.005.

Gonzalez-Olmos, R., Martin, M.J., Georgi, A., Kopinke, F.D., Oller, I., Malato, S., 2012. Fe-zeolites as heterogeneous catalysts in solar Fenton-like reactions at neutral pH. Appl. Catal. B Environ. 125, 51–58. https://doi.org/10.1016/j.apcatb.2012.05.022.
Gonzalez-Olmos, R., Roland, U., Toufar, H., Kopinke, F.D., Georgi, A., 2009. Fe-zeolites as catalysts for chemical oxidation of MTBE in water with H2O2. Appl. Catal. B Environ. 89, 356–364. https://doi.org/10.1016/j.apcatb.2008.12.014.
Guimarães, V., Teixeira, A.R., Lucas, M.S., Silva, A.M.T., Peres, J.A., 2019. Pillared interlayered natural clays as heterogeneous photocatalysts for H_2O_2 -assisted treatment of a winery wastewater. Sep. Purif. Technol. 228, 115768 https://doi.org/10.1016/j.seppur.2019.115768.
Guimaraes, V., Teixeira, A.R., Lucas, M.S., Silva, A.M.T., Peres, J.A., 2019. Pillared interlayered natural clays as heterogeneous photocatalysts for H2O2-assisted treatment of a winery wastewater. Sep. Purif. Technol. 228, 11. https://doi.org/10.1016/j.seppur.2019.115768.
Guo, T., Wang, K., Zhang, G., Wu, X., 2019. A novel α-Fe $_2$ O $_3$ @g-C 3 N 4 catalyst: synthesis derived from Fe-based MOF and its superior photo-Fenton performance. Appl. Surf. Sci. 469, 331–339. https://doi.org/10.1016/j.apsusc.2018.10.183.
Guo, S., Yuan, N., Zhang, G., Yu, J.C., 2017. Graphene modified iron sludge derived from homogeneous Fenton process as an efficient heterogeneous Fenton catalyst for degradation of organic pollutants. Microporous Mesoporous Mater. 238, 62–68. https://doi.org/10.1016/j.micromeso.2016.02.033.
Gursky, J.A., Blough, S.D., Luna, C., Gomez, C., Luevano, A.N., Gardner, E.A., 2006. Particle-particle interactions between layered double hydroxide nanoparticles. J. Am. Chem. Soc. 128, 8376–8377. https://doi.org/10.1021/ja0612100.
Hadjltaief, H.B., Ben Zina, M., Galvez, M.E., Da Costa, P., 2015. Photo-Fenton oxidation of phenol over a Cu-doped Fe-pillared clay. Comptes Rendus Chim. 18, 1161–1169. https://doi.org/10.1016/j.crci.2015.08.004.
Hamers, R.J., 2017. Nanomaterials and global sustainability. Acc. Chem. Res. 50, 633–637. https://doi.org/10.1021/acs.accounts.6b00634.
Han, S., Hu, L., Liang, Z., Wageh, S., Al-Ghamdi, A.A., Chen, Y., Fang, X., 2014. One-step hydrothermal synthesis of 2D Hexagonal nanoplates of α-Fe_2O_3 /Graphene composites with enhanced photocatalytic activity. Adv. Funct. Mater. 24, 5719–5727. https://doi.org/10.1002/adfm.201401279.
Hartmann, M., Kullmann, S., Keller, H., 2010. Wastewater treatment with heterogeneous Fenton-type catalysts based on porous materials. J. Mater. Chem. 20, 9002–9017. https://doi.org/10.1039/c0jm00577k.
Hasija, V., Raizada, P., Sudhaik, A., Sharma, K., Kumar, A., Singh, P., Jonnalagadda, S.B., Thakur, V.K., 2019. Recent advances in noble metal free doped graphitic carbon nitride based nanohybrids for photocatalysis of organic contaminants in water: A review. Appl. Mater. Today 15, 494–524. https://doi.org/10.1016/j.apmt.2019.04.003.
Hassan, H., Hameed, B.H., 2011. Fe-clay as effective heterogeneous Fenton catalyst for the decolorization of Reactive Blue 4. Chem. Eng. J. 171, 912–918. https://doi.org/10.1016/j.cej.2011.04.040.
Hermosilla, D., Han, C., Nadagouda, M.N., Machala, L., Gascó, A., Campo, P., Dionysiou, D.D., 2020. Environmentally friendly synthesized and magnetically recoverable designed ferrite photo-catalysts for wastewater treatment applications. J. Hazard. Mater. 381, 121200 https://doi.org/10.1016/j.jhazmat.2019.121200.
Herney-Ramirez, J., Lampinen, M., Vicente, M.A., Costa, C.A., Madeira, L.M., 2008. Experimental design to optimize the oxidation of orange II dye solution using a clay-based fenton-like catalyst. Ind. Eng. Chem. Res. 47, 284–294. https://doi.org/10.1021/ie070990y.
Herney-Ramirez, J., Vicente, M.A., Madeira, L.M., 2010. Heterogeneous photo-Fenton oxidation with pillared clay-based catalysts for wastewater treatment: a review. Appl. Catal. B Environ. 98, 10–26. https://doi.org/10.1016/j.apcatb.2010.05.004.
Herney-Ramirez, J., Vicente, M.A., Madeira, L.M., 2010. Heterogeneous photo-Fenton oxidation with pillared clay-based catalysts for wastewater treatment: a review. Appl. Catal. B Environ. 98, 10–26. https://doi.org/10.1016/j.apcatb.2010.05.004.
He, D.L., Chen, Y.F., Situ, Y., Zhong, L., Huang, H., 2017. Synthesis of ternary g-C3N4/Ag/gamma-FeOOH photocatalyst: an integrated heterogeneous Fenton-like system for effectively degradation of azo dye methyl orange under visible light. Appl. Surf. Sci. 425, 862–872. https://doi.org/10.1016/j.apsusc.2017.06.124.
He, J., Yang, X.F., Men, B., Wang, D.S., 2016. Interfacial mechanisms of heterogeneous Fenton reactions catalyzed by iron-based materials: a review. J. Environ. Sci. 39, 97–109. https://doi.org/10.1016/j.jes.2015.12.003.
He, J., Yang, X., Men, B., Wang, D., 2016. Interfacial mechanisms of heterogeneous Fenton reactions catalyzed by iron-based materials: a review. J. Environ. Sci. 39, 97–109. https://doi.org/10.1016/j.jes.2015.12.003.
Hodges, B.C., Cates, E.L., Kim, J.H., 2018. Challenges and prospects of advanced oxidation water treatment processes using catalytic nanomaterials. Nat. Nanotechnol. 13, 642–650. https://doi.org/10.1038/s41565-018-0216-x.
Holland Cheng, R., Kuhn, R.J., Olson, N.H., Rossmannˆ Hok-Kin Choi, M.G., Smith, T.J., Baker, T.S., 1995. Nucleocapsid and glycoprotein organization in an enveloped virus. Cell 80, 621–630. https://doi.org/10.1016/0092-8674(95)90516-2.
Horcajada, P., Gref, R., Baati, T., Allan, P.K., Maurin, G., Couvreur, P., Férey, G., Morris, R.E., Serre, C., 2012. Metal-organic frameworks in biomedicine. Chem. Rev. 112, 1232–1268. https://doi.org/10.1021/cr200256v.
Hossain, F., Perales-Perez, O.J., Hwang, S., Román, F., 2014. Antimicrobial nanomaterials as water disinfectant: applications, limitations and future perspectives. Sci. Total Environ. 466–467, 1047–1059. https://doi.org/10.1016/j.scitotenv.2013.08.009.
Hou, X.J., Huang, X.P., Jia, F.L., Ai, Z.H., Zhao, J.C., Zhang, L.Z., 2017. Hydroxylamine promoted goethite surface Fenton degradation of organic pollutants. Environ. Sci. Technol. 51, 5118–5126. https://doi.org/10.1021/acs.est.6b05906.
Hou, Y., Li, X.Y., Zhao, Q.D., Chen, G.H., 2013. ZnFe2O4 multi-porous microbricks/graphene hybrid photocatalyst: facile synthesis, improved activity and photocatalytic mechanism. Appl. Catal. B Environ. 142, 80–88. https://doi.org/10.1016/j.apcatb.2013.04.062.
Hou, Y., Li, X., Zhao, Q., Chen, G., 2013. ZnFe2O4 multi-porous microbricks/graphene hybrid photocatalyst: facile synthesis, improved activity and photocatalytic mechanism. Appl. Catal. B Environ. 142–143, 80–88. https://doi.org/10.1016/j.apcatb.2013.04.062.
Howarth, A.J., Liu, Y., Li, P., Li, Z., Wang, T.C., Hupp, J.T., Farha, O.K., 2016. Chemical, thermal and mechanical stabilities of metal-organic frameworks. Nat. Rev. Mater. 1, 1–15. https://doi.org/10.1038/natrevmats.2015.18.
Hrudey, S.E., 2009. Chlorination disinfection by-products, public health risk tradeoffs and me. Water Res 43, 2057–2092. https://doi.org/10.1016/j.watres.2009.02.011.
Huang, X.P., Hou, X.J., Zhao, J.C., Zhang, L.Z., 2016. Hematite facet confined ferrous ions as high efficient Fenton catalysts to degrade organic contaminants by lowering H2O2 decomposition energetic span. Appl. Catal. B Environ. 181, 127–137. https://doi.org/10.1016/j.apcatb.2015.06.061.
Huang, X., Zhu, N., Mao, F., Ding, Y., Zhang, S., Liu, H., Li, F., Wu, P., Dang, Z., Ke, Y., 2020. Enhanced heterogeneous photo-Fenton catalytic degradation of tetracycline over yCeO2/Fh composites: performance, degradation pathways, Fe2+ regeneration and mechanism. Chem. Eng. J. 392, 123636 https://doi.org/10.1016/j.cej.2019.123636.
Hua, G., Reckhow, D.A., 2007. Comparison of disinfection byproduct formation from chlorine and alternative disinfectants. Water Res. 41, 1667–1678. https://doi.org/10.1016/j.watres.2007.01.032.
Hughes, E.W., 1941. The crystal structure of melamine. J. Am. Chem. Soc. 63, 1737–1752. https://doi.org/10.1021/ja01851a069.
Huling, S.G., Arnold, R.G., Sierka, R.A., Miller, M.R., 2001. Influence of peat on Fenton oxidation. Water Res. 35, 1687–1694. https://doi.org/10.1016/S0043-1354(00)00443-7.
Hurtado, L., Romero, R., Mendoza, A., Brewer, S., Donkor, K., Gomez-Espinosa, R.M., Natividad, R., 2019. Paracetamol mineralization by photo Fenton process catalyzed by a Cu/Fe-PILC under circumneutral pH conditions. J. Photochem. Photobiol. A Chem. 373, 162–170. https://doi.org/10.1016/j.jphotochem.2019.01.012.
Hu, Z.T., Liang, Y.N., Zhao, J., Zhang, Y., Yang, E.H., Chen, J., Lim, T.T., 2018. Ultra-effective integrated technologies for water disinfection with a novel ^{0}D–^{2}D-3D nanostructured rGO-AgNP/Bi2Fe4O9 composite. Appl. Catal. B Environ. 227, 548–556. https://doi.org/10.1016/j.apcatb.2018.01.047.
Hu, X., Yu, J.C., Gong, J., Li, Q., Li, G., 2007. α-Fe2O3 Nanorings prepared by a microwave-assisted hydrothermal process and their sensing properties. Adv. Mater. 19, 2324–2329. https://doi.org/10.1002/adma.200602176.
Hu, J., Zhang, P., An, W., Liu, L., Liang, Y., Cui, W., 2019. In-situ Fe-doped g-C3N4 heterogeneous catalyst via photocatalysis-Fenton reaction with enriched photocatalytic performance for removal of complex wastewater. Appl. Catal. B Environ. 245, 130–142. https://doi.org/10.1016/j.apcatb.2018.12.029.
Jack, R.S., Ayoko, G.A., Adebajo, M.O., Frost, R.L., A review of iron species for visible-light photocatalytic water purification, (2015) 7439–7449. https://doi.org/10.1007/s11356–015-4346–5.
Janiak, C., Vieth, J.K., 2010. MOFs, MILs and more: concepts, properties and applications for porous coordination networks (PCNs). New J. Chem. 34, 2366–2388. https://doi.org/10.1039/c0nj00275e.
Jaramillo-Paez, C., Navio, J.A., Hidalgo, M.C., Bouziani, A., El Azzouzi, M., 2017. Mixed alpha-Fe2O3/Bi2WO6 oxides for photoassisted hetero-Fenton degradation of methyl orange and phenol. J. Photochem. Photobiol. A Chem. 332, 521–533. https://doi.org/10.1016/j.jphotochem.2016.09.031.
Jiang, W., Dionysiou, D.D., Kong, M., Liu, Z., Sui, Q., Lyu, S., 2020. Utilization of formic acid in nanoscale zero valent iron-catalyzed Fenton system for carbon tetrachloride degradation. Chem. Eng. J. 380, 122537 https://doi.org/10.1016/j.cej.2019.122537.
Jiang, Q., Zhu, R., Zhu, Y., Chen, Q., 2019. Efficient degradation of cefotaxime by a UV+ferrihydrite/TiO2+H2O2 process: the important role of ferrihydrite in transferring photo-generated electrons from TiO2 to H2O2. J. Chem. Technol. Biotechnol. 94, 2512–2521. https://doi.org/10.1002/jctb.6041.
Jia, M.D., Chen, B., Noble, R.D., Falconer, J.L., 1994. Ceramic-zeolite composite membranes and their application for separation of vapor/gas mixtures. J. Memb. Sci. 90, 1–10. https://doi.org/10.1016/0376-7388(94)80029-4.
Jin, H., Tian, X.K., Nie, Y.L., Zhou, Z.X., Yang, C., Li, Y., Lu, L.Q., 2017. Oxygen vacancy promoted heterogeneous Fenton-like degradation of ofloxacin at pH 3.2-9.0 by Cu substituted magnetic Fe3O4@FeOOH nanocomposite. Environ. Sci. Technol. 51, 12699–12706. https://doi.org/10.1021/acs.est.7b04503.
Ju, L.L., Chen, Z.Y., Fang, L., Dong, W., Zheng, F.G., Shen, M.R., 2011. Sol-Gel synthesis and photo-Fenton-like catalytic activity of EuFeO3 nanoparticles. J. Am. Ceram. Soc. 94, 3418–3424. https://doi.org/10.1111/j.1551-2916.2011.04522.x.
Kakavandi, B., Takdastan, A., Pourfadakari, S., Ahmadmoazzam, M., Jorfi, S., 2019. Heterogeneous catalytic degradation of organic compounds using nanoscale zero-valent iron supported on kaolinite: mechanism, kinetic and feasibility studies. J. Taiwan Inst. Chem. Eng. 96, 329–340. https://doi.org/10.1016/j.jtice.2018.11.027.
Kasiri, M.B., Aleboyeh, H., Aleboyeh, A., 2008. Degradation of Acid Blue 74 using Fe-ZSM5 zeolite as a heterogeneous photo-Fenton catalyst. Appl. Catal. B Environ. 84, 9–15. https://doi.org/10.1016/j.apcatb.2008.02.024.
Keijer, T., Bakker, V., Slootweg, J.C., 2019. Circular chemistry to enable a circular economy. Nat. Chem. 11, 190–195. https://doi.org/10.1038/s41557-019-0226-9.
Khankhasaeva, S.T., Dashinamzhilova, E.T., Dambueva, D.V., 2017. Oxidative degradation of sulfanilamide catalyzed by Fe/Cu/Al-pillared clays. Appl. Clay Sci. 146, 92–99. https://doi.org/10.1016/j.clay.2017.05.018.

Kita, H., Inoue, T., Asamura, H., Tanaka, K., Okamoto, K., 1997. NaY zeolite membrane for the pervaporation separation of methanol-methyl tert-butyl ether mixtures. Chem. Commun. 45–46. https://doi.org/10.1039/a605708j.

Kofuji, Y., Isobe, Y., Shiraishi, Y., Sakamoto, H., Tanaka, S., Ichikawa, S., Hirai, T., 2016. Carbon nitride-aromatic diimide-graphene nanohybrids: metal-free photocatalysts for solar-to-hydrogen peroxide energy conversion with 0.2% efficiency. J. Am. Chem. Soc. 138, 10019–10025. https://doi.org/10.1021/jacs.6b05806.

Koonin, E.V., Makarova, K.S., Aravind, L., 2001. Horizontal gene transfer in prokaryotes: quantification and classification. Annu. Rev. Microbiol. 55, 709–742. https://doi.org/10.1146/annurev.micro.55.1.709.

Krumina, L., Lyngsie, G., Tunlid, A., Persson, P., 2017. Oxidation of a dimethoxyhydroquinone by ferrihydrite and goethite nanoparticles: iron reduction versus surface catalysis. Environ. Sci. Technol. 51, 9053–9061. https://doi.org/10.1021/acs.est.7b02292.

Kuan, C.C., Chang, S.Y., Schroeder, S.L.M., 2015. Fenton-Like Oxidation of 4-Chlorophenol: homogeneous or Heterogeneous? Ind. Eng. Chem. Res. 54, 8122–8129. https://doi.org/10.1021/acs.iecr.5b02378.

Kuan, C.C., Chang, S.Y., Schroeder, S.L.M., 2015. Fenton-like oxidation of 4-chlorophenol: homogeneous or heterogeneous? Ind. Eng. Chem. Res. 54, 8122–8129. https://doi.org/10.1021/acs.iecr.5b02378.

Kumar, S.G., Devi, L.G., 2011. Review on modified TiO2 photocatalysis under UV/visible light: selected results and related mechanisms on interfacial charge carrier transfer dynamics. J. Phys. Chem. A. 115, 13211–13241. https://doi.org/10.1021/jp204364a.

Kundu, S., Jayachandran, M., 2013. Shape-selective synthesis of non-micellar cobalt oxide (CoO) nanomaterials by microwave irradiations. J. Nanopart. Res. 15, 1–13. https://doi.org/10.1007/s11051-013-1543-3.

Kuppler, R.J., Timmons, D.J., Fang, Q.R., Li, J.R., Makal, T.A., Young, M.D., Yuan, D., Zhao, D., Zhuang, W., Zhou, H.C., 2009. Potential applications of metal-organic frameworks. Coord. Chem. Rev. 253, 3042–3066. https://doi.org/10.1016/j.ccr.2009.05.019.

Kusic, H., Koprivanac, N., Selanec, I., 2006. Fe-exchanged zeolite as the effective heterogeneous Fenton-type catalyst for the organic pollutant minimization: UV irradiation assistance. Chemosphere 65, 65–73. https://doi.org/10.1016/j.chemosphere.2006.02.053.

Lado Ribeiro, A.R., Moreira, N.F.F., Li Puma, G., Silva, A.M.T., 2019. Impact of water matrix on the removal of micropollutants by advanced oxidation technologies. Chem. Eng. J. 363, 155–173. https://doi.org/10.1016/j.cej.2019.01.080.

Lan, Q., Li, F., Liu, C., Li, X.Z., 2008. Heterogeneous photodegradation of pentachlorophenol with maghemite and oxalate under UV illumination. Environ. Sci. Technol. 42, 7918–7923. https://doi.org/10.1021/es801220n.

Laurent, S., Forge, D., Port, M., Roch, A., Robic, C., Vander Elst, L., Muller, R.N., 2008. Magnetic iron oxide nanoparticles: synthesis, stabilization, vectorization, physicochemical characterizations and biological applications. Chem. Rev. 108, 2064–2110. https://doi.org/10.1021/cr068445e.

Laxma Reddy, P.V., Kavitha, B., Kumar Reddy, P.A., Kim, K.H., 2017. TiO2-based photocatalytic disinfection of microbes in aqueous media: a review. Environ. Res. 154, 296–303. https://doi.org/10.1016/j.envres.2017.01.018.

Lee, C., Kim, J.Y., Lee, W.I., Nelson, K.L., Yoon, J., Sedlak, D.L., 2008. Bactericidal effect of zero-valent iron nanoparticles on *Escherichia coli*. Environ. Sci. Technol. 42, 4927–4933. https://doi.org/10.1021/es800408u.

Lee, S.Y., Park, S.J., 2013. TiO2 photocatalyst for water treatment applications. J. Ind. Eng. Chem. 19, 1761–1769. https://doi.org/10.1016/j.jiec.2013.07.012.

Lesthaeghe, D., De Sterck, B., Van Speybroeck, V., Marin, G.B., Waroquier, M., 2007. Zeolite shape-selectivity in thegem-methylation of aromatic hydrocarbons. Angew. Chem. Int. Ed. 46, 1311–1314. https://doi.org/10.1002/anie.200604309.

Liang, R., Shen, L., Jing, F., Qin, N., Wu, L., 2015. Preparation of MIL-53(Fe)-reduced graphene oxide nanocomposites by a simple self-assembly strategy for increasing interfacial contact: efficient visible-light photocatalysts. ACS Appl. Mater. Interfaces 7, 9507–9515. https://doi.org/10.1021/acsami.5b00682.

Liao, X., Wang, F., Wang, F., Cai, Y., Yao, Y., Teng, B.T., Hao, Q., Shuxiang, L., 2019. Synthesis of (100) surface oriented MIL-88A-Fe with rod-like structure and its enhanced fenton-like performance for phenol removal. Appl. Catal. B Environ. 259 https://doi.org/10.1016/j.apcatb.2019.118064.

Lindsey, M.E., Tarr, M.A., 2000. Inhibition of hydroxyl radical reaction with aromatics by dissolved natural organic matter. Environ. Sci. Technol. 34, 444–449. https://doi.org/10.1021/es990457c.

Lindsey, M.E., Tarr, M.A., 2000. Quantitation of hydroxyl radical during Fenton oxidation following a single addition of iron and peroxide. Chemosphere 41, 409–417. https://doi.org/10.1016/S0045-6535(99)00296-9.

Ling, R., Chen, J.P., Shao, J., Reinhard, M., 2018. Degradation of organic compounds during the corrosion of ZVI by hydrogen peroxide at neutral pH: Kinetics, mechanisms and effect of corrosion promoting and inhibiting ions. Water Res. 134, 44–53. https://doi.org/10.1016/j.watres.2018.01.065.

Lin, S.S., Gurol, M.D., 1998. Catalytic decomposition of hydrogen peroxide on iron oxide: Kinetics, mechanism, and implications. Environ. Sci. Technol. 32, 1417–1423. https://doi.org/10.1021/es970648k.

Lin, H., Zhang, H., Wang, X., Wang, L.G., Wu, J., 2014. Electro-Fenton removal of Orange II in a divided cell: reaction mechanism, degradation pathway and toxicity evolution. Sep. Purif. Technol. 122, 533–540. https://doi.org/10.1016/j.seppur.2013.12.010.

Liu, S.Q., Feng, L.R., Xu, N., Chen, Z.G., Wang, X.M., 2012. Magnetic nickel ferrite as a heterogeneous photo-Fenton catalyst for the degradation of rhodamine B in the presence of oxalic acid. Chem. Eng. J. 203, 432–439. https://doi.org/10.1016/j.cej.2012.07.071.

Liu, Y., Guo, Z., Li, F., Xiao, Y., Zhang, Y., Bu, T., Jia, P., Zhe, T., Wang, L., 2019. Multifunctional magnetic copper ferrite nanoparticles as fenton-like reaction and near-infrared photothermal agents for synergetic antibacterial therapy. ACS Appl. Mater. Interfaces 11, 31649–31660. https://doi.org/10.1021/acsami.9b10096.

Liu, N., Huang, W., Zhang, X., Tang, L., Wang, L., Wang, Y., Wu, M., 2018. Ultrathin graphene oxide encapsulated in uniform MIL-88A(Fe) for enhanced visible light-driven photodegradation of RhB. Appl. Catal. B Environ. 221, 119–128. https://doi.org/10.1016/j.apcatb.2017.09.020.

Liu, Y., Mao, Y.Y., Tang, X.X., Xu, Y., Li, C.C., Li, F., 2017. Synthesis of Ag/AgCl/Fe-S plasmonic catalyst for bisphenol A degradation in heterogeneous photo-Fenton system under visible light irradiation. Chin. J. Catal. 38, 1726–1735. https://doi.org/10.1016/s1872-2067(17)62902-4.

Liu, J., Wang, H., Antonietti, M., 2016. Graphitic carbon nitride “reloaded”: emerging applications beyond (photo)catalysis. Chem. Soc. Rev. 45, 2308–2326. https://doi.org/10.1039/c5cs00767d.

Liu, H., Wang, Y., Ma, Y., Wei, Y., Pan, G., 2010. The microstructure of ferrihydrite and its catalytic reactivity. Chemosphere 79, 802–806. https://doi.org/10.1016/j.chemosphere.2010.03.007.

Liu, X., Zhou, Y., Zhang, J., Tang, L., Luo, L., Zeng, G., 2017. Iron containing metal-organic frameworks: structure, synthesis, and applications in environmental remediation. ACS Appl. Mater. Interfaces 9, 20255–20275. https://doi.org/10.1021/acsami.7b02563.

Li, X., Chen, S., Angelidaki, I., Zhang, Y., 2018. Bio-electro-Fenton processes for wastewater treatment: advances and prospects. Chem. Eng. J. 354, 492–506. https://doi.org/10.1016/j.cej.2018.08.052.

Li, Y., Jiang, J., Fang, Y., Cao, Z., Chen, D., Li, N., Xu, Q., Lu, J., 2018. TiO2 nanoparticles anchored onto the metal-organic framework NH2-MIL-88B(Fe) as an adsorptive photocatalyst with enhanced fenton-like degradation of organic pollutants under visible light irradiation. ACS Sustain. Chem. Eng. 6, 16186–16197. https://doi.org/10.1021/acssuschemeng.8b02968.

Li, J.R., Kuppler, R.J., Zhou, H.C., 2009. Selective gas adsorption and separation in metal-organic frameworks. Chem. Soc. Rev. 38, 1477–1504. https://doi.org/10.1039/b802426j.

Li, H.Y., Li, Y.L., Xiang, L.J., Huang, Q.Q., Qiu, J.J., Zhang, H., Sivaiah, M.V., Baron, F., Barrault, J., Petit, S., Valange, S., 2015. Heterogeneous photo-Fenton decolorization of orange II over Al-pillared Fe-smectite: response surface approach, degradation pathway, and toxicity evaluation. J. Hazard. Mater. 287, 32–41. https://doi.org/10.1016/j.jhazmat.2015.01.023.

Li, J.R., Ma, Y., McCarthy, M.C., Sculley, J., Yu, J., Jeong, H.K., Balbuena, P.B., Zhou, H.C., 2011. Carbon dioxide capture-related gas adsorption and separation in metal-organic frameworks. Coord. Chem. Rev. 255, 1791–1823. https://doi.org/10.1016/j.ccr.2011.02.012.

Li, S.L., Wang, W., Liang, F.P., Zhang, W.X., 2017. Heavy metal removal using nanoscale zero-valent iron (nZVI): theory and application. J. Hazard. Mater. 322, 163–171. https://doi.org/10.1016/j.jhazmat.2016.01.032.

Li, J., Xiao, C., Wang, K., Li, Y., Zhang, G., 2019. Enhanced generation of reactive oxygen species under visible light irradiation by adjusting the exposed facet of FeWO4 nanosheets to activate oxalic acid for organic pollutant removal and Cr(VI) reduction. Environ. Sci. Technol. 53, 11023–11030. https://doi.org/10.1021/acs.est.9b00641.

Luo, W., Zhu, L., Wang, N., Tang, H., Cao, M., She, Y., 2010. Efficient removal of organic pollutants with magnetic nanoscaled BiFeO 3 as a reusable heterogeneous fenton-like catalyst. Environ. Sci. Technol. 44, 1786–1791. https://doi.org/10.1021/es903390g.

Lv, H.J., Ma, L., Zeng, P., Ke, D.N., Peng, T.Y., 2010. Synthesis of floriated ZnFe2O4 with porous nanorod structures and its photocatalytic hydrogen production under visible light. J. Mater. Chem. 20, 3665–3672. https://doi.org/10.1039/b919897k.

Mai, H.X., Sun, L.D., Zhang, Y.W., Si, R., Feng, W., Zhang, H.P., Liu, H.C., Yan, C.H., 2005. Shape-selective synthesis and oxygen storage behavior of ceria nanopolyhedra, nanorods, and nanocubes. J. Phys. Chem. B. 109, 24380–24385. https://doi.org/10.1021/jp055584b.

Malato, S., Fernandez-Ibanez, P., Maldonado, M.I., Blanco, J., Gernjak, W., 2009. Decontamination and disinfection of water by solar photocatalysis: Recent overview and trends. Catal. Today 147, 1–59. https://doi.org/10.1016/j.cattod.2009.06.018.

Martinez-Macias, C., Serna, P., Gates, B.C., 2015. Isostructural zeolite-supported rhodium and iridium complexes: tuning catalytic activity and selectivity by ligand modification. ACS Catal. 5, 5647–5656. https://doi.org/10.1021/acscatal.5b00995.

Masarwa, M., Cohen, H., Meyerstein, D., Hickman, D.L., Bakac, A., Espenson, J.H., 1988. Reactions of low-valent transition-metal complexes with hydrogen-peroxide - are they fenton-like or not .1. the case of CU+AQ and CR-2+AQ. J. Am. Chem. Soc. 110, 4293–4297. https://doi.org/10.1021/ja00221a031.

Matafonova, G., Batoev, V., 2018. Recent advances in application of UV light-emitting diodes for degrading organic pollutants in water through advanced oxidation processes: a review. Water Res. 132, 177–189. https://doi.org/10.1016/j.watres.2017.12.079.

Ma, S., Jing, J., Liu, P., Li, Z., Jin, W., Xie, B., Zhao, Y., 2020. High selectivity and effectiveness for removal of tetracycline and its related drug resistance in food wastewater through schwertmannite/graphene oxide catalyzed photo-Fenton-like oxidation. J. Hazard. Mater. 392, 122437 https://doi.org/10.1016/j.jhazmat.2020.122437.

Ma, Y., Wang, B.B., Wang, Q., Xing, S.T., 2018. Facile synthesis of alpha-FeOOH/gamma-Fe2O3 by a pH gradient method and the role of gamma-Fe2O3 in H2O2 activation under visible light irradiation. Chem. Eng. J. 354, 75–84. https://doi.org/10.1016/j.cej.2018.08.011.

Ma, J., Yang, Q., Wen, Y., Liu, W., 2017. Fe-g-C3N4/graphitized mesoporous carbon composite as an effective Fenton-like catalyst in a wide pH range. Appl. Catal. B Environ. 201, 232–240. https://doi.org/10.1016/j.apcatb.2016.08.048.

Ma, J., Yang, M., Yu, F., Chen, J., 2015. Easy solid-phase synthesis of pH-insensitive heterogeneous CNTs/FeS Fenton-like catalyst for the removal of antibiotics from aqueous solution. J. Colloid Interface Sci. 444, 24–32. https://doi.org/10.1016/j.jcis.2014.12.027.

Mccullagh, C., Robertson, J.M.C., Bahnemann, D.W., Robertson, P.K.J., 2007. The application of TiO2 photocatalysis for disinfection of water contaminated with pathogenic micro-organisms: a review. Res. Chem. Intermed. 33, 359–375. https://doi.org/10.1163/156856707779238775.

Minella, M., Bertinetti, S., Hanna, K., Minero, C., Vione, D., 2019. Degradation of ibuprofen and phenol with a Fenton-like process triggered by zero-valent iron (ZVI-Fenton). Environ. Res. 179, 108750 https://doi.org/10.1016/j.envres.2019.108750.

Moncayo-Lasso, A., Sanabria, J., Pulgarin, C., Benítez, N., 2009. Simultaneous E. coli inactivation and NOM degradation in river water via photo-Fenton process at natural pH in solar CPC reactor. a new way for enhancing solar disinfection of natural water. Chemosphere 77, 296–300. https://doi.org/10.1016/j.chemosphere.2009.07.007.

Mondal, S.K., Saha, A.K., Sinha, A., 2018. Removal of ciprofloxacin using modified advanced oxidation processes: kinetics, pathways and process optimization. J. Clean. Prod. 171, 1203–1214. https://doi.org/10.1016/j.jclepro.2017.10.091.

Moon, G.H., Fujitsuka, M., Kim, S., Majima, T., Wang, X., Choi, W., 2017. Eco-Friendly photochemical production of H2O2 through O2 reduction over carbon nitride frameworks incorporated with multiple heteroelements. ACS Catal. 7, 2886–2895. https://doi.org/10.1021/acscatal.6b03334.

Moreira, N.F.F., Narciso-da-Rocha, C., Polo-López, M.I., Pastrana-Martínez, L.M., Faria, J.L., Manaia, C.M., Fernández-Ibáñez, P., Nunes, O.C., Silva, A.M.T., 2018. Solar treatment (H2O2, TiO2-P25 and GO-TiO2 photocatalysis, photo-Fenton) of organic micropollutants, human pathogen indicators, antibiotic resistant bacteria and related genes in urban wastewater. Water Res. 135, 195–206. https://doi.org/10.1016/j.watres.2018.01.064.

Munoz, M., de Pedro, Z.M., Casas, J.A., Rodriguez, J.J., 2015. Preparation of magnetite-based catalysts and their application in heterogeneous Fenton oxidation - a review. Appl. Catal. B Environ. 176, 249–265. https://doi.org/10.1016/j.apcatb.2015.04.003.

Navalon, S., Alvaro, M., Garcia, H., 2010. Heterogeneous Fenton catalysts based on clays, silicas and zeolites. Appl. Catal. B Environ. 99, 1–26. https://doi.org/10.1016/j.apcatb.2010.07.006.

Navalon, S., Dhakshinamoorthy, A., Alvaro, M., Garcia, H., 2011. Heterogeneous Fenton catalysts based on activated carbon and related materials. ChemSusChem 4, 1712–1730. https://doi.org/10.1002/cssc.201100216.

Nguyen, X.S., Zhang, G.K., Yang, X.F., 2017. Mesocrystalline Zn-Doped Fe3O4 hollow submicrospheres: formation mechanism and enhanced photo-Penton catalytic performance. ACS Appl. Mater. Interfaces 9, 8900–8909. https://doi.org/10.1021/acsami.6b16839.

Nidheesh, P.V., Gandhimathi, R., 2012. Trends in electro-Fenton process for water and wastewater treatment: an overview. Desalination 299, 1–15. https://doi.org/10.1016/j.desal.2012.05.011.

Nidheesh, P.V., 2015. Heterogeneous Fenton catalysts for the abatement of organic pollutants from aqueous solution: a review. RSC Adv. 5, 40552–40577. https://doi.org/10.1039/c5ra02023a.

Nidheesh, P.V., Gandhimathi, R., Velmathi, S., Sanjini, N.S., 2014. Magnetite as a heterogeneous electro Fenton catalyst for the removal of Rhodamine B from aqueous solution. RSC Adv. 4, 5698–5708. https://doi.org/10.1039/c3ra46969g.

Nidheesh, P.V., 2017. Graphene-based materials supported advanced oxidation processes for water and wastewater treatment: a review. Environ. Sci. Pollut. Res. 24, 27047–27069. https://doi.org/10.1007/s11356-017-0481-5.

Nieto-Juarez, J.I., Kohn, T., 2013. Virus removal and inactivation by iron (hydr)oxide-mediated Fenton-like processes under sunlight and in the dark. Photochem. Photobiol. Sci. 12, 1596–1605. https://doi.org/10.1039/c3pp25314g.

Nieto-Juarez, J.I., Pierzchla, K., Sienkiewicz, A., Kohn, T., 2010. Inactivation of MS2 coliphage in Fenton and Fenton-like systems: role of transition metals, hydrogen peroxide and sunlight. Environ. Sci. Technol. 44, 3351–3356. https://doi.org/10.1021/es903739f.

Nie, Y., Zhang, L., Li, Y.Y., Hu, C., 2015. Enhanced Fenton-like degradation of refractory organic compounds by surface complex formation of LaFeO3 and H2O2. J. Hazard. Mater. 294, 195–200. https://doi.org/10.1016/j.jhazmat.2015.03.065.

Nogueira, F.G.E., Lopes, J.H., Silva, A.C., Lago, R.M., Fabris, J.D., Oliveira, L.C.A., 2011. Catalysts based on clay and iron oxide for oxidation of toluene. Appl. Clay Sci. 51, 385–389. https://doi.org/10.1016/j.clay.2010.12.007.

Noorjahan, A., Kumari, V.D., Subrahmanyam, A., Panda, L., 2005. Immobilized Fe(III)-HY: an efficient and stable photo-Fenton catalyst. Appl. Catal. B Environ. 57, 291–298. https://doi.org/10.1016/j.apcatb.2004.11.006.

Ola, O., Maroto-Valer, M.M., 2015. Review of material design and reactor engineering on TiO2 photocatalysis for CO_2 reduction. J. Photochem. Photobiol. C Photochem. Rev. 24, 16–42. https://doi.org/10.1016/j.jphotochemrev.2015.06.001.

Oller, I., Malato, S., Sánchez-Pérez, J.A., 2011. Combination of advanced oxidation processes and biological treatments for wastewater decontamination-a review. Sci. Total Environ. 409, 4141–4166. https://doi.org/10.1016/j.scitotenv.2010.08.061.

Ortega-Gómez, E., Ballesteros Martín, M.M., Carratalà, A., Fernández Ibañez, P., Sánchez Pérez, J.A., Pulgarín, C., 2015. Principal parameters affecting virus inactivation by the solar photo-Fenton process at neutral pH and μM concentrations of H2O2 and Fe2+/3+. Appl. Catal. B Environ. 174–175, 395–402. https://doi.org/10.1016/j.apcatb.2015.03.016.

O'Carroll, D., Sleep, B., Krol, M., Boparai, H., Kocur, C., 2013. Nanoscale zero valent iron and bimetallic particles for contaminated site remediation. Adv. Water Resour. 51, 104–122. https://doi.org/10.1016/j.advwatres.2012.02.005.

O'Dowd, K., Pillai, S.C., 2020. Photo-Fenton disinfection at near neutral pH: process, parameter optimization and recent advances. J. Environ. Chem. Eng. 8, 104063 https://doi.org/10.1016/j.jece.2020.104063.

O'Keeffe, M., Yaghi, O.M., 2012. Deconstructing the crystal structures of metal-organic frameworks and related materials into their underlying nets. Chem. Rev. 112, 675–702. https://doi.org/10.1021/cr200205j.

Pan, K., Yang, C., Hu, J., Yang, W., Liu, B., Yang, J., Liang, S., Xiao, K., Hou, H., 2020. Oxygen vacancy mediated surface charge redistribution of Cu-substituted LaFeO3 for degradation of bisphenol A by efficient decomposition of H2O2. J. Hazard. Mater. 389, 122072 https://doi.org/10.1016/j.jhazmat.2020.122072.

Patra, A.K., Kundu, S.K., Bhaumik, A., Kim, D., 2016. Morphology evolution of single-crystalline hematite nanocrystals: magnetically recoverable nanocatalysts for enhanced facet-driven photoredox activity. Nanoscale 8, 365–377. https://doi.org/10.1039/c5nr06509g.

Pecson, B.M., Decrey, L., Kohn, T., 2012. Photoinactivation of virus on iron-oxide coated sand: enhancing inactivation in sunlit waters. Water Res. 46, 1763–1770. https://doi.org/10.1016/j.watres.2011.12.059.

Pelaez, M., Nolan, N.T., Pillai, S.C., Seery, M.K., Falaras, P., Kontos, A.G., Dunlop, P.S.M., Hamilton, J.W.J., Byrne, J.A., O'Shea, K., Entezari, M.H., Dionysiou, D.D., 2012. A review on the visible light active titanium dioxide photocatalysts for environmental applications. Appl. Catal. B Environ. 125, 331–349. https://doi.org/10.1016/j.apcatb.2012.05.036.

Pera-Titus, M., García-Molina, V., Baños, M.A., Giménez, J., Esplugas, S., 2004. Degradation of chlorophenols by means of advanced oxidation processes: a general review. Appl. Catal. B Environ. 47, 219–256. https://doi.org/10.1016/j.apcatb.2003.09.010.

Pereira, M.C., Oliveira, L.C.A., Murad, E., 2012. Iron oxide catalysts: Fenton and Fentonlike reactions – a review. Clay Min. 47, 285–302. https://doi.org/10.1180/claymin.2012.047.3.01.

Pérez, M.H., Peñuela, G., Maldonado, M.I., Malato, O., Fernández-Ibáñez, P., Oller, I., Gernjak, W., Malato, S., 2006. Degradation of pesticides in water using solar advanced oxidation processes. Appl. Catal. B Environ. 64, 272–281. https://doi.org/10.1016/j.apcatb.2005.11.013.

Perisic, D.J., Gilja, V., Stankov, M.N., Katancic, Z., Kusic, H., Stangar, U.L., Dionysiou, D.D., Bozic, A.L., 2016. Removal of diclofenac from water by zeolite-assisted advanced oxidation processes. J. Photochem. Photobiol. a-Chem. 321, 238–247. https://doi.org/10.1016/j.jphotochem.2016.01.030.

Plakas, K.V., Sklari, S.D., Yiankakis, D.A., Sideropoulos, G.T., Zaspalis, V.T., Karabelas, A.J., 2016. Removal of organic micropollutants from drinking water by a novel electro-Fenton filter: pilot-scale studies. Water Res. https://doi.org/10.1016/j.watres.2016.01.013.

Polo, D., García-Fernández, I., Fernández-Ibañez, P., Romalde, J.L., 2018. Hepatitis a virus disinfection in water by solar photo–Fenton systems. Food Environ. Virol. 10, 159–166. https://doi.org/10.1007/s12560-018-9339-3.

Polshettiwar, V., Luque, R., Fihri, A., Zhu, H., Bouhrara, M., Basset, J.M., 2011. Magnetically recoverable nanocatalysts. Chem. Rev. 111, 3036–3075. https://doi.org/10.1021/cr100230z.

Poree, C., Schoenebeck, F., 2017. A holy grail in chemistry: computational catalyst design: feasible or fiction? Acc. Chem. Res. 50, 605–608. https://doi.org/10.1021/acs.accounts.6b00606.

Pouran, S.R., Aziz, A., Raman, A., Mohd, W., Wan, A., 2014. Review on the application of modi fi ed iron oxides as heterogeneous catalysts in Fenton reactions. J. Clean. Prod. 64, 24–35. https://doi.org/10.1016/j.jclepro.2013.09.013.

Pradhan, G.K., Sahu, N., Parida, K.M., 2013. Fabrication of S, N co-doped alpha-Fe2O3 nanostructures: effect of doping, OH radical formation, surface area, 110 plane and particle size on the photocatalytic activity. RSC Adv. 3, 7912–7920. https://doi.org/10.1039/c3ra23088k.

Primo, A., Garcia, H., 2014. Zeolites as catalysts in oil refining. Chem. Soc. Rev. 43, 7548–7561. https://doi.org/10.1039/c3cs60394f.

Qian, X.F., Wu, Y.W., Kan, M., Fang, M.Y., Yue, D.T., Zeng, J., Zhao, Y.X., 2018. FeOOH quantum dots coupled g-C3N4 for visible light driving photo- Fenton degradation of organic pollutants. Appl. Catal. B Environ. 237, 513–520. https://doi.org/10.1016/j.apcatb.2018.05.074.

Qin, Y., Zhang, L., An, T., 2017. Hydrothermal carbon-mediated fenton-like reaction mechanism in the degradation of alachlor: direct electron transfer from hydrothermal carbon to Fe(III). ACS Appl. Mater. Interfaces 9, 17115–17124. https://doi.org/10.1021/acsami.7b03310.

Quan, L.N., Rand, B.P., Friend, R.H., Mhaisalkar, S.G., Lee, T.W., Sargent, E.H., 2019. Perovskites for Next-Generation Optical Sources. Chem. Rev. 119, 7444–7477. https://doi.org/10.1021/acs.chemrev.9b00107.

Rahim Pouran, S., Abdul Aziz, A.R., Wan Daud, W.M.A., 2015. Review on the main advances in photo-Fenton oxidation system for recalcitrant wastewaters. J. Ind. Eng. Chem. 21, 53–69. https://doi.org/10.1016/j.jiec.2014.05.005.

Rahim Pouran, S., Abdul Raman, A.A., Wan, W.M.A., 2014. Daud, review on the application of modified iron oxides as heterogeneous catalysts in Fenton reactions. J. Clean. Prod. 64, 24–35. https://doi.org/10.1016/j.jclepro.2013.09.013.

Raming, T.P., Winnubst, A.J.A., Van Kats, C.M., Philipse, A.P., 2002. The synthesis and magnetic properties of nanosized hematite (α-Fe2O3) particles. J. Colloid Interface Sci. 249, 346–350. https://doi.org/10.1006/jcis.2001.8194.

Ramirez, J.H., Maldonado-Hódar, F.J., Pérez-Cadenas, A.F., Moreno-Castilla, C., Costa, C.A., Madeira, L.M., 2007. Azo-dye Orange II degradation by heterogeneous Fenton-like reaction using carbon-Fe catalysts. Appl. Catal. B Environ. 75, 312–323. https://doi.org/10.1016/j.apcatb.2007.05.003.

Rasheed, H.U., Lv, X., Zhang, S., Wei, W., Ullah, N., Xie, J., 2018. Ternary MIL-100(Fe) @Fe3O4/CA magnetic nanophotocatalysts (MNPCs): magnetically separable and Fenton-like degradation of tetracycline hydrochloride. Adv. Powder Technol. 29, 3305–3314. https://doi.org/10.1016/j.apt.2018.09.011.

Rincon, A.G., Pulgarin, C., 2006. Comparative evaluation of Fe3+ and TiO2 photoassisted processes in solar photocatalytic disinfection of water. Appl. Catal. B Environ. 63, 222–231. https://doi.org/10.1016/j.apcatb.2005.10.009.

Rodríguez-Chueca, J., Mosteo, R., Ormad, M.P., Ovelleiro, J.L., 2012. Factorial experimental design applied to *Escherichia coli* disinfection by Fenton and photo-Fenton processes. Sol. Energy 86, 3260–3267. https://doi.org/10.1016/j.solener.2012.08.015.

Rodriguez-Chueca, J., Polo-Lopez, M.I., Mosteo, R., Ormad, M.P., Fernandez-Ibanez, P., 2014. Disinfection of real and simulated urban wastewater effluents using a mild solar photo-Fenton. Appl. Catal. B Environ. 150, 619–629. https://doi.org/10.1016/j.apcatb.2013.12.027.

Ruales-lonfat, C., Barona, J.F., Sienkiewicz, A., Bensimon, M., Vélez-colmenares, J., 2015a. Environmental Iron oxides semiconductors are efficients for solar water disinfection : a comparison with photo-Fenton processes at neutral pH. Appl. Catal. B Environ. 166-167, 497–508. https://doi.org/10.1016/j.apcatb.2014.12.007.

Ruales-Lonfat, C., Barona, J.F., Sienkiewicz, A., Bensimon, M., Velez-Colmenares, J., Benitez, N., Pulgarin, C., 2015b. Iron oxides semiconductors are efficients for solar water disinfection: a comparison with photo-Fenton processes at neutral pH. Appl. Catal. B Environ. 166, 497–508. https://doi.org/10.1016/j.apcatb.2014.12.007.

Ruales-Lonfat, C., Benitez, N., Sienkiewicz, A., Pulgarin, C., 2014. Deleterious effect of homogeneous and heterogeneous near-neutral photo-Fenton system on Escherichia coli. Comparison with photo-catalytic action of TiO2 during cell envelope disruption. Appl. Catal. B-Environ. 160, 286–297. https://doi.org/10.1016/j.apcatb.2014.05.001.

Rubin, B.S., 2011. Bisphenol A: an endocrine disruptor with widespread exposure and multiple effects. J. Steroid Biochem. Mol. Biol. 127, 27–34. https://doi.org/10.1016/j.jsbmb.2011.05.002.

Rubio, D., Nebot, E., Casanueva, J.F., Pulgarin, C., 2013. Comparative effect of simulated solar light, UV, UV/H202 and photo-Fenton treatment (UV Vis/H2O2/Fe-2+,Fe-3+) in the *Escherichia* colt inactivation in artificial seawater. Water Res. 47, 6367–6379. https://doi.org/10.1016/j.watres.2013.08.006.

Rusevova, K., Koferstein, R., Rosell, M., Richnow, H.H., Kopinke, F.D., Georgi, A., 2014. LaFeO3 and BiFeO3 perovskites as nanocatalysts for contaminant degradation in heterogeneous Fenton-like reactions. Chem. Eng. J. 239, 322–331. https://doi.org/10.1016/j.cej.2013.11.025.

Saenger, W., 1980. Cyclodextrin inclusion compounds in research and industry. Angew. Chem. Int. Ed. Engl. 19, 344–362. https://doi.org/10.1002/anie.198003441.

Saha, D., Visconti, M.C., Desipio, M.M., Thorpe, R., 2020. Inactivation of antibiotic resistance gene by ternary nanocomposites of carbon nitride, reduced graphene oxide and iron oxide under visible light. Chem. Eng. J. 382 https://doi.org/10.1016/j.cej.2019.122857.

Serrà, A., Artal, R., García-Amorós, J., Gómez, E., Philippe, L., 2020. Circular zero-residue process using microalgae for efficient water decontamination, biofuel production, and carbon dioxide fixation. Chem. Eng. J. 388, 124278 https://doi.org/10.1016/j.cej.2020.124278.

Shannon, M.A., Bohn, P.W., Elimelech, M., Georgiadis, J.G., Mariñas, B.J., Mayes, A.M., 2008. Science and technology for water purification in the coming decades. Nature 452, 301–310. https://doi.org/10.1038/nature06599.

Shao, M.F., Wei, M., Evans, D.G., Duan, X., 2013. Hierarchical structures based on functionalized magnetic cores and layered double-hydroxide shells: concept, controlled synthesis, and applications. Chem. Eur. J. 19, 4100–4108. https://doi.org/10.1002/chem.201204205.

Sharma, R., Bansal, S., Singhal, S., 2015. Tailoring the photo-Fenton activity of spinel ferrites (MFe2O4) by incorporating different cations (M = Cu, Zn, Ni and Co) in the structure. RSC Adv. 5, 6006–6018. https://doi.org/10.1039/c4ra13692f.

Sharma, V.K., Feng, M., 2019. Water depollution using metal-organic frameworks-catalyzed advanced oxidation processes: a review. J. Hazard. Mater. 372, 3–16. https://doi.org/10.1016/j.jhazmat.2017.09.043.

Sharma, R., Singhal, S., 2015. Photodegradation of textile dye using magnetically recyclable heterogeneous spinel ferrites. J. Chem. Technol. Biotechnol. 90, 955–962. https://doi.org/10.1002/jctb.4409.

Shen, L., Luo, M., Liu, Y., Liang, R., Jing, F., Wu, L., 2015. Noble-metal-free MoS2 co-catalyst decorated UiO-66/CdS hybrids for efficient photocatalytic H2 production. Appl. Catal. B Environ. 166–167, 445–453. https://doi.org/10.1016/j.apcatb.2014.11.056.

Shen, X., Tian, J., Li, J., Li, X., Chen, Y., 1992. Formation of the excited ferryl species following fenton reaction. Free Radic. Biol. Med. 13, 585–592. https://doi.org/10.1016/0891-5849(92)90152-7.

Sheydaei, M., Aber, S., Khataee, A., 2014. Preparation of a novel gamma-FeOOH-GAC nano composite for decolorization of textile wastewater by photo Fenton-like process in a continuous reactor. J. Mol. Catal. A Chem. 392, 229–234. https://doi.org/10.1016/j.molcata.2014.05.019.

Singh, P., Shandilya, P., Raizada, P., Sudhaik, A., Rahmani-Sani, A., Hosseini-Bandegharaei, A., 2020. Review on various strategies for enhancing photocatalytic activity of graphene based nanocomposites for water purification. Arab. J. Chem. 13, 3498–3520. https://doi.org/10.1016/j.arabjc.2018.12.001.

Sin, J.-C., Lam, S.-M., Mohamed, A.R., Lee, K.-T., 2012. Degrading endocrine disrupting chemicals from wastewater by TiO 2 photocatalysis: a review. Int. J. Photo 2012. https://doi.org/10.1155/2012/185159.

Smith, M.D., Connor, B.A., Karunadasa, H.I., 2019. Tuning the luminescence of layered halide perovskites. Chem. Rev. 119, 3104–3139. https://doi.org/10.1021/acs.chemrev.8b00477.

Soltani, T., Lee, B., 2017. Enhanced formation of sulfate radicals by metal-doped BiFeO 3 under visible light for improving photo-Fenton catalytic degradation of 2-chlorophenol. Chem. Eng. J. 313, 1258–1268. https://doi.org/10.1016/j.cej.2016.11.016.

Soon, A.N., Hameed, B.H., 2011. Heterogeneous catalytic treatment of synthetic dyes in aqueous media using Fenton and photo-assisted Fenton process. Desalination 269, 1–16. https://doi.org/10.1016/j.desal.2010.11.002.

Spuhler, D., Rengifo-Herrera, J.A., Pulgarin, C., 2010. The effect of Fe2+, Fe3+, H2O2 and the photo-Fenton reagent at near neutral pH on the solar disinfection (SODIS) at low temperatures of water containing *Escherichia coli* K12. Appl. Catal. B Environ. 96, 126–141. https://doi.org/10.1016/j.apcatb.2010.02.010.

Suárez-Iglesias, O., Collado, S., Oulego, P., Díaz, M., 2017. Graphene-family nanomaterials in wastewater treatment plants. Chem. Eng. J. 313, 121–135. https://doi.org/10.1016/j.cej.2016.12.022.

Sudhaik, A., Raizada, P., Shandilya, P., Jeong, D.Y., Lim, J.H., Singh, P., 2018. Review on fabrication of graphitic carbon nitride based efficient nanocomposites for photodegradation of aqueous phase organic pollutants. J. Ind. Eng. Chem. 67, 28–51. https://doi.org/10.1016/j.jiec.2018.07.007.

Suib, S.L., 1993. Zeolitic and layered materials. Chem. Rev. 93, 803–826. https://doi.org/10.1021/cr00018a009.

Sun, H.Q., Liu, S.Z., Zhou, G.L., Ang, H.M., Tade, M.O., Wang, S.B., 2012. Reduced graphene oxide for catalytic oxidation of aqueous organic pollutants. ACS Appl. Mater. Interfaces 4, 5466–5471. https://doi.org/10.1021/am301372d.

Sun, H., Wang, J., Jiang, Y., Shen, W., Jia, F., Wang, S., Liao, X., Zhang, L., 2019. Rapid Aerobic inactivation and facile removal of escherichia coli with amorphous zero-valent iron microspheres: indispensable roles of reactive oxygen species and Iron corrosion products. Environ. Sci. Technol. 53, 3707–3717. https://doi.org/10.1021/acs.est.8b06499.

Tabet, D., Saidi, M., Houari, M., Pichat, P., Khalaf, H., 2006. Fe-pillared clay as a Fenton-type heterogeneous catalyst for cinnamic acid degradation. J. Environ. Manag. 80, 342–346. https://doi.org/10.1016/j.jenvman.2005.10.003.

Tang, J., Wang, J., 2018. Metal organic framework with coordinatively unsaturated sites as efficient fenton-like catalyst for enhanced degradation of sulfamethazine. Environ. Sci. Technol. 52, 5367–5377. https://doi.org/10.1021/acs.est.8b00092.

Tan, C., Xiang, B., Li, Y.J., Fang, J.W., Huang, M., 2011. Preparation and characteristics of a nano-PbO2 anode for organic wastewater treatment. Chem. Eng. J. 166, 15–21. https://doi.org/10.1016/j.cej.2010.08.018.

Thakur, I., Örmeci, B., verma, A., 2020. Inactivation of E. coli in water employing Fe-TiO2 composite incorporating in-situ dual process of photocatalysis and photo-Fenton in fixed-mode. J. Water Process Eng. 33, 101085 https://doi.org/10.1016/j.jwpe.2019.101085.

Thomas, C.M., Nielsen, K.M., 2005. Mechanisms of, and barriers to, horizontal gene transfer between bacteria. Nat. Rev. Microbiol. 3, 711–721. https://doi.org/10.1038/nrmicro1234.

Tong, M., Liu, F., Dong, Q., Ma, Z., Liu, W., 2020. Magnetic Fe3O4-deposited flower-like MoS2 nanocomposites for the Fenton-like Escherichia coli disinfection and diclofenac degradation. J. Hazard. Mater. 385, 121604 https://doi.org/10.1016/j.jhazmat.2019.121604.

To, T., Phan, N., Nikoloski, A.N., Bahri, P.A., Li, D., 2018. Journal of industrial and engineering chemistry heterogeneous photo-Fenton degradation of organics using highly ef fi cient Cu-doped LaFeO 3 under visible light. J. Ind. Eng. Chem. 61, 53–64. https://doi.org/10.1016/j.jiec.2017.11.046.

Tucek, J., Prucek, R., Kolarik, J., Zoppellaro, G., Petr, M., Filip, J., Sharma, V.K., Zboril, R., 2017. Zero-Valent iron nanoparticles reduce arsenites and arsenates to As (0) firmly embedded in core-shell superstructure: challenging strategy of arsenic treatment under anoxic conditions. Acs Sustain. Chem. Eng. 5, 3027–3038. https://doi.org/10.1021/acssuschemeng.6b02698.

Usman, M., Byrne, J.M., Chaudhary, A., Orsetti, S., Hanna, K., Ruby, C., Kappler, A., Haderlein, S.B., 2018. Magnetite and green rust: synthesis, properties, and environmental applications of mixed-valent Iron minerals. Chem. Rev. 118, 3251–3304. https://doi.org/10.1021/acs.chemrev.7b00224.

Valdés-Solís, T., Valle-Vigón, P., Álvarez, S., Marbán, G., Fuertes, A.B., 2007. Manganese ferrite nanoparticles synthesized through a nanocasting route as a highly active Fenton catalyst. Catal. Commun. 8, 2037–2042. https://doi.org/10.1016/j.catcom.2007.03.030.

Vayssieres, L., Sathe, C., Butorin, S.M., Shuh, D.K., Nordgren, J., Guo, J., 2005. One-dimensional quantum-confinement effect in α-Fe 2 O 3 ultrafine nanorod arrays. Adv. Mater. 17, 2320–2323. https://doi.org/10.1002/adma.200500992.

Vilardi, G., Mpouras, T., Dermatas, D., Verdone, N., Polydera, A., Di Palma, L., 2018. Nanomaterials application for heavy metals recovery from polluted water: The combination of nano zero-valent iron and carbon nanotubes. Competitive adsorption non-linear modeling. Chemosphere 201, 716–729. https://doi.org/10.1016/j.chemosphere.2018.03.032.

Vione, D., Falletti, G., Maurino, V., Minero, C., Pelizzetti, E., Malandrino, M., Ajassa, R., Olariu, R.I., Arsene, C., 2006. Sources and sinks of hydroxyl radicals upon irradiation of natural water samples. Environ. Sci. Technol. 40, 3775–3781. https://doi.org/10.1021/es052206b.

Voelker, B.M., Morel, F.M.M., Sulzberger, B., 1997. Iron redox cycling in surface waters: effects of humic substances and light. Environ. Sci. Technol. 31, 1004–1011. https://doi.org/10.1021/es9604018.

Vorontsov, A.V., 2019. Advancing Fenton and photo-Fenton water treatment through the catalyst design. J. Hazard. Mater. 372, 103–112. https://doi.org/10.1016/j.jhazmat.2018.04.033.

Walte, T.D., Morel, F.M.M., 1984. Photoreductive dissolution of colloidal iron oxides in natural waters. Environ. Sci. Technol. 18, 860–868. https://doi.org/10.1021/es00129a010.

Wang, S., 2008. A comparative study of Fenton and Fenton-like reaction kinetics in decolourisation of wastewater. Dye. Pigment. 76, 714–720. https://doi.org/10.1016/j.dyepig.2007.01.012.
Wang, Q., Astruc, D., 2020. State of the art and prospects in Metal-Organic Framework (MOF)-based and MOF-derived nanocatalysis. Chem. Rev. 120, 1438–1511. https://doi.org/10.1021/acs.chemrev.9b00223.
Wang, X., Blechert, S., Antonietti, M., 2012. Polymeric graphitic carbon nitride for heterogeneous photocatalysis. ACS Catal. 2, 1596–1606. https://doi.org/10.1021/cs300240x.
Wang, H., Jing, M., Wu, Y., Chen, W., Ran, Y., 2018. Effective degradation of phenol via Fenton reaction over CuNiFe layered double hydroxides. J. Hazard. Mater. 353, 53–61. https://doi.org/10.1016/j.jhazmat.2018.03.053.
Wang, Y., Liang, M.X., Fang, J.S., Fu, J., Chen, X.C., 2017. Visible-light photo-Fenton oxidation of phenol with rGO-alpha-FeOOH supported on Al-doped mesoporous silica (MCM-41) at neutral pH: performance and optimization of the catalyst. Chemosphere 182, 468–476. https://doi.org/10.1016/j.chemosphere.2017.05.037.
Wang, X., Lin, Y., Ding, X.F., Jiang, J.G., 2011. Enhanced visible-light-response photocatalytic activity of bismuth ferrite nanoparticles. J. Alloy. Compd. 509, 6585–6588. https://doi.org/10.1016/j.jallcom.2011.03.074.
Wang, X.G., Liu, C.S., Li, X.M., Li, F.B., Zhou, S.G., 2008. Photodegradation of 2-mercaptobenzothiazole in the gamma-Fe2O3/oxalate suspension under UVA light irradiation. J. Hazard. Mater. 153, 426–433. https://doi.org/10.1016/j.jhazmat.2007.08.072.
Wang, X., Liu, W., Qin, J., Lei, L., 2020. Improvement of H2O2 utilization by the persistent heterogeneous Fenton reaction with the Fe3O4-zeolite-cyclodextrin composite. Ind. Eng. Chem. Res. 59, 2192–2202. https://doi.org/10.1021/acs.iecr.9b06091.
Wang, Y., Song, H., Chen, J., Chai, S., Shi, L., Chen, C., Wang, Y., He, C., 2020. A novel solar photo-Fenton system with self-synthesizing H2O2: enhanced photo-induced catalytic performances and mechanism insights. Appl. Surf. Sci. 512 https://doi.org/10.1016/j.apsusc.2020.145650.
Wang, W.M., Song, J., Han, X., 2013. Schwertmannite as a new Fenton-like catalyst in the oxidation of phenol by H2O2. J. Hazard. Mater. 262, 412–419. https://doi.org/10.1016/j.jhazmat.2013.08.076.
Wang, D., Wang, M., Li, Z., 2015. Fe-based metal-organic frameworks for highly selective photocatalytic benzene hydroxylation to phenol. ACS Catal. 5, 6852–6857. https://doi.org/10.1021/acscatal.5b01949.
Wang, X.Y., Wang, A.Q., Ma, J., Fu, M.L., 2017. Facile green synthesis of functional nanoscale zero-valent iron and studies of its activity toward ultrasound-enhanced decolorization of cationic dyes. Chemosphere 166, 80–88. https://doi.org/10.1016/j.chemosphere.2016.09.056.
Wang, X., Yin, R., Zeng, L., Zhu, M., 2019. A review of graphene-based nanomaterials for removal of antibiotics from aqueous environments. Environ. Pollut. 253, 100–110. https://doi.org/10.1016/j.envpol.2019.06.067.
Wang, J., Zhang, Q., Deng, F., Luo, X., Dionysiou, D.D., 2020. Rapid toxicity elimination of organic pollutants by the photocatalysis of environment-friendly and magnetically recoverable step-scheme SnFe2O4/ZnFe2O4 nano-heterojunctions. Chem. Eng. J. 379, 122264.
Wang, J., Zhang, P., Liang, B., Liu, Y., Xu, T., Wang, L., Cao, B., Pan, K., 2016. Graphene oxide as an effective barrier on a porous nanofibrous membrane for water treatment. ACS Appl. Mater. Interfaces 8, 6211–6218. https://doi.org/10.1021/acsami.5b12723.
Wang, Y., Zhao, H., Li, M., Fan, J., Zhao, G., 2014. Magnetic ordered mesoporous copper ferrite as a heterogeneous Fenton catalyst for the degradation of imidacloprid. Appl. Catal. B Environ. 147, 534–545. https://doi.org/10.1016/j.apcatb.2013.09.017.
Wang, N., Zheng, T., Zhang, G., Wang, P., 2016. A review on Fenton-like processes for organic wastewater treatment. J. Environ. Chem. Eng. 4, 762–787. https://doi.org/10.1016/j.jece.2015.12.016.
Wang, W., Zhou, M., Mao, Q., Yue, J., Wang, X., 2010. Novel NaY zeolite-supported nanoscale zero-valent iron as an efficient heterogeneous Fenton catalyst. Catal. Commun. 11, 937–941. https://doi.org/10.1016/j.catcom.2010.04.004.
Wang, N., Zhu, L., Lei, M., She, Y., Cao, M., Tang, H., 2011. Ligand-induced drastic enhancement of catalytic activity of nano-BiFeO 3 for oxidative degradation of bisphenol A. ACS Catal. 1, 1193–1202. https://doi.org/10.1021/cs2002862.
Wan, Z., Wang, J., 2017. Degradation of sulfamethazine using Fe3O4-Mn3O4/reduced graphene oxide hybrid as Fenton-like catalyst. J. Hazard. Mater. 324, 653–664. https://doi.org/10.1016/j.jhazmat.2016.11.039.
Weckhuysen, B.M., Yu, J., 2015. Recent advances in zeolite chemistry and catalysis. Chem. Soc. Rev. 44, 7022–7024. https://doi.org/10.1039/c5cs90100f.
Wei, S., Ren, H., Li, J., Shi, J., Shao, Z., 2013. Decolorization of organic dyes by zero-valent iron in the presence of oxalic acid and influence of photoirradiation and hexavalent chromium. J. Mol. Catal. A Chem. 379, 309–314. https://doi.org/10.1016/j.molcata.2013.09.002.
Wu, M., Wang, Q., Sun, Q., Jena, P., 2013. Functionalized graphitic carbon nitride for efficient energy storage. J. Phys. Chem. C. 117, 6055–6059. https://doi.org/10.1021/jp311972f.
Wu, Q., Yang, H., Kang, L., Gao, Z., Ren, F., 2020. Fe-based metal-organic frameworks as Fenton-like catalysts for highly efficient degradation of tetracycline hydrochloride over a wide pH range: acceleration of Fe(II)/ Fe(III) cycle under visible light irradiation. Appl. Catal. B Environ. 263 https://doi.org/10.1016/j.apcatb.2019.118282.
Xiang, Y., Huang, Y., Xiao, B., Wu, X., Zhang, G., 2020. Magnetic yolk-shell structure of ZnFe2O4 nanoparticles for enhanced visible light photo-Fenton degradation towards antibiotics and mechanism study. Appl. Surf. Sci. 513, 145820 https://doi.org/10.1016/j.apsusc.2020.145820.
Xiao, C., Li, J., Zhang, G., 2018. Synthesis of stable burger-like α-Fe2O3 catalysts: formation mechanism and excellent photo-Fenton catalytic performance. J. Clean. Prod. 180, 550–559. https://doi.org/10.1016/j.jclepro.2018.01.127.
Xie, Y., Carbone, L., Nobile, C., Grillo, V., D'Agostino, S., Della Sala, F., Giannini, C., Altamura, D., Oelsner, C., Kryschi, C., Cozzoli, P.D., 2013. Metallic-like stoichiometric copper sulfide nanocrystals: phase- and shape-selective synthesis, near-infrared surface plasmon resonance properties, and their modeling. ACS Nano 7, 7352–7369. https://doi.org/10.1021/nn403035s.
Xie, A., Cui, J., Yang, J., Chen, Y., Lang, J., Li, C., Yan, Y., Dai, J., 2020. Graphene oxide/Fe(III)-based metal-organic framework membrane for enhanced water purification based on synergistic separation and photo-Fenton processes. Appl. Catal. B Environ. 264, 118548 https://doi.org/10.1016/j.apcatb.2019.118548.
Xiong, S., Xu, J., Chen, D., Wang, R., Hu, X., Shen, G., Wang, Z.L., 2011. Controlled synthesis of monodispersed hematite microcubes and their properties. CrystEngComm 13, 7114–7120. https://doi.org/10.1039/c1ce05569k.
Xu, J.G., Li, Y.Q., Yuan, B.L., Shen, C.H., Fu, M.L., Cui, H.J., Sun, W.J., 2016. Large scale preparation of Cu-doped alpha-FeOOH nanoflowers and their photo-Fenton-like catalytic degradation of diclofenac sodium. Chem. Eng. J. 291, 174–183. https://doi.org/10.1016/j.cej.2016.01.059.
Xu, P., Ming, G., Lian, D., Ling, C., Hu, S., Hua, M., 2012. Science of the Total Environment Use of iron oxide nanomaterials in wastewater treatment : a review. Sci. Total Environ. 424, 1–10. https://doi.org/10.1016/j.scitotenv.2012.02.023.
Xu, P.A., Zeng, G.M., Huang, D.L., Feng, C.L., Hu, S., Zhao, M.H., Lai, C., Wei, Z., Huang, C., Xie, G.X., Liu, Z.F., 2012. Use of iron oxide nanomaterials in wastewater treatment: a review. Sci. Total Environ. 424, 1–10. https://doi.org/10.1016/j.scitotenv.2012.02.023.
Xu, T.Y., Zhu, R.L., Liu, J., Zhou, Q., Zhu, J.X., Liang, X.L., Xi, Y.F., He, H.P., 2016. Fullerol modification ferrihydrite for the degradation of acid red 18 under simulated sunlight irradiation. J. Mol. Catal. A Chem. 424, 393–401. https://doi.org/10.1016/j.molcata.2016.09.024.
Xu, T.Y., Zhu, R.L., Zhu, J.X., Liang, X.L., Liu, Y., Xu, Y., He, H.P., 2016. BiVO4/Fe/Mt composite for visible-light-driven degradation of acid red 18. Appl. Clay Sci. 129, 27–34. https://doi.org/10.1016/j.clay.2016.04.018.
Xu, T.Y., Zhu, R.L., Zhu, G.Q., Zhu, J.X., Liang, X.L., Zhu, Y.P., He, H.P., 2017. Mechanisms for the enhanced photo-Fenton activity of ferrihydrite modified with BiVO4 at neutral pH. Appl. Catal. B Environ. 212, 50–58. https://doi.org/10.1016/j.apcatb.2017.04.064.
Yang, X., Cheng, X., Elzatahry, A.A., Chen, J., Alghamdi, A., Deng, Y., 2019. Recyclable Fenton-like catalyst based on zeolite Y supported ultrafine, highly-dispersed Fe2O3 nanoparticles for removal of organics under mild conditions. Chin. Chem. Lett. 30, 324–330. https://doi.org/10.1016/j.cclet.2018.06.026.
Yang, G.C.C., Huang, S.C., Wang, C.L., Jen, Y.S., 2016. Degradation of phthalate esters and acetaminophen in river sediments using the electrokinetic process integrated with a novel Fenton-like process catalyzed by nanoscale schwertmannite. Chemosphere 159, 282–292. https://doi.org/10.1016/j.chemosphere.2016.04.119.
Yang, Z., Yu, A., Shan, C., Gao, G., Pan, B., 2018. Enhanced Fe(III)-mediated Fenton oxidation of atrazine in the presence of functionalized multi-walled carbon nanotubes. Water Res. 137, 37–46. https://doi.org/10.1016/j.watres.2018.03.006.
Yang, X., Zhang, Y.F., Xu, G., Wei, X., Ren, Z.H., Shen, G., Han, G.R., 2013. Phase and morphology evolution of bismuth ferrites via hydrothermal reaction route. Mater. Res. Bull. 48, 1694–1699. https://doi.org/10.1016/j.materresbull.2013.01.032.
Yang, Z.Z., Zhang, C., Zeng, G.M., Tan, X.F., Wang, H., Huang, D.L., Yang, K.H., Wei, J.J., Ma, C., Nie, K., 2020. Design and engineering of layered double hydroxide based catalysts for water depollution by advanced oxidation processes: a review. J. Mater. Chem. 8 https://doi.org/10.1039/c9ta13522g.
Yan, J., Qian, L., Gao, W., Chen, Y., Ouyang, D., Chen, M., 2017. Enhanced Fenton-like degradation of trichloroethylene by hydrogen peroxide activated with nanoscale zero valent iron loaded on biochar. Sci. Rep. 7, 1–9. https://doi.org/10.1038/srep43051.
Yao, Y., Chen, H., Qin, J., Wu, G., Lian, C., Zhang, J., Wang, S., 2016. Iron encapsulated in boron and nitrogen codoped carbon nanotubes as synergistic catalysts for Fenton-like reaction. Water Res. 101, 281–291. https://doi.org/10.1016/j.watres.2016.05.065.
Yao, Y., Wang, L., Sun, L., Zhu, S., Huang, Z., WangyangLu, Y.M., Chen, W., 2013. Efficient removal of dyes using heterogeneous Fenton catalysts based on activated carbon fibers with enhanced activity. Chem. Eng. Sci. 101, 424–431. https://doi.org/10.1016/j.ces.2013.06.009.
Yin, J., Zhu, G., Deng, B., 2016. Graphene oxide (GO) enhanced polyamide (PA) thin-film nanocomposite (TFN) membrane for water purification. Desalination 379, 93–101. https://doi.org/10.1016/j.desal.2015.11.001.
You, Y., Han, J., Chiu, P.C., Jin, Y., 2005. Removal and inactivation of waterborne viruses using zerovalent iron. Environ. Sci. Technol. 39, 9263–9269.
Zaleska, A., 2008. Doped-TiO2: a review. Recent Pat. Eng. 2, 157–164. https://doi.org/10.2174/187221208786306289.
Zarei, A.R., Rezaei-Vahidian, H., Mehrabi, G.R., Farajpour, T., 2019. Application of response surface methodology to optimize degradation of TNT using nano Fe-0-assisted Fenton process. Environ. Prog. Sustain. Energy 38, 477–482. https://doi.org/10.1002/ep.12990.
Zeng, X., Lemley, A.T., 2009. Fenton degradation of 4,6-dinitro-o-cresol with Fe2+-substituted ion-exchange resin. J. Agric. Food Chem. 57, 3689–3694. https://doi.org/10.1021/jf900764q.
Zhang, X.H., Chen, Y.Z., Zhao, N., Liu, H., Wei, Y., 2014. Citrate modified ferrihydrite microstructures: facile synthesis, strong adsorption and excellent Fenton-like catalytic properties. RSC Adv. 4, 21575–21583. https://doi.org/10.1039/c4ra00978a.

Zhang X., Chen Y., Zhao N., Wei Y., RSC Advances synthesis , strong adsorption and excellent Fenton-, (2014) 21575–21583. https://doi.org/10.1039/c4ra00978a.
Zhang, H., Fei, C.Z., Zhang, D.B., Tang, F., 2007. Degradation of 4-nitrophenol in aqueous medium by electro-Fenton method. J. Hazard. Mater. 145, 227–232. https://doi.org/10.1016/j.jhazmat.2006.11.016.
Zhang, L., Jin, H., Ma, H., Gregory, K., Qi, Z., Wang, C., Wu, W., Cang, D., Li, Z., 2020. Oxidative damage of antibiotic resistant E. coli and gene in a novel sulfidated micron zero-valent activated persulfate system. Chem. Eng. J. 381, 122787 https://doi.org/10.1016/j.cej.2019.122787.
Zhang, L.H., Li, F., Evans, D.G., Duan, X., 2010a. Evolution of structure and performance of Cu-based layered double hydroxides. J. Mater. Sci. 45, 3741–3751. https://doi.org/10.1007/s10853-010-4423-6.
Zhang, L.H., Li, F., Evans, D.G., Duan, X., 2010b. Cu-Zn-(Mn)-(Fe)-Al layered double hydroxides and their mixed metal oxides: physicochemical and catalytic properties in wet hydrogen peroxide oxidation of phenol. Ind. Eng. Chem. Res 49, 5959–5968. https://doi.org/10.1021/ie9019193.
Zhang, M., Yao, Q., Guan, W., Lu, C., Lin, J.M., 2014. Layered double hydroxide-supported carbon dots as an efficient heterogeneous Fenton-like catalyst for generation of hydroxyl radicals. J. Phys. Chem. C. 118, 10441–10447. https://doi.org/10.1021/jp5012268.
Zhang, L., Zhang, Z., Lu, C., Lin, J.M., 2012. Improved chemiluminescence in Fenton-Like reaction via dodecylbenzene- sulfonate-intercalated layered double hydroxides. J. Phys. Chem. C. 116, 14711–14716. https://doi.org/10.1021/jp304147x.
Zhang, G., Zhang, X., Meng, Y., Pan, G., Ni, Z., Xia, S., 2020. Layered double hydroxides-based photocatalysts and visible-light driven photodegradation of organic pollutants: a review. Chem. Eng. J. 392, 123684 https://doi.org/10.1016/j.cej.2019.123684.
Zhao, L., Han, T., Wang, H., Zhang, L., Liu, Y., 2016. Ni-Co alloy catalyst from LaNi1-xCoxO3 perovskite supported on zirconia for steam reforming of ethanol. Appl. Catal. B Environ. 187, 19–29. https://doi.org/10.1016/j.apcatb.2016.01.007.
Zhao, Z., Sun, Y., Dong, F., 2015. Graphitic carbon nitride based nanocomposites: a review. Nanoscale 7, 15–37. https://doi.org/10.1039/c4nr03008g.
Zhao, H., Tian, C., Mei, J., Yang, S., Wong, P.K., 2020. Synergistic effect and mechanism of catalytic degradation toward antibiotic contaminants by amorphous goethite nanoparticles decorated graphitic carbon nitride. Chem. Eng. J. 390 https://doi.org/10.1016/j.cej.2020.124551.
Zheng, X., Cheng, H., Yang, J., Chen, D., Jian, R., Lin, L., 2018. One-Pot solvothermal preparation of Fe3O4-urushiol-graphene hybrid nanocomposites for highly improved fenton reactions. ACS Appl. Nano Mater. 1, 2754–2762. https://doi.org/10.1021/acsanm.8b00446.
Zheng, X.L., Weng, J.B., Hu, B.H., Lv, X.Z., Meng, D.L., Chan, A.S.C., 2011. Fabrication of a stable superhydrophobic film constructed by poly(vinylpyrrolidone)/poly (urushiol)-CuS through layer-by-layer assembly. Mater. Chem. Phys. 130, 1054–1060. https://doi.org/10.1016/j.matchemphys.2011.08.032.
Zheng, X., Weng, J., Li, S., Liu, H., Hu, B., Li, Y., Meng, X., Ruan, H., 2014. Anticorrosive ultrathin film derived from bio-based urushiol-Ti by layer-by-layer self-assembly. Chem. Eng. J. 245, 265–275. https://doi.org/10.1016/j.cej.2014.02.039.
Zhong, X., Royer, S., Zhang, H., Huang, Q., Xiang, L., Valange, S., Barrault, J., 2011. Mesoporous silica iron-doped as stable and efficient heterogeneous catalyst for the degradation of C.I. Acid Orange 7 using sono-photo-Fenton process. Sep. Purif. Technol. 80, 163–171. https://doi.org/10.1016/j.seppur.2011.04.024.
Zhou, S., Qian, Z., Sun, T., Xu, J., Xia, C., 2011. Catalytic wet peroxide oxidation of phenol over Cu-Ni-Al hydrotalcite. Appl. Clay Sci. 53, 627–633. https://doi.org/10.1016/j.clay.2011.05.013.
Zhou, Y.Z., Wang, T., Zhi, D., Guo, B.L., Zhou, Y.Y., Nie, J., Huang, A.Q., Yang, Y., Huang, H.L., Luo, L., 2019. Applications of nanoscale zero-valent iron and its composites to the removal of antibiotics: a review. J. Mater. Sci. 54, 12171–12188. https://doi.org/10.1007/s10853-019-03606-5.
Zhu, J.J., Thomas, A., 2009. Perovskite-type mixed oxides as catalytic material for NO removal. Appl. Catal. B Environ. 92, 225–233. https://doi.org/10.1016/j.apcatb.2009.08.008.
Zhu, R., Zhu, Y., Xian, H., Yan, L., Fu, H., Zhu, G., Xi, Y., Zhu, J., He, H., 2020. CNTs/ferrihydrite as a highly efficient heterogeneous Fenton catalyst for the degradation of bisphenol A: the important role of CNTs in accelerating Fe(III)/Fe(II) cycling. Appl. Catal. B Environ. 270, 118891 https://doi.org/10.1016/j.apcatb.2020.118891.
Zhu, Y.P., Zhu, R.L., Xi, Y.F., Xu, T.Y., Yan, L.X., Zhu, J.X., Zhu, G.Q., He, H.P., 2018. Heterogeneous photo-Fenton degradation of bisphenol A over Ag/AgCl/ferrihydrite catalysts under visible light. Chem. Eng. J. 346, 567–577. https://doi.org/10.1016/j.cej.2018.04.073.
Zhu, Y., Zhu, R., Xi, Y., Zhu, J., Zhu, G., He, H., 2019. Strategies for enhancing the heterogeneous fenton catalytic reactivity: a review. Appl. Catal. B Environ. 255, 117739 https://doi.org/10.1016/j.apcatb.2019.05.041.
Zhu, Y.P., Zhu, R.L., Yan, L.X., Fu, H.Y., Xi, Y.F., Zhou, H.J., Zhu, G.Q., Zhu, J.X., He, H. P., 2018b. Visible-light Ag/AgBr/ferrihydrite catalyst with enhanced heterogeneous photo-Fenton reactivity via electron transfer from Ag/AgBr to ferrihydrite. Appl. Catal. B Environ. 239, 280–289. https://doi.org/10.1016/j.apcatb.2018.08.025.
Zubir, N.A., Yacou, C., Motuzas, J., Zhang, X., Diniz Da Costa, J.C., 2014. Structural and functional investigation of graphene oxide-Fe 3 O 4 nanocomposites for the heterogeneous Fenton-like reaction. Sci. Rep. 4, 1–8. https://doi.org/10.1038/srep04594.
Zubir, N.A., Yacou, C., Motuzas, J., Zhang, X.W., Zhao, X.S., da Costa, J.C.D., 2015. The sacrificial role of graphene oxide in stabilising a Fenton-like catalyst GO-Fe3O4. Chem. Commun. 51, 9291–9293. https://doi.org/10.1039/c5cc02292d.

Nishanth Thomas is a Ph.D. candidate in the Nanotechnology and Bio-Engineering Research Group at the Institute of Technology Sligo, Ireland. He completed his BSMS dual degree in Chemistry (major) with Biology minor from Indian Institute of Science Education and Research (IISER) Bhopal. During his master's thesis, he investigated the shape-selective synthesis of silver nanostructures by a modified polyol method. Currently, he is working in the EU-Horizon 2020 PANI Water Project for developing Advanced Oxidation Processes (AOPs) for the removal of antimicrobial-resistant organisms from water. His research interest involves the design of unique nanomaterials for the sustainable environment and energy applications.

Professor Dionysiou is currently a Herman Schneider Professor of Environmental Engineering and has served as a UNESCO co-Chair Professor on "Water Access and Sustainability" at the University of Cincinnati. He teaches courses on drinking water quality, treatment and reuse, advanced unit operations for water treatment, advanced oxidation technologies, and physical-chemical processes for water quality control. Professor Dionysiou is leading several projects of local, state, national and international importance focused on water quality, treatment, reuse, and monitoring. His work encompasses surface water, groundwater, agricultural water, and industrial waters of complex mixtures. His research interests include (i) physical chemical processes for water treatment, (ii) urban water quality, (iii) advanced oxidation processes, (iv) UV and solar light-based remediation processes, (v) treatment of contaminants of emerging concern (i.e., pharmaceuticals and personal care products, biotoxins, heavy metals), (vi) remediation of Harmful Algal Blooms/cyanotoxins, (vii) environmental nanotechnology and nanosensing, (viii) water-energy-food (WEF) nexus, and (ix) water sustainability. Several of his current projects are focused on the treatment, sensing, and monitoring of cyanotoxins formed in freshwater aquatic systems such as Lake Erie and several inland lakes and rivers in Ohio.

Prof. Suresh C. Pillai obtained his PhD in the area of Nanotechnology from Trinity College Dublin and then performed postdoctoral research at California Institute of Technology (Caltech), USA. Upon the completion of this appointment he returned to Trinity College Dublin as a Research Fellow before joining CREST-DIT as a Senior Research Manager in April 2004. Suresh joined IT Sligo as a Senior Lecturer in Nanotechnology in October 2013 and currently heads the Nanotechnology and Bio-Engineering Research group. He is the recipient of 'Boyle-Higgins Award – 2019' from the Institute of Chemistry Ireland. He is an elected fellow of the UK's Royal Microscopical Society (FRMS) and the Institute of Materials, Minerals and Mining (FIMMM). Suresh was responsible for acquiring more than €5 million direct R&D funding. He has published several scientific articles in leading peer reviewed journals and has presented papers in several international conferences. He has delivered over hundred international invited talks including several key-note and plenary talks. His research work was featured in the BBC London, BBC World Radio, Times UK, 'The Investigators (RTE TV)' programme, RTE-1 TV News, Aljazeera TV, Ocean FM Radio and a number of national and international news media. He was also the recipient of the 'Hothouse Commercialisation Award 2009' from the Minister of Science, Technology and Innovation and also the recipient of the 'Enterprise Ireland Research Commercialization Award 2009'. He is an associate editor for the Chemical Engineering Journal (Elsevier) and Editorial Board Member for Applied Catalysis B (Elsevier)